The climate and vegetation of Europe, North Africa and the Middle East during the Last Glacial Maximum (21,000 years BP) based on pollen data

Basil A.S. Davis[1], Marc Fasel[2], Jed O. Kaplan[3], Emmanuele Russo[4], Ariane Burke[5]

[1]Institute of Earth Surface Dynamics, University of Lausanne, Lausanne, 1015, Switzerland
[2]enviroSPACE lab, Institute for Environmental Sciences, University of Geneva, Geneva, 1211, Switzerland
[3]Department of Earth Sciences, The University of Hong Kong, Hong Kong, Peoples Republic of China
[4]Department of Environmental Systems Science, ETH Zurich, Zurich, 8092, Switzerland
[5]Laboratoire d'Ecomorphologie et de Paleoanthropologie, Departement d'Anthropologie, Universite de Montreal, Montreal, Quebec, H3C 3J7, Canada

Correspondence to: Basil A. S. Davis (basil.davis@unil.ch)

Abstract. Pollen data represents one of the most widely available and spatially-resolved sources of information about the past land cover and climate of the Last Glacial Maximum (21,000 years BP). Previous pollen data compilations for Europe, the Mediterranean and the Middle East however have been limited by small numbers of sites and poor dating control. Here we present a new compilation of pollen data from the region that improves on both the number of sites (63) and the quality of the chronological control. Data has been sourced from both public data archives and published (digitized) diagrams. Analysis is presented based on a standardized pollen taxonomy and sum, with maps shown for the major pollen taxa, biomes and total arboreal pollen, as well as quantitative reconstructions of forest cover and winter, summer and annual temperatures and precipitation. The reconstructions are based on the modern analogue technique (MAT) with a modern calibration dataset taken from the latest Eurasian Modern Pollen Database (~8000 samples). A site-by-site comparison of MAT and Inverse Modelling methods shows little or no significant difference between the methods for the LGM, indicating that no-modern-analogue and low CO2 conditions during the LGM do not appear to have had a major effect on MAT transfer function performance. Previous pollen-based climate reconstructions ~~based on~~ using modern pollen ~~analogues~~ calibration datasets show a much colder and drier climate for the LGM than both Inverse Modelling and climate model simulations, but our new results suggest much greater agreement. Differences between our latest MAT reconstruction and those in earlier studies can be largely attributed to bias in the small modern calibration dataset previously used. We also find that quantitative forest cover reconstructions show more forest than that previously suggested by biome reconstructions, but less forest than that suggested by simple percentage arboreal pollen, although uncertainties remain large. Overall, we find that LGM climatic cooling/drying was significantly greater in winter than in summer, but with large site to site variance that emphasizes the importance of topography and other local factors in controlling the climate and vegetation of the LGM.

1 Introduction

During the Last Glacial Maximum (LGM) ~21,000 years BP (Mix et al., 2001), the climate, vegetation and landscape of Europe and its surrounding regions were very different than today. Scandinavia and a large part of the British Isles were covered by a single ice sheet, with separate ice sheets covering the Alps and Pyrenees, while many smaller and lower mountainous areas were also glaciated (Ehlers et al. 2011). As a result of this global build-up of ice on land, sea levels were around 120 meters lower than today, resulting in the retreat of Atlantic and Mediterranean coastlines and the emergence on land of the English Channel and North Sea basin. Falling sea levels also led to the disconnection of the Black Sea from the Mediterranean, and a subsequent drop in Black Sea water levels as evaporation exceeded inflow (Arslanov et al. 2007). On land, permafrost and periglacial processes occurred immediately to the south of the Scandinavian ice sheet, while the massive discharge of glacial clays and sands provided material to be redeposited by the wind as belts of loess across northern France, Benelux, Germany and central Europe (Lehmkuhl et al. 2021). Under these cooler and drier climatic conditions, forests are thought to have retreated to the relative shelter of Southern Europe and the Mediterranean, while relatively unproductive steppe and tundra dominated the region north of the Alps (Grichuk 1992).

This traditional view of the LGM has been established for many years, but many details concerning the climate and vegetation of the LGM remain debated. Much of this debate concerns information derived from the pollen record, which represents one of the most widely available and spatially-resolved sources of information concerning LGM vegetation and climate, and the primary terrestrial proxy used to evaluate climate models in the Palaeoclimate Modelling~~-model~~ Inter-comparison Project (PMIP) (Bartlein et al., 2011; Harrison et al., 2014).

For example, climate model simulations continue to indicate a climate that is less cold and more humid than pollen-based reconstructions (Jost et al., 2005). These ~~pollen climate reconstructions~~results are similar to ~~those~~ reconstructions based on glaciological modelling (Allen et al., 2008b~~a~~). On the other hand, the pollen-based reconstructions that show the greatest disagreement with climate models have themselves been criticized for not considering the possible effect of low atmospheric CO2 on the physiological relationship between plants and climate (Ramstein et al., 2007). Methods that use modern pollen samples for calibration purposes are based on the assumption that the relationship between vegetation and climate remains the same through time, and that this is independent of change in CO2 concentration. Studies have shown however that plant growth processes and plant resilience are sensitive to CO2 concentration, and particularly water-use efficiency which would make plants more drought sensitive in low CO2 environments (Cowling & Sykes 1999). Atmospheric CO2 during the LGM was around 190 ppm, some 100 ppm lower than the pre-industrial period, and 200 ppm lower than the levels experienced in the last 50 years. Concerns about the effects of lower CO2 during the LGM has directly led to the development of pollen-climate reconstruction methods that can take account of CO2 effects, either through use of a process-based vegetation model run in inverse mode (Guiot et al. 2000, Guiot et al. 2009), or through the use of a correction algorithm (Prentice et al. 2017). Pollen-climate reconstructions based on inverse modelling that account for these low CO2 effects show less cooling and drying and consequently greater agreement with climate models (Ramstein et al., 2007; Wu et al., 2007).

Further data-model discrepancies have also been highlighted concerning LGM vegetation cover. Earlier pollen synthesis studies, especially those that applied the biomisation method (Elenga et al., 2000) give the impression that non-glaciated areas of LGM Europe were dominated by treeless steppe, while vegetation models driven by climate model simulations indicate large areas of forest and woodlands (Binney et al., 2017; Kaplan et al., 2016; Velasquez et al., 2021). The apparent data-model discrepancy associated with steppe has led to the suggestion that early humans, which are not included in vegetation models, could have reduced the forest cover with only a relatively moderate use of fire because of the cold climate and slow speed of vegetation recovery (Kaplan et al., 2016). This debate is important because of studies that have shown the sensitivity of the climate system to vegetation boundary conditions during the LGM (Ludwig et al., 2017; Velasquez et al., 2021). This suggests that accurate knowledge of the vegetation cover during the LGM is a necessary prerequisite to understanding the role of other influences on the climate system at this time.

More recent pollen and macrofossil studies from eastern Central Europe have shown that at least in this region there existed areas of open boreal forest and woodland with some temperate broadleaf species (Kuneš et al., 2008; Willis and Van Andel, 2004). The evidence of forest, and particularly elements of temperate broadleaf forest, north of the Alps has come to represent a challenge to the traditional view that forest species only survived the LGM in sheltered refugia far to the south of the Fenoscandian ice sheet and close to the moderating influence of the Mediterranean Sea. The presence of micro-refugia north of the Alps is important because it would represent a very different baseline for understanding the later rate and route of plant migrations under the rapid warming that occurred during the Late Glacial to Holocene transition (Douda et al., 2014; Giesecke, 2016; Krebs et al., 2019; Nolan et al., 2018), as well as understanding patterns of present-day genetic diversity (Normand et al., 2011; Svenning et al., 2008). Modelling studies have shown difficulty in supporting the very high rates of postglacial expansion that would be necessary for southern refugia (Feurdean et al., 2013, Nogués-Bravo et al. 2018).

Much of this debate has been informed by an increasing number of LGM pollen studies from an ever-broader geographical area, and especially from an increasing number of studies from north of the Alps. Nevertheless, the synthesis of these studies into a single narrative is made difficult by several factors, for instance: different taxonomic definitions, pollen percentages calculated from non-standardized pollen sums, and quantitative analyses such as climate reconstructions that are based on different training sets and methodologies. This has led to some modelling studies ignoring the pollen record completely, on the basis that data from the LGM is too scarce (Janská et al., 2017). Where standardized methods have been applied to multiple LGM pollen records, poor dating control has resulted in the inclusion of many records that may not actually be from the selected LGM time window. This is particularly important because the 21 ± 2.0 ka time slice commonly used to represent the LGM period in PMIP data-model comparisons and other synthesis studies (MARGO members, 2009; Bartlein et al., 2011) occurs immediately after the glacial maxima in the Alps~~, which occurs~~ around 26-23 ka (Heiri et al., 2014; Spötl et al., 2021) and ~~, and is therefore likely to be represented by a different vegetation and climate.~~ Heinrich stadial HS-2 (24.3-26.5), whilst also being closely followed by Heinrich stadial HS-1(15.6-18.0 ka) (Sanchez-Goñi & Harrison, 2010). These closely associated time periods can therefore be expected to represent both a different vegetation and climate than the LGM itself.

For example, of the 18 European pollen records used in the PMIP benchmarking dataset (Bartlein et al., 2011), 10 fall into the worst class ('poor') in the COHMAP chronological quality classification scheme if relative dating such as pollen correlation is excluded. More recent synthesis studies have also relied heavily on records from the European Pollen Database (EPD) which currently has 116 records with samples of LGM age (as of June 2022). Many of these records however are based on chronologies that are considered reliable for the Holocene (Giesecke et al., 2014), but have large uncertainties for the LGM as a result of 1) excessive extrapolation back in time from Holocene age dates, 2) the use of pollen correlation or other relative dating despite poorly defined regional biostratigraphy, or 3) the inappropriate use of radiocarbon dates contaminated with old carbon. We found that 104 of these 116 EPD records (Neotoma, 2021) fall into the worst class (‘poor’) in the COHMAP chronological quality classification.

Here we address these problems using a new synthesis of LGM pollen records from throughout Europe, the Mediterranean and the Middle East (EurMedMidEst) based on rigorous quality control criteria. Records were compiled from an extensive review of public databases and archives, and the scientific literature. Pollen records were selected according to the robustness of their chronological control around the PMIP LGM time-window (21 ± 2 ka), and combined into a single dataset based on a harmonized taxonomy and standardized pollen sum. The dataset was then analysed so that standardised maps could be produced to show the distribution of the major pollen taxa, biomes and total arboreal pollen at the LGM. In addition, quantitative reconstructions of forest cover as well as winter, summer and annual temperatures and precipitation were undertaken using the Modern Analogue Technique (MAT), utilizing the latest Eurasian Modern Pollen Database v2~~II~~ calibration dataset. These climate reconstructions are compared and evaluated against previous LGM pollen-climate reconstructions, as well as reconstructions based on other proxies. The dataset and results are fully documented and the complete data files are provided in the supplementary information.

2 Methods

2.1 Pollen Data

LGM fossil pollen data from Europe and bordering regions including North Africa and the Middle East were selected and collated into a single standardized project database. This data was sourced from the EPD/Neotoma database (Williams et al., 2021), the Pangaea data archive, publications in scientific journals, and from the original authors. We selected LGM pollen sites/data according to strict quality control criteria. Where possible, primary raw pollen counts were used where this was available. Where the original electronic data was not available, the data was digitized from the published diagram. Overall we have included~~, 35 out of~~ 63 records in our study, of which 35 were digitized and 28 consisted of the original ~~, while the rest of the data consisted of raw~~ pollen counts (Table 1).

The distribution of the 63 sites ~~included in our study~~ reflects the distribution of suitable archives, with fewer records available from climatically or environmentally challenging regions (Fig. 1). High rates of erosion and a drier and colder climate during the LGM reduced the number of suitable anoxic sediment sinks for pollen preservation, especially in Central Europe between the Scandinavian and Alpine ice sheets. Nevertheless, our dataset includes sites from this region, as well as North Africa and eastern Central Europe through to Iran, although most sites are located in an arc across eastern Spain, the Alps, and Italy. Lakes sites are the most numerous archive and tend to be located in the more sheltered and topographically favourable regions of Southern Europe and the Mediterranean. Peat is the next most important archive, followed by alluvial and colluvial sediments, as well as cave sites, the later also often being known for their archaeological significance. Sites located at the ice margins that appear to be under the ice reflect uncertainties in the location of the ice margin both in time and space during the LGM, as well as the fact that the selected time window for this study (21 ± 2 ka) is later than the maximum ice advance in some regions (Hughes and Gibbard, 2015). For completeness, we also include 7 marine records which have the advantage of more continuous deposition and often better dating over the LGM period, but which are prone to taphonomic biases compared to terrestrial records. These biases are discussed later in this section.

LGM pollen records were selected according to a number of quality control criteria, but primary amongst these was the existence of sufficient independent chronological control points to accurately identify samples that would fall within the 21 ± 2 ka BP time-slice of interest. We have used all of the samples within this time frame where the samples have been available in electronic form, else we have used the sample closest to the target time (21 ka BP). For records taken from the EPD we have used the latest Bayesian age-depth models where these were available (Giesecke et al., 2014), otherwise we have used the dates and chronology proposed by the original authors. We classified chronologies according to the COHMAP chronological quality scheme for the LGM period (Anderson et al., 1988; Yu and Harrison, 1995), which classifies record quality from 1-6 depending on whether a date falls within 2000 14C years (or less) of the time being assessed, or whether bracketing dates fall within 6000 and 8000 14C years (or less) about the time being assessed (Table~~.~~ A1~~2~~). Chronologies based on dates that fall outside of these limits fall into COHMAP class 7, and are regarded as 'poorly dated' with respect to the LGM. Importantly, we have only included radiometric and other absolute dates (such as varves) in this assessment, and have excluded dates based on correlation with regional pollen records. These pollen-based stratigraphic dates have been widely used in previous LGM studies, but do not include estimates of uncertainty and are generally regarded as unreliable at this time given the sparsity of well dated pollen sites and samples on which to base any correlation (Giesecke et al., 2014).

All records that were classified as poorly dated (COHMAP class 7) were subsequently excluded from our analysis. This has meant that many of the pollen records used in previous studies were excluded, including 16~~0~~ of the 26~~18~~ LGM records used by PMIP and associated studies in Europe (Bartlein et al., 2011; Elenga et al., 2000; Tarasov et al. 2000, Jost et al., 2005; Peyron et al., 1998; Wu et al., 2007; Cleator et al., 2020). We also excluded 104 of the 116 records in the EPD with samples that fall within our LGM time window. Many of these EPD pollen records have been used in more recent studies, although the exact record (EPD ~~site #~~Entity number) is often not stated. We estimate that we have excluded 16 of the 17 European sites used by Binney et al. (2017) (this study only included sites above latitude 40N), 5 of the 6 European sites used by Allen et al. (2010), 28 of the 33 sites used by Cao et al. (2019) and 27 of the 71 sites used by Kaplan et al. (2016).

Other quality control criteria were also used in the selection of LGM pollen records. Published pollen diagrams that only included a small part of the terrestrial pollen assemblage, or only presented summary taxa, were excluded. Records were also excluded where the dating information was incomplete, for instance where radiocarbon dating uncertainties were not published or where it was not possible to determine if the date shown was in calibrated or uncalibrated radiocarbon years.

The modern pollen data for the climate and tree cover reconstructions were sourced from the latest version 2 of the Eurasian Modern Pollen Database (Davis et al., 2020), which is managed as part of the EPD. The EMPD2 includes 8133 modern pollen samples from across the Palearctic biogeographic region from Europe to the far East of Asia. The taxa from both the fossil and modern pollen data were consolidated into 120 of the most commonly-occurring terrestrial taxa types. This taxa list was designed to be compatible with the biomisation scheme used in our study (Peyron et al., 1998; Tarasov et al., 2000) and that used in the Holocene mapping study of Brewer et al. (2017). The count of *Larix* was amplified by a factor of 10 due to its low pollen representation (Edwards et al. 2000, Bigelow et al. 2003, Tarasov et al. 1998, 2000, 2013, Binney et al., 2017).

2.2 Biomisation

We converted pollen assemblages to biomes based on the European biomisation scheme of Peyron et al (1998), which in turn is based on Prentice et al. (1996). The method is described in detail in Collins et al. (2012). We expanded the number of taxa included in the biomisation procedure proposed by Peyron et al (1998) to include taxa from the Northern Eurasian biomisation procedure of Tarasov et al. (1998). The inclusion of additional Northern Eurasian taxa reflects recent evidence that modern analogues of LGM vegetation occur in parts of Siberia (Magyari et al., 2014a). The biomisation procedure (Prentice et al. 1996) assigns each taxa to a plant functional type (PFT) and calculates a score for each of these PFT's based on the sum of the square root of the percentage of each of the taxa included in that PFT. To reduce the influence of long-distance transport, taxa below 0.5% are removed at the start of the procedure. Each biome is then assigned one or more PFT's and a score for each biome is calculated as the sum of the associated PFT scores. The biome with the highest score is then viewed as the dominant biome. Where the highest score is the same for more than one biome, the dominant biome is decided based on a hierarchy of unique PFT's. Peyron et al. (1998) also included a procedure for distinguishing warm and cold steppe biomes based on re-assigning certain steppe PFT's according to the presence or otherwise of PFT's indicative of cold or warm conditions. Following the Biome6000 project ~~(~~(Elenga et al., 2000) and Allen et al. (2010), we did not apply this additional procedure and present only the merged steppe biome. In summary, the biomisation procedure categorised 39 arboreal pollen taxa and 39 non-arboreal taxa into 22 plant functional types (PFT's), which were then combined into 12 biomes.

2.3 Quantitative climate reconstruction

We reconstructed climate from pollen data based on a standard Modern Analogue Technique (MAT) that used PFT scores to match fossil samples with modern calibration pollen samples (as used by Davis et al., 2003). This is a similar approach to that used by Peyron et al. (1998) and Jost et al. (2005) who also applied pollen PFT scores to reconstruct LGM climate from pollen data, but who used a neural network technique ~~which is a variant of the standard MAT~~ (Chevalier et al., 2020). PFT scores have been used in previous large-scale European pollen-based climate reconstructions for the Holocene (Davis et al., 2003; Mauri et al., 2014, 2015), where performance was found to be better than the conventional approach based on individual taxa (eg Marsicek et al., 2018). A particular advantage of the PFT approach for the LGM is that it can help overcome problems associated with vegetation (pollen) assemblages that may have no modern analogue (Davis et al. 2003). This can be a problem during the LGM when the climate and environment could be expected to be very different from today, and when many taxa formed unusual vegetation assemblages as a result of their forced retreat to sheltered refugia locations. The problem of modern analogues is also addressed in our reconstruction by using the latest EMPD2 modern pollen dataset for calibration purposes.

The EMPD2 provides a large number of potential modern analogues for many different LGM vegetation types and climates found today across the Palearctic region. PFT scores were calculated according to the methods outlined already in the Biomisation section, then normalized so that each sample was proportional to every other sample (Juggins and Birks, 2012).

The MAT method was applied using the Rioja program for R (Juggins, 2020). The modern calibration data was taken from the latest version 2 of the EMPD (as detailed earlier). The EMPD2 includes 8133 samples, which is considerably larger than the modern datasets used in previous LGM pollen-based reconstructions. For instance, Peyron et al. (1998) used a calibration dataset of 683 samples, which was updated by Jost et al (2005) to include an additional 185 samples. These datasets were also mainly taken from the steppes of Kazakstan and Mongolia, while the EMPD2 covers a much wider area, spanning most of the Eurasian Palearctic region (Davis et al., 2020). The size and distribution of the modern training set in climate and vegetation space is important because in order for the method to work effectively, it is necessary to have samples representative of the likely vegetation and climate space that could be occupied by the fossil assemblage (Turner et al. 2021, Chevalier et al., 2020; Salonen et al. 2012, Juggins, 2013).

A known problem with MAT is the role of spatial auto-correlation in providing unrealistically low estimates of uncertainty (Chevalier et al., 2020; Telford and Birks, 2009). This results from the fact that closely analogous modern pollen samples can also be located closely in physical space, and therefore in climate space. To reduce this problem it is possible to ~~systematically~~ exclude closely located ~~closely located modern samples from the analogue matching process, for instance, by excluding~~ samples from the analogue matching process ~~that fall within a certain spatial range~~using a filter based on a set distance (h-block filter) (Telford and Birks, 2009). While this approach can help, there are also three main problems associated with it. The first is error substitution, since removing samples also reduces the number of potential analogues, creating a different source of error that is not easy to categorise. Secondly, multiple samples taken from the same location are actually a strength of pollen training sets, since they are more likely to capture the full range of the assemblage diversity associated with a given climate. Thirdly, current methods that limit spatial range such as the h-block filter only do so on the horizontal axis, and do not consider the fact that samples can also be found at different elevations. In hilly or mountainous regions samples can therefore be excluded because they are closely located in horizontal space, but in fact they actually occupy very different climates and vegetation associations, contradicting the logical premise of the h-block filter. It was therefore decided not to apply this filter.

Uncertainties for the pollen-climate reconstructions were calculated using a standard method for MAT (Juggins 2020) based on the spread of the climates associated with the best modern pollen analogues used for each fossil sample. The closer the climates of the best modern pollen analogues (6 in the case of this study) then the smaller are the calculated uncertainties assigned to the reconstructed climate of the fossil pollen sample.

Climate reconstructions are presented as anomalies. These have been calculated with respect to modern climate (1970-2000 average) at each core site location using WorldClim 2 (Fick and Hijmans, 2017) (Table A2), which was also used to assign the modern climate for the modern pollen samples in the transfer function (Davis et al., 2020).

2.4 Quantitative tree cover reconstruction

It has long been recognized that the proportional representation of individual pollen taxa in a pollen assemblage does not necessarily reflect the proportion of land area covered by that taxa in the pollen source area surrounding the sample site (Davis 1963, Gaillard et al. 2010, Zanon et al. 2018). These differences can be caused by varations in pollen productivity, differential transport, deposition and preservation of pollen grains, and even the ease or otherwise of the identification of pollen grains themselves. This can make the interpretation of pollen taxa percentages difficult, even for relatively simple questions such as the proportion of forest to non-forest in the landscape.

There have been two main methods developed to account for this quantification problem, one using a physical modelling technique (PMT) based on estimates of pollen production for individual taxa (Gaillard et al., 2010), and the other using a MAT very similar to that used in pollen-climate reconstructions (Williams and Jackson, 2003). Both approaches have been widely applied during the Holocene in Europe (Zanon et al., 2018), but we know of no previous study that has applied either of these approaches to the LGM. The LGM presents a number of challenges, not least the problem of potential missing vegetation analogues, as well as low atmospheric CO2, which has been shown to influence pollen productivity (Leroy and Arpe, 2007).

Here we use the MAT to provide quantitative estimates of forest cover, following the approach of Zanon et al. (2018) who applied this method to the Holocene pollen record of Europe. We apply MAT in exactly the same way as for the climate reconstructions described earlier, including the use of PFT scores to match fossil and modern pollen samples. Instead of modern climate values, we assigned an estimate of modern forest cover to each of our modern pollen sites. To do this we use a high resolution (~100m) remote sensing dataset derived from satellite observations (Hansen et al., 2013). Zanon et al. (2018) have shown that the MAT calibrated in this way gives comparable results to the PMT approach in Europe, at least for the Holocene. One of the main differences however is that the PMT is designed to provide estimates of the proportions of different taxa, whereas the MAT (as applied here) is designed to provide estimates of the proportion of forest cover. Where the PMT can only reconstruct the proportion of forest forming trees, irrespective of their size, the MAT (following Zanon et al. 2018) is calibrated specifically to reconstruct forest composed of trees over 5m tall. This follows the FAO definition of forest as "land spanning more than 0.5 hectares with trees higher than 5 meters and a canopy cover of more than 10 percent, or trees able to reach these thresholds in situ" (FAO Terms and definitions 2020 http://www.fao.org/3/I8661EN/i8661en.pdf).

2.5 Maps

We present our results in the form of maps that include the main physiographic features of the LGM in the study area. The maps are based on the WGS84 projection. Coastlines reflect LGM sea level at 120m below present, while ice sheets are based on Ehlers et al. (2011). Modern national country boundaries are also included for reference.

2.6 Marine pollen records

We have included marine pollen records in our analysis for reasons explained below, but it is important that these records should be viewed with caution, particularly when used for biome and quantitative MAT reconstructions, and when compared with terrestrial records from different archives. Biomisation methods have been applied to individual marine pollen records (Combourieu Nebout et al., 2009), as well as multi-site synthesis studies such as the ACER project (ACER project members et al., 2017). However, marine records were specifically excluded from the Biome6000 project (Elenga et al., 2000). Similarly, quantitative climate methods have been applied to individual marine pollen records (Combourieu Nebout et al., 2009; Fletcher et al., 2010), as well as multi-site synthesis studies (Brewer et al., 2008). However, marine records have also been specifically excluded from other major pollen-climate studies (Cheddadi et al., 1996; Davis et al., 2003; Marsicek et al., 2018), as well as quantitative forest cover reconstructions (Zanon et al. 2018).

Discussion on the advantages and problems associated with marine records can be found elsewhere (Chevalier et al., 2020; Daniau et al., 2019), but are reviewed briefly here where relevant to the methodologies applied in this study. Marine sedimentary records provide continuous and well dated pollen records for the LGM that are often lacking from many terrestrial regions, especially in arid areas with few alternative anaeorobic sediment sinks. Conversely however, pollen source areas for marine sites may be many hundreds of kilometers from the coring site and may be liable to change through time in response to changes in distance to the coastline, rates of river discharge and ocean and atmospheric dynamics. This can theoretically give rise to changes in the vegetation shown in the pollen assemblage recorded at the marine site without any actual change in climate or other environmental pressure. The large and indeterminable source area of marine records also mean that it is difficult to apply quantitative MAT reconstruction methods, not least because the mean climate or forest cover of the source area is almost impossible to determine. In addition, the pollen record and the calibration dataset to which it is being compared are composed largely of terrestrial lakes and bog sites with much smaller and more homogeneous source areas. This creates a series of problems, the more obvious of which is the calculation of anomalies, since we cannot assume that the modern climate at the (marine) coring site location is representative of the (terrestrial) source area. In this study we have taken the closest point on land as the modern climate for the calculation of anomalies, but provide the absolute values for all sites so that these can be recalculated if necessary (Table A2). The next problem is that the large source area may capture a combination of different vegetation types that is not going to be represented in a calibration dataset based on samples from terrestrial sites with much smaller source areas, for instance a mixture of coastal and mountain vegetation, or even vegetation from different continents (Magri and Parra, 2002). However, in our analysis we did not find any sample from a marine record (or terrestrial record) that did not have a reasonable modern analogue in our training set (chord distance <0.3)(Huntley, 1990), even though we did not adjust the pollen assemblage for the over-representation of ~~*Pinus*~~*Pinus* in the marine pollen samples.

Typically, the Pine component is excluded from the terrestrial pollen sum when calculating percentages for marine pollen samples, and in some cases Pine has been excluded entirely from the samples used in marine pollen-climate reconstructions (Combourieu Nebout et al., 2009). The problem with excluding ~~Pinus~~Pinus is two-fold, the first is that ~~*Pinus*~~*Pinus* often represents the main forest forming tree in the Koeppen Csb climate zone on the Atlantic coast where many marine sites are located (García-Amorena et al., 2007), as well as representing the most abundant tree taxa in Europe during the LGM (Figure A3~~1~~c). Removing *Pinus* from the assemblage would almost certainly create an artificially arid assemblage in these circumstances, undermining the ability of the transfer function to reconstruct precipitation, although temperature would likely be less affected since *Pinus* is a generalist found in both hot and cold temperature regions. The second problem is that the remaining terrestrial taxa often constitute a very small number of pollen grains in a typical marine pollen sample (<100 grains), which can result in pollen assemblages that are not based on a statistically stable count of the pollen sample (Chevalier et al., 2020).

3. Results

3.1 Vegetation & Biomes

Results of the biomisation analysis shows that steppe (STEP) was the most common biome at the LGM across the study area, occurring at 36 out of 63 sites, indicating that the landscape was largely dominated by cool temperate grasslands across much of western Central Europe, central and eastern Mediterranean, as well as North Africa and the Middle East (Fig. 2). However, at the same time we also find that there were a significant number of sites where we find that woody and forest biomes occur, more particularly in southern and eastern Iberia, northern Italy and central eastern Europe. The most dominant of these forest and woody biomes are taiga (TAIG) in the north, and cool-mixed forest (COMX) and xerophytic woodlands (XERO) in the south.

As would be expected, the dominance of STEP biomes is generally reflected in low arboreal pollen percentages across the same areas/sites (Fig. 3 & 4). Exceptions to this rule can be found at marine sites such as ~~[site #3]~~[MD99-2331 site #3] and ~~[site #58]~~[MD01-2430 site #58] where STEP is reconstructed despite arboreal pollen percentages of 71 and 80 percent respectively. This apparent contradiction illustrates some of the idiosyncrasies of the biomisation method, especially when applying the method to marine pollen samples. In this case it is important to remember that the AP% is calculated from the sum of the percentages of each relevant taxa, but the score for each biome is the sum of the square root of the percentages of each of its constituent taxa. This results in biomes with taxa with large percentage values scoring proportionally smaller, and biomes with taxa with small percentage values scoring proportionally larger. For example, a single taxa at 50% has a square root of 7.07, but the sum of the square roots of 10 taxa each at 5% is 22.36 even though the sum of the percentages is the same 50%. This effect can be particularly pronounced in marine pollen samples because they are usually dominated by a single taxa (~~*Pinus*~~*Pinus*) that forms a high percentage of the total assemblage. Since there are often more non-arboreal taxa than arboreal taxa in a pollen assemblage, the non-arboreal taxa can dominate in the biomisation process even if collectively their percentage of the assemblage is a lot less than the arboreal taxa, resulting in a non-arboreal biome such as STEP having the highest biome score.

Of ~~The~~the main arboreal biomes, ~~found at the LGM include~~ Taiga (TAIG) is the dominant biome at 3 sites at the eastern end of the Alpine ice sheet, as well as at a site just to the north in northern Germany and a site in Slovakia, while Cool Conifer Forest (COCO) is found at 1 site close to the Scandinavian ice sheet in Lithuania. ~~,~~ Cool Mixed Forest (COMX) is found much more widely at 8 sites south of the Alps from south-west Iberia to Romania, with ~~, Cool Conifer Forest (COCO) and~~ Xerophytic Scrub (XERO) occurring at 8 sites with a similar distribution but not as far east or west. ~~, with just a single occurrence of~~ Cold Mixed Forest (CL~~O~~MX) occurs at just two sites in Georgia and the Alboran Sea at the far east and west of the study area, while~~and~~ Warm Mixed Forest (WAMX) is the dominant biome at just 1 site in Southern Spain. We do not record ~~any~~ Temperate Deciduous Forest (TEDE), Tundra (TUND) or Desert (DESE) as the dominant biome~~s~~ at any site at the LGM, although they do occur as sub-dominant biomes.

An alternative picture of LGM tree-cover is provided by the MAT reconstructions (Fig. 4~~5~~). MAT performance statistics for tree cover are shown in table 2~~3~~, based on an evaluation using the modern training set. This shows a relatively large root mean square error (RMSE) of 21.03. and an R2 of 0.52 that is not as good as for the MAT climate analysis, but overall the results are comparable with previous MAT tree cover studies (Zanon et al., 2018). In general, the MAT values (site average 34%) show forest-cover around 16% less than that suggested from AP% (site average 50%) (Fig. A1~~3~~), although sites with very low AP% also show higher values based on MAT. These differences are consistent with comparisons between MAT and AP% in Zanon et al (2018), although it should be noted that uncertainties related to the MAT reconstructions are large (± 23%). Zanon et al (2018) found that the differences between MAT and AP% were greatest over Northern Europe and in Arctic and sub-Arctic climate regions that are likely to be comparable to many areas of Europe during the LGM. These regions today are associated with tree-forming taxa such as Birch that fail to grow to a height of 5m or more, developing only as shrubs or krummholz forms.

Pollen taxa percentages are shown in supplementary figure A2~~6~~, and distribution maps of the 33 most common taxa are shown in the supplementary figures A3~~1~~a-f. Of the 21 arboreal taxa, *~~Pinus~~Pinus* generally has the highest values and is the most widespread, being present at all 63 sites. Other acicular arboreal taxa include *Juniperus*, which also has a wide distribution across EurMedMidEst although at lower values. The rest of the acicular arboreal taxa have more regional distributions. *Picea* is found mainly to the north of the study region, away from the Mediterranean, whilst Abies is generally found more to the south. *Larix* occurs only in the central European area including the northern edge of the Po plain just south of the Alps, whilst *Cedrus* is found mainly across south and west Europe in locations much further north than its Holocene and modern distribution which is confined mainly to Morocco and Lebanon (Collins et al., 2012). Temperate broadleaf arboreal taxa which also include cold-tolerant species such as *Betula* and *Salix* are relatively widely spread across the EurMedMidEst during the LGM, while less dought tolerant taxa such as *Alnus*, *Car~~ppinus~~inus* and *Corylus* are found more to the south-west through to the north-east. Other temperate broadleaf arboreal taxa such as *Quercus* (deciduous) and *Ulmus* have a much more southern distribution, with *Fraxinus*, *Olea*, and *Quercus* (evergreen) being more prevalent in the south-west. In contrast, *Fagus* occurs more to centre and the east, while *Tilia* is found even in more northern locations of central Europe. The remaining arboreal taxa are more shrubby and drought adapted, with *Ephedra* and particularly *Ephedra fragilis* having a southern distribution, whilst the more cold adapted *Hippophae* being found even in the north of central Europe (similar to *Tilia*).

The main non-arboreal taxa generally indicate cool, dry and environmentally disturbed conditions across much of the EurMedMidEst. The most widely distributed taxon is Poaceae, which like ~~Pinus~~Pinus, is found in all records. Other non-arboreal taxa with a widespread distribution include Rubiaceae, Apiaceae and Asteraceae (Asteroideae), while *Plantago*, Cayophyllaceae, Brassicaceae and Asteraceae (Cichorioideae) have a more southern and western distribution. *Thalictrum* can be found mostly at sites in the centre of the EurMedMidEst, along with *Helianthemum* which also extends to sites in the south-west. Other taxa such as *Chenopodiaceae* and *Artemisia* have a more southern distribution, reflecting their preference for drier and less cold climates.

3.2 Climate reconstruction evaluation

Evaluation of transfer function performance based on the modern training set is presented in table 2~~3~~. This shows that root mean square error predicted (RMSEP) values were smallest for summer temperatures (2.21C), and largest for winter temperature (3.35C), with mean annual temperatures in between (2.28C). The weaker performance for winter temperatures largely reflects the much greater range of winter temperatures in the training set. In turn, this contributes to a better R2 performance for winter temperatures (0.91) than annual temperatures (0.9) and summer temperatures (0.81). Overall R2 performance for precipitation is weaker than for temperature, which is typical because of the higher spatial variability of precipitation compared to temperature. Summer precipitation has the strongest R2 performance (0.75) compared to winter and annual precipitation (both 0.69), as well as smaller RMSE values (52mm) than winter (78mm).

Given the widespread occurrence of steppe during the LGM, we also undertook a separate evaluation of transfer function performance in this type of environment. For this we used a subset of 1588 pollen samples from the EMPD2 that are classified with the steppe pollen-biome (Davis et al. 2020). The results indicate (Figure A3) little difference in performance compared to the full dataset, with a small decrease in performance in annual and summer seasons in both precipitation and temperature, and a slight increase in performance in winter.

The~~se~~ results overall indicate good transfer function performance especially for temperature, and are comparable with those found in other continental scale pollen-climate studies (Bartlein et al., 2011). It is important to remember though that comparisons between studies can only be made with caution because results are often heavily dependent on the nature of the modern pollen dataset used as the training set, which is not the same in all studies (Juggins, 2013).

~~The evaluation of pollen-climate transfer function performance using the modern training set necessarily only indicates performance for the present-day climate and vegetation. We therefore undertook two additional tests of our MAT methodology to assess performance during the LGM. The first test was to compare our MAT results with previous pollen-climate reconstructions based on the same LGM sites but using different methods. These previous reconstructions include the neural-network methodology of Peyron et al. (1998) and Jost et al. (2005) which we call MAT-NN, as well as the Inverse Modelling approach by Wu et al. (2007) which we call INV.~~

~~We found 10 sites/records in our dataset which were also included in these earlier analysis (Fig. 7). All of the other sites used in these earlier studies were excluded from our study because of poor dating control. While these previous studies almost certainly shared the same pollen dataset, this dataset has never been placed in the public domain and no metadata provided other than the name of the site and the publication. In other words, it is not known if 1) the data represented a single sample or the mean of multiple samples within a time-window, 2) what the actual depth/age of those samples were or the actual sediment core in the case of multiple cores, 3) if the data was digitized or had a restricted taxa list (as was the case with the data from Huntley & Birks (1983), which is a likely source). While these aspects are unknown, it seems likely that the pollen data we used in our analysis was very similar if not identical in most cases, and in fact we found that the biomes reconstructed from our pollen dataset for these 10 sites are identical to the biomes reconstructed using the earlier pollen dataset (Elenga et al., 2000).~~

~~We compare our MAT with the MAT-NN and INV reconstructions in figure 7. On average across all 10 records, the MAT and INV methods give almost identical results for both anomalies of mean annual temperature (MAT -6.6C, INV -7.2C) and precipitation (MAT 158mm, INV 165mm). Uncertainties are also similar for both methods. In contrast, the MAT-NN method gives much cooler mean annual temperature anomalies (MAT-NN -13.9C) and drier precipitation anomalies (MAT-NN -474mm). On a site by site basis the MAT and INV methods show closer agreement for temperatures than precipitation, although precipitation has proportionally larger uncertainties. The reconstructions based on these two methods are close enough that the uncertainties overlap at all sites for both temperature and precipitation, except the precipitation reconstruction at Lac de Bouchet (site 25). The reason for this is not clear, but there could easily be differences with the pollen data analysed by Wu et al. (2007) in their INV reconstruction since the pollen record at Lac de Bouchet (Reille and de Beaulieu, 1988) includes multiple cores each with many different samples covering the LGM period.~~

~~The second evaluation of the MAT reconstruction method is based on comparison with a chironomid summer temperature record from Lago della Costa (site #34) in Northern Italy, analyzed by Samartin et al. (2016). We compare the chironomid record with our MAT reconstruction using pollen data that Samaratin et al (2016) also analysed from the same core. The results are presented in Fig. 8 and are shown as anomalies compared to the present day over our LGM time-window (19-23k BP). Our pollen-climate reconstruction is for JJA mean temperate, while the chironomid reconstruction is for July mean temperature, with the anomalies based on the modern equivalent JJA and July mean temperatures respectively. The average anomaly values for all 8 samples reconstructed by the pollen-climate MAT are -10.2 ± 3.5C, and for the chironomids -9.5 ± 3.0C. This indicates that pollen and chironomid average summer temperature reconstructions are almost identical taking into account the overlapping uncertainties, while also showing a strong similarity on a sample-by-sample basis throughout the time-series.~~

3.3 Climate reconstruction

Reconstructed LGM temperatures indicate an overall mean annual cooling of -7.2 ± 3.3C, with a greater cooling of around -9.3 ± 4.5C in winter and -5.0 ± 3.2C in summer (Fig. 5~~9~~). All sites apart from Lake Van [site #62] in eastern Turkey show cooler temperatures at the LGM compared to modern (Fig. ~~10~~6), and even at this site cooler conditions fall within the uncertainties. With greater cooling in winter compared to summer, the difference in temperature between winter and summer also increased (shown by positive anomalies) at most (but not all) sites (Fig. ~~10~~6). This increase in continentality was around +4.2C on average across all sites (Fig. ~~9~~5).

We reconstruct an overall decline in mean annual precipitation of around -91 ± 270mm (-13%) at the LGM. Most of this decline is in winter (-38 ± 90mm) (-21%), while in summer a small increase is shown (10 ± 57mm) (6%), although uncertainties are large (Fig. ~~11~~7). Compared to temperature there is significant seasonal and spatial variability in positive and negative precipitation anomalies (Fig. ~~12~~8). Positive anomalies appear more predominant in eastern and southern Spain and in central eastern Europe in both summer and winter, while positive anomalies are found more generally in summer across sites in Southern Europe and the Mediterranean. These more positive summer anomalies also reflect a relative shift from winter to summer in the seasonality of precipitation in this region.

4.0 Discussion

Before we consider the results of our analysis it is important to provide some context in terms of European LGM geography and environment, which was very different from today (Fig. 1). Major ice sheets covered Scandinavia and much of the UK, the Alps, and the Pyrenees. Sea level was 120m lower, resulting in much of the North Sea and English Channel becoming dry land, and the European coastline extending over 100 km out into the Atlantic and Mediterranean, especially around the Bay of Biscay and Adriatic. The Black Sea was no longer connected to the Mediterranean, and was smaller with a water level around 100m lower than today (Genov, 2016). These changes in sea or water level had two main consequences, the first being that the marine sites were closer to land, and therefore closer to (low lying) terrestrial vegetation and (pollen carrying) river discharge points than they are today. The second consequence of lower seas levels is that terrestrial pollen sites were located further from the moderating effect of the ocean than they are today, resulting in a localised modification of the climate experienced by the site irrespective of regional or global changes (Geiger, 1960).

The maps used in our analysis shows the maximum ice sheet at 21k ± 2k (Ehlers et al., 2011). The precise geographical location of the ice sheet is difficult to resolve at a fine spatial scale, however, which explains why some sites close to the ice margin appear to be actually located under the ice (for example sites Kersdorf-Briesen site #46 & Mickunai site #54). The resolution of the map also shows the occurrence of permanent ice not only to the north and over the Alps, but also on many subsidiary areas of high ground across central and southern Europe, including areas such as the Pyrenees, Massif Central, Vosges and Carpathian Mountains. While global ice volume may have peaked ~21 ka individual ice sheets in Europe and other areas are known to have reached their maximum extent at different times (Hughes et al., 2016). The larger ice sheets are likely to have had a significant influence on regional climate and environmental conditions across Europe, but the smaller ice sheets had similar if more localized impacts as well. Surrounding each ice sheet would have been an unglaciated area of active peri-glacial processes and newly created and unstable ground. This would include outwash plains, impounded lakes and recently drained lake beds, seasonally and sporadically flooded areas, moraines, kettle holes and other glaciological and peri-glacial features. Soils in these areas would be non-existent or skeletal, and vegetation would find it difficult to obtain nutrients and water for survival, irrespective of the prevailing climatic conditions. Outside of these areas, permafrost is also likely to have been present, particularly north of the Alps (Vandenberghe et al., 2014), which would also act as an impediment to vegetation growth.

In terms of regional climate, the major ice sheets would have provided significant barriers to westerly atmospheric circulation, or even north-south circulation in the case of the Alps and Pyrenees. As well as representing a physical obstruction, the thermodynamic response of the atmosphere to these high, cold obstructions would have been to encourage the formation of areas of semi-permanent high pressure, similar to those found today for instance over the Greenland ice sheet. In addition, the Laurentide ice sheet located over North America would have generated downstream effects over Europe (COHMAP, 1988). These physical and thermodynamic effects would have affected the direction of storm tracks, as well as more local climatic effects commonly associated with ice sheets such as strong katabatic winds (Kageyama,et al. 2021, Velasquez et al. 2021, Luetscher et al. 2015, Lefort et al. 2019)

4.1 Vegetation Cover

The nature and extent of forest cover during the LGM remains a matter of considerable debate. Vegetation models driven by LGM climate model simulations generally indicate extensive areas of boreal forest north of the Alps, and a mix of temperate and warm-temperate woodland to the south across southern Europe and much of the Mediterranean. Treeless areas such as steppe are mainly confined to those areas where it is also found today, namely inland Iberia, Ukraine, southern Russia and Turkey, while Tundra is found to the north close to the Scandinavian Ice Sheet (Allen et al., 2010; Cao et al., 2019; Prentice et al., 2011; Velasquez et al., 2021).

Evaluation of these vegetation-model simulations against data has been largely based on comparison with compilations of pollen-biome reconstructions (Prentice et al., 2011; Allen et al., 2010; Cao et al., 2019; Velasquez et al., 2021). Early studies were based on only a limited number of sites from southern Europe, and showed steppe at all sites in contradiction with model simulations (Elenga et al. 2000). More recent pollen compilations have included more sites especially to the north that have revealed a more mixed picture of vegetation cover, with forest biomes at some sites both south and north of the Alps that appear more consistent with model simulations (Binney et al., 2017; Cao et al., 2019). However, many of these pollen sites used in these studies were assigned an LGM age based on poor or incorrect dating control, and likely date to MIS3, the Late-Glacial or even the Holocene. Nevertheless, based on our compilation of more securely dated LGM pollen sites, we also show a wider distribution of forest biomes particularly in Iberia, northern Italy and Central Europe, although with greater areas of steppe than suggested by the models over the remaining regions.

However, the interpretation of biome reconstructions requires care since the forest cover and vegetation composition may not be as clear as the dominant biome suggests. For instance, we find that steppe is still reconstructed as the dominant biome at some sites despite arboreal pollen forming 70-80% of the pollen assemblage. In addition, it is important to remember that pollen-biomes are based only on the proportion of taxa that can form forest and woodland, while these taxa may in fact exist only as shrubs or stunted krummholz forms in the challenging climate and environment of the LGM. Alternatively, similar conditions may favour low-lying non-arboreal taxa forms with poor pollen dispersion or even insect pollinated taxa forms that may be poorly represented in the pollen assemblage, giving greater prominence to arboreal taxa whose pollen may be the result of long-distance transport particularly *Pinus*. However there also appear to be plenty of samples with low or even very low (<20%) arboreal percentages, so not all sites in open areas may be affected by long-distance transport of *Pinus* in the same way.

Quantitative MAT based reconstructions of forest cover can overcome some of these problems where they can be detected based on the composition of the pollen assemblage when compared with the modern land-cover. Chord-distance measurements of the match between fossil and modern pollen assemblages indicate good LGM analogues exist in our large Eurasian modern pollen dataset. The results of the MAT forest cover reconstruction indicates that forest cover was low but not entirely devoid of woodland in most areas, similar to the modern boreal forests of Siberia and consistent with a steppe-tundra-woodland mosaic proposed by many authors (e.g. Birks and Willis, 2008; Willis and Van Andel, 2004). This is confirmed in an analysis of the most commonly found modern analogue ecoregions for LGM pollen samples at each site (Table A4). Uncertainties are large, but for comparison the MAT site-average of 33% forest cover is slightly less than the average today over the Boreal region of Europe (43%) and slightly more than the average today over Mediterranean region (27%) (Zanon et al. 2018).

By calculating the percentage of each of the taxa in each LGM pollen sample using a standardized pollen sum, we are able to make direct comparisons between different LGM pollen records and their taxa percentages (Figure A2, ~~Figure 6,~~ A3~~1~~). The results show a preponderance of boreal forest taxa to the north of the Alps, consistent with biome results mentioned earlier. ~~*Pinus*~~*Pinus* is the most common forest forming taxa in this boreal zone, together with *Picea*, and including *Larix* to the east and *Abies* to the west. The occurrence of *Betula* and *Juniperus* also suggests shrubby elements consistent with arctic shrub-tundra, although high Poaceae and other herbaceous taxa such as *Artemisia* and *Chenopodiaceae* indicate more steppe than tundra. Other deciduous taxa found north of the Alps include cold tolerant generalists such as *Corylus* and *Alnus*, as well as low percentages of relatively thermophilous taxa in the east, such as *Carp~~pinus~~inus* and *Tilia*.

These results are consistent with charcoal (Magyari et al., 2014a; Willis and Van Andel, 2004), malacological (Juřičková et al., 2014), biomarkers (Zech et al., 2010) and genetic evidence (Stivrins et al., 2016; Willis and Van Andel, 2004) that the main forest region north of the Alps was in the eastern region of Central Europe around the Carpathian basin. This was also an area where cold and moisture sensitive deciduous taxa were also able to survive (Magyari et al., 2014), although evidence of temperate taxa found in the pollen record has yet to be supported by charcoal and macrofossil records (Feurdean et al., 2014). Our pollen evidence indicates an open taiga or cool mixed forest that extended in central and eastern Europe to areas close to the Scandinavian and Alpine ice caps, as proposed by Willis and Van Andel (2004) and Huntley and Allen (2003), although whether this represents isolated pockets of forest or an extended open steppe-forest is difficult to determine (Kuneš et al., 2008). Even steppe or tundra areas in western Europe show a low but significant presence of the pollen of tree taxa at sites close to the ice sheets that are unlikely to be solely the result of long distance transport or reworking (Kelly et al., 2010). The presence of woodland in these areas is also supported by mammalian remains, for instance at Kents Cavern in SW England (Stewart and Lister, 2001).

Overall however, our results clearly show a much greater predominance of thermophilious and moisture sensitive deciduous taxa south of the Alps, particularly in Iberia and Northern Italy, where temperate broadleaf forests survived in sheltered refugia (Kaltenrieder et al., 2009). Most of these appear to be in hilly areas with the ability to generate orographic rainfall (Monegato et al., 2015), on south facing slopes to make the most of the sun's radiant energy and located above the valley floor to escape frost and flooding. We might also expect these areas to be sheltered from cold northerly winds, and benefit from relatively mild and moisture laden winds coming from the Mediterranean Sea. For instance, the presence of woodland and low glacier altitudes along the southern slopes of the Alps around the Po Valley and Trentino region is consistent with strong orographic rains generated by southerly and easterly winds that today can be generated by low pressure located south of the Alps in the Gulf of Genoa, and consistent with a southerly storm track around the Alps (Kehrwald et al., 2010; Luetscher et al., 2015). Generally, as might be expected, areas of forest reconstruct similar or increased precipitation compared to today, and areas of steppe indicate deceased precipitation (see next section).

Independent evidence of LGM vegetation is provided by archaeozoological data. This data supports the palynological evidence for the existence of forest and woodland refugia across the ice-free areas of Europe at latitudes north of the Alps. For instance, large vertebrates in these areas show patterns of extirpation and extinction in response to shifts in climate and vegetation cover that is different for different species, indicating a variety of environments and niches (Lister and Stuart, 2008; Stewart and Lister, 2001). As with the pollen record, the presence of temperate adapted large vertebrate taxa within the glacial landscape of Western Europe also suggests the existence of temperate “micro-refugia” (Stewart and Lister, 2001) , consistent with suggestions that temperate arboreal taxa were not entirely extirpated from the region during the LGM (Magri, 2010). Further east, mammal assemblages indicate generalized loss of forest components in the East European Plain (Demay et al. 2021, Puzachenko et al., 2021) which is consistent with our data indicating low forest cover in this region. In other areas, evidence of the prevailing land cover at the LGM comes from studies of small vertebrate communities, which have a closer affinity to the prevailing environment than large vertebrates (López-García and Blain, 2020) that have the propensity to migrate large distances, often on a seasonal basis. These studies of small vertebrate assemblages also support the existence of temperate “micro-refugia” in France (Royer et al., 2016) and the existence of woodland components in many regions across Southern Europe including parts of Iberia (Bañuls-Cardona et al., 2014) Italy (Berto et al., 2019) and the Balkan Peninsula (Mauch Lenardić et al., 2018).

Other paleobotanical evidence also supports our land cover reconstruction. Schafer et al. (2016) suggest leaf wax patterns from palaeosols in Spain may indicate the presence of drought intolerant deciduous trees and more humid conditions during the LGM. Significantly, none of the pollen sites indicate that temperate broadleaf forests were dominant, and broadleaf temperate taxa always appear part of a mixed woodland together with cold or aridity adapted evergreen and needleaf taxa, including typical Mediterranean taxa. This type of mixed vegetation probably extended to the Balkans where the hilly terrain and proximity to the Mediterranean would appear to have provided favourable climatic conditions, although we still lack LGM sites from this region. At sites in central and southern Italy and east through Greece and Turkey to the Middle East (and including North Africa), the vegetation appears drier with a greater prevalence of steppe. Only a site in Georgia at the edge of~~in~~ the Caucasian mountains indicates the presence of significant amounts of forest (mainly ~~*Pinus*~~*Pinus*), a result that was also found by Tarasov et al. (2000), and probably linked to favourable orographic precipitation and proximity to the Black Sea.

Comparison with LGM land cover from vegetation modelling studies driven by climate model simulations indicate a much wider presence of forest than that shown by the pollen data (Kaplan et al., 2016). Data-model agreement appears to be closest over eastern-central Europe where pollen indicates the presence of open Boreal forest, and over south-west Europe with the presence of cool mixed temperate forest, including broadleaf deciduous and thermophilious elements (Prentice et al., 2011; Allen et al., 2010; Cao et al., 2019; Velasquez et al., 2021). Nevertheless, agreement still appears to be weak over western-central Europe and Southern and Eastern Europe through to the Middle East, where pollen data continues to indicate widespread steppe. One proposed explanation for this data-model discrepancy has been the role of fire (including man-made fire) in maintaining forest openness, a factor influencing forest cover that is not included in most vegetation models (Kaplan et al., 2016). In the Carpathian basin Magyari et al. (2014a) noted that charcoal increased as forest cover declined, suggesting that wildfires played a role in decreasing forest cover during the LGM. Other studies have noted low levels of charcoal and therefore fires during the LGM, although these tend to be from steppe areas with low biomass and fuel availability (Connor et al., 2013; Kaltenrieder et al., 2009). Recent LGM vegetation simulations that include fire indicate much lower values of forest cover than those without fire over western central Europe, while forest remains in central eastern Europe (see figure 6 in Velasquez et al., 2021). This appears closer to the data, but the values are perhaps too low compared with our MAT reconstructions here (Figure 45).

4.2 Climate: Temperature

4.21 Comparison with previous pollen-based reconstructions

The climate of the LGM is generally considered to have been cooler and drier than today, but data-model comparisons continue to highlight important discrepancies, not only in the degree of cooling and drying but also in their seasonal and spatial distribution. Data-model comparisons over Europe have mainly used quantitative pollen-based climate reconstructions, especially the Palaeeoclimate- Mmodelling Intercomparison Project (PMIP/CMIP) (Kageyama et al., 2021, Bartlein et al., 2011; Harrison et al., 2015; Kageyama et al., 2006). These pollen reconstructions use many of the same compilations of LGM pollen data used in the biome reconstructions mentioned earlier (Elenga et al., 2000), and therefore suffer from the same problems of dating control, unclear provenance and a potentially limited taxa assemblages.The most commonly used reconstructions have been based on two main methods, a neural-network methodology (ANN) of Peyron et al. (1998) and Jost et al. (2005), and an Inverse Modelling approach (INV) applied by Wu et al. (2007). The ANN method uses modern pollen samples for calibration and does not include any correction for CO_2 effects, being similar in these respects with the MAT method used in this study. In contrast the INV method does not use modern pollen samples for calibration, but instead uses a process-based vegetation model run in inverse mode. Ordinarily, a vegetation model will use climate as an input to generate a vegetation as an output, but in inverse mode the model is reconfigured to generate climate as an output given a particular vegetation (pollen) assemblage as an input. One of the advantages of the INV method is that CO_2 can also be varied as an input, and therefore the effect of changes in CO_2 on the vegetation, and therefore reconstructed climate, can be investigated. Comparison of these ANN and INV reconstructions have shown important differences, with the INV reconstruction generally not as cold and somewhat drier than ANN (Wu et al. 2007). These differences between pollen-climate methods have often been attributed to CO_2 effects (Wu et al. 2007) but this is not clear since there may be other factors, such as the size and location of the training set used in the ANN reconstruction.

We identified 10 LGM pollen records where we could directly compare our MAT-based pollen-climate reconstruction with previous pollen-climate reconstructions based on Inverse Modelling (INV) (Wu et al., 2007), and the Neural Networks method which is a version of MAT (MAT-NN) (Peyron et al., 1998a). This comparison showed that our MAT reconstructions were very similar to the INV method, but not as cold or dry as the MAT-NN method. This has two main implications. The first is that our reconstructions indicate greater agreement with the results of climate model simulations since climate models indicate temperatures closer to the INV reconstructions (Latombe et al., 2018) than the MAT-NN reconstructions (Jost et al., 2005; Kageyama et al., 2006). The difference between our MAT and the MAT-NN reconstructions is likely the result of the modern calibration datasets used, since the MAT-NN reconstruction by Peyron et al. (1998a) was based on a considerably smaller number of samples taken mainly from the cold dry steppes of Kazakstan and

~~Mongolia. The second implication is that the MAT method may not be significantly impacted by the effects of lower CO_2 (Cowling and Sykes, 1999; Prentice and Harrison, 2009; Williams et al., 2000) or indeed insolation changes during the LGM, since the MAT results are similar to those based on the INV method which specifically takes account of these non-climatic factors (Wu et al., 2007). This would also suggest that MAT could also work well for pollen-based climate reconstructions on longer glacial-interglacial timescales where insolation and CO_2 vary significantly from their modern values.~~
We make a comparison with these earlier reconstructions based on 10 sites/records in our dataset which we identified as also being included in these earlier studies (Fig. 9). While we were able to identify the site and data source, as well as the time window, we were unable to establish if the the data represented a single sample or the mean of multiple samples within a time-window or the exact depth of those samples, or the actual sediment core in the case of multiple cores from the same site. While these aspects are unknown, it seems likely that the pollen data we used in our analysis was very similar if not identical in most cases, and reconstructed biomes for these sites from our pollen dataset are identical to the biomes reconstructed using the earlier pollen dataset (Elenga et al., 2000).

We compare our MAT with the ANN and INV reconstructions in figure 9. On average across all 10 records, the MAT and INV methods give almost identical results for both anomalies of mean annual temperature (MAT -6.6C, INV -7.2C) and precipitation (MAT 158mm, INV 165mm). Uncertainties are also similar for both methods. In contrast, the ANN method gives much cooler mean annual temperature anomalies (ANN -13.9C) and drier precipitation anomalies (ANN -474mm). On a site by site basis the MAT and INV methods show closer agreement for temperatures than precipitation, although precipitation has proportionally larger uncertainties. The reconstructions based on these two methods are close enough that the uncertainties overlap at all sites for both temperature and precipitation, except the precipitation reconstruction at Lac de Bouchet (site #25). The reason for this is not clear, but there could easily be minor differences with the pollen data analysed by Wu et al. (2007) in their INV reconstruction since the pollen record (Reille and de Beaulieu, 1988) includes multiple cores each with many different samples covering the LGM period.

This comparison shows that our MAT reconstructions are very similar to the INV method, but not as cold or dry as the ANN method. This has two main implications. The first is that our reconstructions indicate greater agreement with the results of climate model simulations since climate models indicate temperatures closer to the INV reconstructions (Latombe et al., 2018) than the ANN reconstructions (Jost et al., 2005; Kageyama et al., 2006). The difference between our MAT and earlier ANN reconstructions is likely the result of the modern calibration datasets used, since the ANN reconstruction was based on a considerably smaller number of samples taken mainly from the cold dry steppes of Kazakstan and Mongolia.

The second implication is that the MAT method may not be significantly impacted by the effects of lower CO_2 (Cowling and Sykes, 1999; Prentice and Harrison, 2009; Williams et al., 2000) or indeed insolation changes during the LGM, since the MAT results are similar to those based on the INV method which specifically takes account of these non-climatic factors (Wu et al., 2007). This would suggest that MAT could also work well for pollen-based climate reconstructions on longer glacial-interglacial timescales where insolation and CO_2 vary significantly from their modern values. This is consistent with the findings of Pini et al. (2021) who applied a correction algorithm developed by Prentice et al. (2017) and Cleator et al. (2020) to a MAT reconstruction of mean annual precipitation at Lake Fimon in Northern Italy. This shows a very small correction of 0mm to 30mm for samples across the LGM time-window, which indicates that CO_2 is not a very significant factor in influencing this type of reconstruction, at least compared to the overall uncertainties (+/- 200mm) of the reconstruction itself. The uncertainties associated with the correction algorithm are not discussed, but given that inputs include estimates of both LGM temperature and cloud cover, it seems likely that these could be significant. Importantly, both Pini et al (2021) and Cleator et al (2020) specifically exclude the necessity of applying a correction algorithm to temperature reconstructions, since they consider only hydrological variables to be affected by changes in atmospheric CO_2.

4.22 Comparison with climate reconstructions based on other proxies

4.221 Temperature

Proxies that are not based on plants should remain unaffected by the CO_2 problem during the LGM, and provide an alternative basis for evaluating pollen-based reconstructions. Samartin et al. (2016) reconstructed LGM summer temperatures based on chironomid remains from Lago della Costa (site #34) in Northern Italy. They also undertook pollen analysis on the same samples down the core, allowing us to make a sample-by-sample comparison between the chironomid temperature record and our MAT reconstruction (Fig. 10). Our pollen-climate reconstruction is for JJA mean temperate, while the chironomid reconstruction is for July mean temperature, with the anomalies based on the modern equivalent JJA and July mean temperatures respectively. The average anomaly values for all 8 samples reconstructed by the pollen-climate MAT are -10.2 ± 3.5C, and for the chironomids -9.5 ± 3.0C. This indicates that pollen and chironomid average summer temperature reconstructions are very similar on average, taking into account the overlapping uncertainties, while also showing a strong similarity on a sample-by-sample basis throughout the time-series.

Other reconstructions based on other proxies provide a basis for more general regional comparisons (Figure A4, A5). ~~Comparison with LGM climate reconstructions based on other (non-pollen) proxies provides another way of evaluating our pollen-based reconstruction.~~ We reconstruct both summer and winter temperatures and show that cooling in winter was greater than in summer at most sites, associated with an increase in continentality (increased temperature difference between summer and winter). A similar seasonal pattern of temperature change has also been shown in other studies that reconstruct both summer and winter LGM temperatures, including Prud'homme et al. (2016) using d18O analysis of earthworm calcite granules at Nussloch near the French-German border, Bañuls-Cardona et al. (2014) using faunal remains of small mammals at 4 locations in western Spain, and Ferguson et al. (2011) who examined seasonal temperature change using d18O and Mg/Ca analysis of limpet shells at Gibraltar in southern Spain. The increase in continentality at Nussloch (Prud'homme et al., 2016) was reconstructed at between 11.6 to 15.6 ºC, comparable at the lower end with nearby pollen sites ~~[site #28]~~[La Grotte Walou site #28] 10.4 ± 5.8 ºC and ~~[site #29]~~[Bergsee site #29] 7.9 ± 5.7 ºC. The faunal sites in western Spain studied by Bañuls-Cardona et al. (2014) gave much reduced increases in continentality, but nevertheless similar to nearby pollen sites. For instance at Valdavara 5.1 ºC ~~[site #3]~~[MD99-2331 site #3] 5.2± 3.1 ºC , El Miron 1.2 ºC ~~[site #19]~~[Tourbiere de l'Estarres site #19] 5.1 ± 6.2 ºC, El Portalon 0.9C ~~[site #16]~~[Torrecilla de Valmadrid site #16] 2.8 ± 1.8 ºC and Cueva de Maltrvieso 6.1C ~~[site #2]~~[SU81-18 site #2] 4.8 ± 3.4 ºC. Further south at Gibraltar the limpet-based study of Ferguson et al. (2011) also shows a relatively small increase of 2 ºC. The nearest pollen site ~~[site #5]~~[Gorham Cave site #5] however shows a larger increase of 4.7

± 2.3 ºC, although differences could be expected given the different temporal resolution of annual laminae on mollusk shells compared to pollen assemblages that reflecting much slower changes in trees and other long-lived flora.

Summer temperatures were warm enough during the LGM over the Alpine areas that Swiss lakes were largely ice free in summer, while glacier ELA's around the time of the LGM suggest summers were -6.5 to -7.7 ºC cooler compared to the LIA (Heiri et al., 2014). This cooling was similar to that found at Nussloch some 200km north of the Swiss border by Prud'homme et al. (2016), who reconstructed anomalies of -6 to -8 ± 4 ºC from d18O analysis of earthworm calcite granules (representing warm season May-September temperatures). Slightly less cooling was found close by at the nearby site of Achenheim where analysis of Mollusc assemblages gave summer (August) cooling estimates of -3.5 to -6.5 ºC based on MAT (Rousseau, 1991), and -5.5 to -9.5 ºC based on the Mutual Climatic Range method (Moine et al., 2002). These reconstructions appear somewhat cooler than nearby pollen sites ~~[site #28]~~[La Grotte Walou site #28] -1.4 ± 3.6 ºC and ~~[site #29]~~[Bergsee site #29] -2.7 ± 5.1 ºC, although comparable with the pollen site ~~[site #32]~~[Pilsensee site #32] -7.3 ± 5.0 ºC 200 km further east. Similar differences also occur at the site of Les Echets on the western edge of the Alps where a d~~D~~iatom based reconstruction of summer (July) temperatures (Ampel et al., 2010) indicated a greater cooling (-10.5 to -11.5 ºC) than our pollen reconstruction ~~[site #27]~~[Les Echets G site #27] (-4 ± 2.7 ºC). However, the authors caution that the results were based on poor analogues and rare taxa, as well as a small training set of only 90 lakes in Switzerland.

South of the Alps, other proxies show the opposite relationship with the pollen reconstructions. For instance, at Lago dela Costa in the Po valley, a summer (July) temperature chironomid reconstruction by Samartin et al. (2016) is around 1-2 ºC less cool than the pollen reconstruction (JJA) for the same site ~~[site #34]~~[Lago della Costa site #34] -11.4 ± 2.7C, although both reconstructions fall within their respective uncertainty ranges (Figure 8). In the Pindus Mountains in Greece, Hughes et al. (~~Hughes et al.,~~ 2006) estimated LGM summer temperature anomalies of - 7 ºC based on glacier modelling, which is comparable with that reconstructed at the nearest pollen site ~~[site #51]~~[Ioannina site #51] -7.7 ± 2.8 ºC. In Spain the analysis of small mammal remains by Bañuls-Cardona et al. (2014) shows similarly less cooling in summer or even warmer than present positive anomalies compared to the nearest pollen sites, such as Valdavara 1.4 ºC ~~[site #3]~~[MD99-2331 site #3] -2.3 ± 2.8 ºC , El Miron -2.3 ºC ~~[site #19]~~[Tourbiere de l'Estarres site #19] -5.7 ± 5.4 C, El Portalon 0.8 ºC ~~[site #16]~~[Torrecilla de Valmadrid site #16] -2.6 ± 1.1 ºC and Cueva de Maltrvieso -1.1C ~~[site #2]~~[SU81-18 site #2] -10.4± 2.8 ºC. Further south at Gibraltar, the limpet-based study of Ferguson et al. (2012) suggests an anomaly of around -7 ºC, which is a greater cooling than the pollen reconstruction from this location ~~[site #5]~~[Gorham Cave site #5] -1.3 ± 2.2 ºC, although comparable with other pollen sites slightly further east.

Winter temperature reconstructions from non-pollen proxies show a similar pattern in relation to pollen reconstructions as for summer temperatures. North of the Alps at Achenheim, Prud'homme et al. (2016) use d18O on earthworm remains to reconstruct particularly cold winter anomalies of -17.6 to -23.6 ºC compared to nearby pollen sites ~~[site #28]~~[La Grotte Walou site #28] -11.8 ± 8.0 ºC and ~~[site #29]~~[Bergsee site #29] -10.6 ± 6.3 ºC. South of the Alps in Spain, the analysis by Bañuls-Cardona et al (2014) based on the remains of small mammals shows less cooling in winter compared to the nearest pollen sites, in particular Valdavara -3.7 ºC ~~[site #3]~~[MD99-2331 site #3] -7.5 ± 3.4 ºC , El Miron -3.5 ºC ~~[site #19]~~[Tourbiere de l'Estarres site #19] -10.8 ± 7.0 ºC, El Portalon -0.1 ºC ~~[site #16]~~[Torrecilla de Valmadrid #16] -5.4 ± 2.5 ºC and Cueva de Maltrvieso -7.2C [site #2][SU81-18 site #2] -15.2 ± 4.0 ºC. And again, in southern Spain at Gibralter, analysis of limpet shells by Ferguson et al (2011) suggests winter cooling of around -9 ºC while the pollen reconstruction suggests [site #5][Gorham Cave site #5] -6.0 ± 2.5 ºC, although sites further east indicate cooler conditions.

A number of additional proxies have also been used to reconstruct LGM mean annual temperature. Heyman et al. (2013) applied glacier mass balance modelling at sites located in the smaller mountain regions north of the Alps. These are generally slightly cooler than our pollen-based reconstructions at sites close to the Vosge Mountains -12.7 ± 2.0 ºC and Black Forest -11.4± 2.3 ºC [site #29][Bergsee site #29] -8.2 ± 3.3 ºC, Bavarian Forest -10.7± 2.2 [site #32][Pilsensee site #32] -9.2 ± 1.2 ºC and Giant Mountains -8.5 ± 1.8 [site #46][Kersdorf-Briesen site #46] -7.3 ± 0.3 ºC. These values obtained by Heyman et al. (2013) are warmer than Pud'homme et al. (2016) who estimated annual mean temperature anomalies of -15.1 to -19.1 ºC based on d18O of earthworm calcite at the Nussloch site just north of the Vosge and Black Forest. The annual temperatures reconstructed by Heyman et al. (2013) are also around 2C warmer than Allen et al. (2008) who applied a similar, although simpler method to over 29 different mountainous regions across Europe that had been glaciated during the LGM. Since glacier mass balance is a function of both snowfall and temperature, these estimated temperatures vary according to estimated changes in precipitation. For instance, mean annual temperature estimates by Allen et al. (2008a) are much cooler than reconstructed by pollen, with an average anomaly of -13.2 ºC for the 29 sites assuming a 40% reduction in precipitation, but this is reduced to -11.8 ºC assuming the same precipitation as modern. This compares with -7.2 ºC for our 63 pollen sites. The glacier mass balance modelling by Allen et al. (2008a) assumes a seasonal distribution of precipitation that is similar to the present day, and does not consider increases in winter precipitation or mean annual precipitation above present day levels. Both of these are suggested by the pollen data in some regions, and both could explain glacier extent found during the LGM based on less extreme temperature anomalies more comparable with the pollen data.

To the east of the Alps in the Panonian basin, mean annual temperature anomaly estimates have been made from noble gas measurements on groundwater ranging from -2 to -4 ºC (Stute and Deak, 1990) up to -9 ºC (Varsányi et al., 2011). These are similar to estimates ranging from -2 to -9 ºC from oxygen isotope ratios from mammoth tooth enamel (Kovács et al., 2012) and are comparable with nearby pollen sites [site #50][Feher Lake site #50] -8.2 ± 3.3 ºC and [site #52][Kokad site #52] -4.5 ± 2.3 ºC. On a broader scale, Sanchi et al (2014) estimated LGM cooling in the Danube and Dneiper basins based on Lipid biomarkers in a core from the Black Sea and came up with similar mean annual temperature anomalies between -6 to -10 ºC, which again are comparable with pollen sites from the region that range from [site #48][Nagymohos site #48] -10.5 ± 4.1 ºC to [site #57][Straldzha site #57] -4.3 ± 5.8 ºC.

Further south and west, García-Amorena et al. (2007) reported mean annual temperature anomalies of -2.0 to -11.3 ºC at LGM sites along the Portuguese coast, based on an indicator species method using plant macrofossils. This is similar to the closest marine pollen sites off the coast, which recorded values of [site #1][MD95-2039 site #1] -10.5 ± 4.6 ºC and [site #3][MD99-2331 site #3] -5.3± 2.9 ºC. Meanwhile, in the far east of the study area, Zaarur et al. (2016) estimated a mean annual temperature anomaly of around -3 ºC based on clumped isotope analysis of Melanopsis shells from LGM sediments in the Sea of Galilee. This limited cooling appears similar to the nearest pollen site ~~[site #63]~~[Lake Zeribar site #63] where we reconstruct a cooling of -2.2 ± 4.6 ºC.

Reconstructions of LGM sea surface temperatures (SST's) provide yet another source of comparison with our terrestrial pollen-based reconstructions, although many of the physical processes controlling surface sea temperatures such as upwelling, surface mixing, surface currents, stratification and thermal inertia through the seasonal cycle, represent quite different processes to those controlling surface temperatures over land, particularly at the sub-regional scale. Nevertheless, the Atlantic coastal waters of Iberia and the waters throughout the Mediterranean Sea include many SST sites that lie in relative proximity to our terrestrial pollen-sites, allowing us to make a comparison at the largest scale. Within this area the MARGO database (MARGO Members, 2009) includes 13 Alkenone, 2 Mg/Ca and 41 Foraminifera based SST records of mean annual temperature, with the Foraminifera records also providing an additional 41 winter (JFM) and summer (JAS) SST estimates. We compare the SST records with the 36 closest terrestrial pollen records which fall within a box of -11 to 35 degrees longitude and 32 to 43 degrees latitude containing all of the SST records. A simple site average indicates a mean annual SST anomaly of -5.5 ± 1.0 ºC which is relatively close to the value of -7.2 ± 3.4 ºC obtained from the terrestrial pollen sites [sites #1-4, 5, 7-24, 25, 26, 30, 35-38, 41, 47, 51, 53, 56-59]. Interestingly the inter-site variance (standard deviation of the reconstructed temperatures across all sites) is almost identical for the two datasets, 2.57 ºC for the SST sites and 2.63 ºC for the pollen sites, despite representing very different environments, proxies and uncertainties. However, when we look at the seasonal temperature anomalies, we find very different results. Site averaged winter SST anomalies are -3.7 ± 1.1 ºC compared to -9.3 ± 4.2 ºC for winter temperatures from terrestrial pollen sites, while in summer the values are reversed, -7.0 ± 0.8 ºC compared to -5.38 ± 3.3 ºC respectively. This suggests that SST's experienced greater cooling in summer compared to winter, which is the opposite to that generally found in terrestrial seasonal temperature reconstructions throughout the region, although this is consistent with model simulations (Mikolajewicz, 2011).

4.221 Precipitation

~~**4.3 Climate: Precipitation**~~

Few proxies apart from pollen provide quantitative reconstructions of precipitation during the LGM. Glacier mass balance modelling includes assumptions about precipitation in order to derive temperatures (Allen et al., 2008a), but neither is independent of the other. Hughes et al. (2006) estimate from glacier modelling that mean annual precipitation during the LGM at sites in the Pindus mountains in Greece was around 2300 ± 200mm, which they consider to be similar to the present day (>2000mm). A small change in precipitation compared to modern values is also indicated by the nearest pollen site, which is around 47 km to the south ~~[site #51]~~[Ioannina #51], and indicates a mean annual precipitation anomaly of -152 ± 294mm, representing just 15% of the modern value. A larger reduction in mean annual precipitation of -45% (maximum) is reconstructed by García-Amorena et al. (2007) based on plant macrofossil remains from sites on the Portuguese coast. In comparison, the closest pollen sites record values which are a little lower, ranging from ~~[site #1]~~[MD95-2039 site #1] -22% to ~~[site #3]~~[MD99-2331 site #3] -34%. Further north in south-west Germany, Prud'homme et al. (2018) reconstructed mean annual precipitation from the delta 13C of earthworm calcite granules at F~~F~~ussloch. They estimate a field site average of 333 (159-574) mm/yr at the LGM, which represents an anomaly of -503 mm/yr (-60%) relative to the modern precipitation of 836 mm/yr. This is comparable with the closest pollen site ~~[site #29]~~[Bergsee #29] with an anomaly of -540 mm/yr.

As with glaciers, lake levels reflect changes in moisture balance that includes the effects of both temperature (via evapotranspiration) and precipitation, rather than just precipitation. They also represent semi-quantitative data at best, with changes often described relative to the modern or other baseline. There are few lake level records available north of the Alps, but to the south, many records indicate high lake levels in areas such as Spain (Lacey et al., 2016; Moreno et al., 2012; Vegas et al., 2010), Italy (Belis et al., 1999; Giraudi, 2017), Greece and Turkey (Harrison et al., 1996; Reimer et al., 2009) and the Middle East (Kolodny et al., 2005; Lev et al., 2019). These lake records are also supported by evidence of higher river levels in Morocco (El Amrani et al., 2008). The cause of the higher lake levels has been the subject of some debate, since many pollen records (and especially early biome reconstructions) show steppe vegetation that would suggest aridity that appears incompatible with higher lake levels. Prentice et al. (1992) proposed that the co-existence of steppe vegetation and high lake levels could be possible if precipitation increased outside of the summer growing season, while summers themselves were drier and cooler with decreased evaporation. However, the results of our analysis tend to indicate the opposite in regions with higher lake levels, with increased summer rainfall and decreased winter rainfall. In addition, the increase in summer precipitation was enough to compensate for the decrease in winter rainfall, leading to an overall increase in mean annual precipitation at many pollen sites in Spain and Greece for instance. This together with depressed temperatures and consequently decreased evaporation could explain the higher lake levels, whilst also limiting the growth of trees as a result of cooler temperatures and prolonged aridity outside of the summer season. Davis & Stevenson (2007) also note a differential hydrological response between summer and winter rainfall in the Mediterranean during the Holocene that may also provide an explanation. In this case sporadic summer storms may result in high rates of runoff that may fill run-off fed lakes, but low rates of soil moisture recharge that fails to benefit vegetation in the same way winter rainfall does.

Overall, we reconstruct only a small reduction in precipitation during the LGM of around 91mm (13%) averaged over all sites, which is less than the ~200mm reduction based on the sites in the pollen-climate compilation used by PMIP (Bartlein et al., 2011). Since our precipitation reconstruction on average matches that of the INV reconstruction by Wu et al (REF), we can attribute much of the difference to the greater aridity shown in the ~~MAT-NN~~ANN reconstruction by Peyron et al and Jost et al (2005) (see figure 9~~7~~). As with temperature, this is probably a reflection of the modern training set used in the ~~MAT-NN~~ANN reconstruction which is much smaller than our training set and is largely taken from the arid steppes of Kazakhstan and Mongolia. However, it is also important to recognize the significant spatial variability in precipitation, which means that a simple average of different sets of sites from different regions may not accurately reflect the change in LGM precipitation at the European scale. Nevertheless, one of the most consistent signals in our dataset is for an increase in summer precipitation over many areas of Southern Europe and the Mediterranean. This is also found in climate models, where it has been attributed to an increase in convection-driven precipitation, although the amount of precipitation generated by this mechanism varies significantly between models (Beghin et al., 2016). It may seem counter-intuative to see an increase in reconstructed precipitation in the same regions where we also find a preponderance of steppe or xerophytic biomes and taxa, including *Artemisia* and Chenopodiaceae. This is attributable to the fact that climate can change quite markedly with necessarily invoking a major change in vegetation, and especially the pollen biome. For instance, a semi-arid climate ranges from 250-500mm rainfall a year, so we could expect a semi-arid vegetation to be dominant even if the rainfall increases 250mm (100%).

A more consistent response in models is for an increase in winter precipitation across Southern Europe and the Mediterranean related to a stronger and more southerly displaced jet stream, with winter precipitation also accounting for much of the change in mean annual precipitation (Beghin et al., 2016). Our reconstruction of winter precipitation however shows less support for this scenario with a more general decrease in winter precipitation apart from southern and eastern Iberia, and with summer precipitation generally more important in those sites that show an overall increase in mean annual precipitation. This may not necessarily contradict the models in terms of the strength and position of the winter jet stream, but may instead indicate that models over-estimate the amount of moisture being carried westward from the cold North Atlantic along the storm track, especially across the far northern Mediterranean. The increase in winter precipitation across southern and eastern Iberia is however entirely consistent with a strengthened and more southerly jet stream, which also brings increased winter precipitation to the region today as a result of blocking over northern Europe/Atlantic and a negative NAO (Vicente-Serrano et al., 2011).

Other areas that show an increase in winter precipitation include pollen sites around the eastern end of the Alps. This is consistent with a recent study by Spötl et al (2021) who argued, on the basis of cryogenic carbonates preserved in a cave in Austria, that heavy winter (and autumn) precipitation was a significant factor in driving LGM glaciation in the region. The seasonally specific nature of this precipitation is also supported by the same pollen sites, which do not show any increase in summer precipitation at this time.

5.0 Conclusions

We have reconstructed the climate and vegetation cover across Europe, North Africa and the Middle East at the time of the LGM based on 63 pollen records. These records were selected using strict quality control criteria, with particular attention paid to dating control, which led to the exclusion of many records that have been used in previous studies. This fully documented dataset represents the most chronologically precise and spatially resolved view of LGM climate and vegetation during the PMIP benchmarking time window at 21 ± 2 ka. Nevertheless, it is important to recognize that there are still significant spatial gaps in pollen sites especially north of the Alps, the Balkans, Turkey and the Middle East, and we continue to have only a partial understanding of the LGM over these areas.

~~Distribution maps were created using a standardized pollen taxonomy and sum to enable direct comparison between sites/records. Pollen biomes and quantitative MAT estimates of tree cover have also been reconstructed allowing us to determine the relative proportion of forest and woodland cover.~~One of the key questions concerning the vegetation landscape of the LGM in Europe has been the extent to which forest rather than steppe covered the continent, and to what extent temperate elements could be found north of the classical refugia areas of Southern Europe and the Mediterranean. Our ~~These~~ results show that although steppe and tundra was extensive at the time of the LGM, areas of open forest also occurred in many regions, particularly (but not exclusively) in Iberia, northern Italy and Central Europe. These forest or woodland stands are likely to have been located in environmentally favourable areas, with good soils, elevated rainfall and shelter from cold, desiccating winds. In those areas where woodland existed, Boreal taxa generally dominated north and east of the Alps, while temperate and thermophilious (mainly drought adapted) taxa were generally confined to areas south of the Alps and around the Mediterranean. The temperate deciduous forests that compose the climax community in many areas of Europe today were displaced to the south and reduced to a partnership role with Boreal elements. Overall our new reconstruction indicates greater agreement with model land cover simulations, but models still appear to over-estimate the amount of forest and woodland over areas such as France and the Benelux, Greece, Turkey and the Far East.

Another key question about the LGM concerns the ability of climate models to simulate the climate of this period and whether pollen-based climate reconstructions which show disagreement with models have been biased by the effects of low CO2 on plant physiology. We find that our new pollen-climate reconstruction shows much closer agreement with climate models than previous reconstructions that did not take account of low CO2 effects. We also find close agreement with previous reconstructions that did take account of CO2 effects. Since our MAT method itself does not specifically take account of low CO2 effects, this would suggest that this problem is not a significant hindrance to MAT performance at the time of the LGM, at least not compared to other uncertainties. Instead, we suggest that the main factor in the performance of pollen-climate transfer functions that use modern analogue methods is the provision of a large enough modern pollen dataset with suitable LGM analogues.

This conclusion is supported by comparison with climate reconstructions based on other proxies. We found little difference between ~~We reconstructed the LGM climate of Europe based on a MAT in combination with a large modern pollen calibration dataset covering the Eurasian region. In a direct comparison we found no significant difference between LGM temperatures and precipitation reconstructed from pollen using MAT, and that reconstructed by Inverse Modelling. We therefore do not find MAT performance at the time of the LGM to be significantly impaired by non-climatic plant growth factors, such as atmospheric CO2 concentration, that were significantly different compared to modern. Our results are also much closer to climate model simulations than previous studies using the Neural Network method (a variant on MAT), which suggested a climate that was much cooler and drier. The difference between our MAT reconstruction and the Neural Network reconstruction is probably attributable to the much smaller size and spatial bias of the modern calibration dataset that was used in this earlier analysis.~~

~~We also found little difference between~~ our MAT reconstruction and a Chironomid-based summer temperature record based on ~~usinga~~ downcore sample by sample comparison, as well as comparsons with records from a variety of other proxies ~~based on a more general site by site comparison~~ at a regional scale. However, it is notable that some studies using glacier mass balance modelling methods indicate LGM temperatures that are much cooler than our pollen-based reconstruction~~as well as reconstructions based on other proxies~~. The reasons behind this are not clear, but our pollen-based results indicate higher than present precipitation in some areas that could potentially explain low ~~altitude~~ elevation ~~LGM~~ glacier ELA's without the need for such cold temperatures.

We also find that although our pollen-based reconstruction and those of SST's generally agree in terms of mean annual temperatures, SST's indicate greater cooling in summer compared to winter, while terrestrial records indicate greater cooling in winter compared to summer. These seasonal differences are~~area~~ also reproduced in climate models, and probably reflect the different processes driving seasonal temperature change in the terrestrial and marine domain.

Our r~~R~~econstructions of precipitation show large spatial and seasonal variability, but generally indicate less overall aridity than previously suggested from smaller scale studies which sampled less of the spatial domain. We find that in some regions of Southern Europe precipitation may actually have been greater than present, especially in summer, but also in winter in southern and eastern Iberia and around the southern slopes of the Alps. This may have important implications in understanding the development of LGM glaciation, which may be less a function of temperature than previously supposed. This could also help better explain the observed asynchronous nature of glaciation even within relatively small regions such as Europe, as a result of more localized controls on ice sheet development such as precipitation.

We hope that this new continental-scale dataset of climate and vegetation reconstructions will provide an improved baseline for data-model comparisons and other studies that will allow us to better understand the complex LGM environment.

Code/Data availability

All of the data shown in the figures together with the fossil and modern pollen datasets will be made available on pangaea.de once the review process has been completed and these datasets are therefore no longer subject to change.

Author contribution

BASD designed the study, undertook the analysis and wrote the manuscript. MF and ER designed and prepared the maps. JOK and AB reviewed the manuscript and provided additional input.

Competing interests

The authors declare that they have no conflict of interest.

Acknowledgements

This work was supported by a grant from the Fonds de Recherche du Québéc Société et Culture (2019-SE3-254686) to AB. Data were obtained from the European Pollen Database (EPD), based within the Neotoma Paleoecology Database (http://www.neotomadb.org). The work of data contributors, data stewards, and the Neotoma and EPD community is gratefully acknowledged. We dedicate this paper in memory of Eric Grimm, whose tireless work for the EPD and Neotoma helped make this study possible.

References

ACER project members, Goñi, M. F. S., Desprat, S., Daniau, A. L., Bassinot, F. C., Polanco-Martínez, J. M., Harrison, S. P., Allen, J. R. M., Scott Anderson, R., Behling, H., Bonnefille, R., Burjachs, F., Carrión, J. S., Cheddadi, R., Clark, J. S., Combourieu-Nebout, N., Mustaphi, C. J. C., Debusk, G. H., Dupont, L. M., Finch, J. M., Fletcher, W. J., Giardini, M., González, C., Gosling, W. D., Grigg, L. D., Grimm, E. C., Hayashi, R., Helmens, K., Heusser, L. E., Hill, T., Hope, G., Huntley, B., Igarashi, Y., Irino, T., Jacobs, B., Jiménez-Moreno, G., Kawai, S., Peter Kershaw, A., Kumon, F., Lawson, I. T., Ledru, M. P., Lézine, A. M., Mei Liew, P., Magri, D., Marchant, R., Margari, V., Mayle, F. E., Merna Mckenzie, G., Moss, P., Müller, S., Müller, U. C., Naughton, F., Newnham, R. M., Oba, T., Pérez-Obiol, R., Pini, R., Ravazzi, C., Roucoux, K. H., Rucina, S. M., Scott, L., Takahara, H., Tzedakis, P. C., Urrego, D. H., Van Geel, B., Guido Valencia, B., Vandergoes, M. J., Vincens, A., Whitlock, C. L., Willard, D. A. and Yamamoto, M.: The ACER pollen and charcoal database: A global resource to document vegetation and fire response to abrupt climate changes during the last glacial period, Earth Syst. Sci. Data, 9(2), 679–695, doi:10.5194/essd-9-679-2017, 2017.

Allen, J. R. M., Hickler, T., Singarayer, J. S., Sykes, M. T., Valdes, P. J. and Huntley, B.: Last glacial vegetation of northern Eurasia, Quat. Sci. Rev., 29(19–20), 2604–2618, doi:10.1016/j.quascirev.2010.05.031, 2010.

Allen, R., Siegert, M. J. and Payne, A. J.: Reconstructing glacier-based climates of LGM Europe and Russia – Part 2 : A dataset of LGM precipitation / temperature relations derived from degree-day modelling of palaeo glaciers, , 249–263, 2008a.

Allen, R., Siegert, M. J. and Payne, A. J.: Reconstructing glacier-based climates of LGM Europe and Russia – Part 3 : Comparison with previous climate reconstructions, , (1999), 265–280, 2008b.

Ampel, L., Bigler, C., Wohlfarth, B., Risberg, J., Lotter, A. F. and Veres, D.: Modest summer temperature variability during DO cycles in western Europe, Quat. Sci. Rev., 29(11–12), 1322–1327, doi:10.1016/j.quascirev.2010.03.002, 2010.

El Amrani, M., Macaire, J. J., Zarki, H., Bréhéret, J. G. and Fontugne, M.: Contrasted morphosedimentary activity of the lower Kert River (northeastern Morocco) during the Late Pleistocene and the Holocene. Possible impact of bioclimatic variations and human action, Comptes Rendus - Geosci., 340(8), 533–542, doi:10.1016/j.crte.2008.05.004, 2008.

Anderson, P. M., Barnosky, C. W., Bartlein, P. J., Behling, P. J., Brubaker, L., Cushing, E. J., Dodson, J., Dworetsky, B., Guetter, P. J., Harrison, S. P., Huntley, B., Kutzbach, J. E., Markgraf, V., Marvel, R., McGlone, M. S., Mix, A., Moar, N. T., Morley, J., Perrott, R. A., Peterson, G. M., Prell, W. L., Prentice, I. C., Ritchie, J. C., Roberts, N., Ruddiman, W. F., Salinger, M. J., Spaulding, W. G., Street-Perrott, F. A., Thompson, R. S., Wang, P. K., Webb, T., Winkler, M. G. and Wright, H. E.: Climatic changes of the last 18,000 years: Observations and model simulations, Science (80-.)., 241(4869), 1043–1052, doi:10.1126/science.241.4869.1043, 1988.

Arpe, K., Leroy, S. A. G. and Mikolajewicz, U.: A comparison of climate simulations for the last glacial maximum with three different versions of the ECHAM model and implications for summer-green tree refugia, Clim. Past, 91–114, doi:10.5194/cp-7-91-2011, 2011.

Arslanov, K. A., Dolukhanov, P. M. and Gei, N. A.: Climate, Black Sea levels and human settlements in Caucasus Littoral 50,000-9000 BP, Quat. Int., 167–168, 121–127, doi:10.1016/j.quaint.2007.02.013, 2007.

Bañuls-Cardona, S., López-García, J. M., Blain, H. A., Lozano-Fernández, I. and Cuenca-Bescós, G.: The end of the Last Glacial Maximum in the Iberian Peninsula characterized by the small-mammal assemblages, J. Iber. Geol., 40(1), 19–27, doi:10.5209/rev_JIGE.2014.v40.n1.44085, 2014.

Bartlein, P. J., Harrison, S. P., Brewer, S., Connor, S., Davis, B. A. S., Gajewski, K., Guiot, J., Harrison-Prentice, T. I., Henderson, A., Peyron, O., Prentice, I. C., Scholze, M., Seppä, H., Shuman, B., Sugita, S., Thompson, R. S., Viau, A. E., Williams, J. and Wu, H.: Pollen-based continental climate reconstructions at 6 and 21 ka: A global synthesis, Clim. Dyn., 37(3), 775–802, doi:10.1007/s00382-010-0904-1, 2011.

de Beaulieu, J.-L. and Reille, M.: Pollen analysis of a long upper Pleistocene continental sequence in a Velay maar (Massif Central, France), Palaeogeogr. Palaeoclimatol. Palaeoecol., 80(1), 35–48, 1990.
Beghin, P., Charbit, S., Kageyama, M., Combourieu-Nebout, N., Hatté, C., Dumas, C. and Peterschmitt, J. Y.: What drives LGM precipitation over the western Mediterranean? A study focused on the Iberian Peninsula and northern Morocco, Clim. Dyn., 46(7–8), 2611–2631, doi:10.1007/s00382-015-2720-0, 2016.

Belis, C. A., Lami, A., Guilizzoni, P., Ariztegui, D. and Geiger, W.: The late Pleistocene ostracod record of the crater lake sediments from Lago di Albano (Central Italy): Changes in trophic status, water level and climate, J. Paleolimnol., 21(2), 151–169, doi:10.1023/A:1008095805748, 1999.

Berto, C., López-García, J. M. and Luzi, E.: Changes in the Late Pleistocene small-mammal distribution in the Italian Peninsula, Quat. Sci. Rev., 225, doi:10.1016/j.quascirev.2019.106019, 2019.

Bigelow, N.H., Brubaker, L.B., Edwards, M.E., Harrison, S.P., Prentice, I.C., Anderson, P.M., Andreev, A.A., Bartlein, P.J., Christiansen, T.R., Cramer, W., Kaplan, J.O., Lozhkin, A.V., Matveyeva, N.V., Murray, D.F., McGuire, A.D., Razzhivin, V.Y., Ritchie, J.C., Smith, B., Walker, D.A., Gajewski, K., Wolf, V., Holmqvist, B.H., Igarashi, Y., Kremenetskii, K., Paus, A., Pisaric, M.F.J., Volkova, V.S.: Climate change and arctic ecosystems: 1. Vegetation changes north of 55 N between the last glacial maximum, mid-Holocene, and present. J. Geophys. Res. 108 (D19), 8170. doi.org/10.1029/2002JD002558, 2013.

Binney, H., Edwards, M., Macias-Fauria, M., Lozhkin, A., Anderson, P., Kaplan, J. O., Andreev, A., Bezrukova, E., Blyakharchuk, T., Jankovska, V., Khazina, I., Krivonogov, S., Kremenetski, K., Nield, J., Novenko, E., Ryabogina, N., Solovieva, N., Willis, K. and Zernitskaya, V.: Vegetation of Eurasia from the last glacial maximum to present: Key biogeographic patterns, Quat. Sci. Rev., 157, 80–97, doi:10.1016/j.quascirev.2016.11.022, 2017.

Birks, H. J. B. and Willis, K. J.: Alpines, trees, and refugia in Europe, Plant Ecol. Divers., 1(2), 147–160, doi:10.1080/17550870802349146, 2008.

Bonatti, E.: Pollen sequence in the lake sediments. In: lanula: an account of the history and development of the Lago di Monterosi, Latium, Italy, in Trans. Am. phil. Soc., vol. 60, edited by G. E. Hutchinson, pp. 26–31., 1970.

Brewer, S., Guiot, J., Sánchez-Goñi, M. F. and Klotz, S.: The climate in Europe during the Eemian: a multi-method approach using pollen data, Quat. Sci. Rev., 27(25–26), 2303–2315, doi:10.1016/j.quascirev.2008.08.029, 2008.

Brewer, S., Giesecke, T., Davis, B. A. S., Finsinger, W., Wolters, S., Binney, H., de Beaulieu, J. L., Fyfe, R., Gil-Romera, G., Kühl, N., Kuneš, P., Leydet, M. and Bradshaw, R. H.: Mapping Lateglacial and Holocene European pollen data: The maps, J. Maps, 13(2), 921–928, doi:10.1080/17445647.2016.1197613, 2017.

Camuera, J., Jiménez-Moreno, G., Ramos-Román, M. J., García-Alix, A., Toney, J. L., Anderson, R. S., Jiménez-Espejo, F., Bright, J., Webster, C., Yanes, Y. and Carrión, J. S.: Vegetation and climate changes during the last two glacial-interglacial cycles in the western Mediterranean: A new long pollen record from Padul (southern Iberian Peninsula), Quat. Sci. Rev., 205, 86–105, doi:10.1016/j.quascirev.2018.12.013, 2019.

Cao, X., Tian, F., Dallmeyer, A. and Herzschuh, U.: Northern Hemisphere biome changes (>30°N) since 40 cal ka BP and their driving factors inferred from model-data comparisons, Quat. Sci. Rev., 220, 291–309, doi:10.1016/j.quascirev.2019.07.034, 2019.

Carrión, J. S.: Late quaternary pollen sequence from Carihuela Cave, southern Spain, Rev. Palaeobot. Palynol., 71(1–4), doi:10.1016/0034-6667(92)90157-C, 1992.

Carrión, J. S.: Patterns and processes of Late Quaternary environmental change in a montane region of southwestern Europe, Quat. Sci. Rev., 21, 2047–2066, 2002.

Carrión, J. S., Finlayson, C., Fernández, S., Finlayson, G., Allué, E., López-Sáez, J. A., López-García, P., Gil-Romera, G., Bailey, G. and González-Sampériz, P.: A coastal reservoir of biodiversity for Upper Pleistocene human populations: palaeoecological investigations in Gorham's Cave (Gibraltar) in the context of the Iberian Peninsula, Quat. Sci. Rev., 27(23–24), 2118–2135, doi:10.1016/j.quascirev.2008.08.016, 2008.

Cheddadi, R., Yu, G., Guiot, J., Harrison, S. P. and Colin Prentice, I.: The climate of Europe 6000 years ago, Clim. Dyn., 13(1), 1–9, 1996.

Chevalier, M., Davis, B. A. S., Heiri, O., Seppä, H., Chase, B. M., Gajewski, K., Lacourse, T., Telford, R. J., Finsinger, W., Guiot, J., Kühl, N., Maezumi, S. Y., Tipton, J. R., Carter, V. A., Brussel, T., Phelps, L. N., Dawson, A., Zanon, M., Vallé, F., Nolan, C., Mauri, A., de Vernal, A., Izumi, K., Holmström, L., Marsicek, J., Goring, S., Sommer, P. S., Chaput, M. and Kupriyanov, D.: Pollen-based climate reconstruction techniques for late Quaternary studies, Earth-Science Rev., 210, doi:10.1016/j.earscirev.2020.103384, 2020.

Cleator, S. F., Harrison, S. P., Nichols, N. K., Colin Prentice, I. and Roulstone, I.: A new multivariable benchmark for Last Glacial Maximum climate simulations, Clim. Past, 16(2), 699–712, doi:10.5194/cp-16-699-2020, 2020.

COHMAP,: Climatic changes of the last 18,000 years: observations and model simulations. *Science*, 241, 1043-1052, 1988.

Collins, P. M., Davis, B. A. S. and Kaplan, J. O.: The mid-Holocene vegetation of the Mediterranean region and southern Europe, and comparison with the present day, J. Biogeogr., 39(10), doi:10.1111/j.1365-2699.2012.02738.x, 2012.

Combourieu Nebout, N., Peyron, O., Dormoy, I., Desprat, S., Beaudouin, C., Kotthoff, U. and Marret, F.: Rapid climatic variability in the west Mediterranean during the last 25 000 years from high resolution pollen data, Clim. Past, 5(3), 503–521, doi:10.5194/cp-5-503-2009, 2009.

Connor, S. E., Ross, S. A., Sobotkova, A., Herries, A. I. R., Mooney, S. D., Longford, C. and Iliev, I.: Environmental conditions in the SE Balkans since the Last Glacial Maximum and their influence on the spread of agriculture into Europe, Quat. Sci. Rev., 68, 200–215, doi:10.1016/j.quascirev.2013.02.011, 2013.

Cowling, S. A. and Sykes, M. T.: Physiological significance of low atmospheric CO2 for plant-climate interactions, Quat. Res., 52(2), 237–242, doi:10.1006/qres.1999.2065, 1999.

Damblon, F.: L'enregistrement palynologique de la sequence pléistocène et holocène de la grotte Walou, in La grotte Walou à Trooz (Belgique), edited by C. Draily, S. Pirson, and M. Toussaint, pp. 84–129, Service public de Wallonie (Etudes et Documents, Archéologie, 21)., 2011.

Daniau, A.-L., Desprat, S., Aleman, J. C., Bremond, L., Davis, B., Fletcher, W., Marlon, J. R., Marquer, L., Montade, V., Morales-Molino, C., Naughton, F., Rius, D. and Urrego, D. H.: Terrestrial plant microfossils in palaeoenvironmental studies, pollen, microcharcoal and phytolith. Towards a comprehensive understanding of vegetation, fire and climate changes over the past one million years, Rev. Micropaleontol., 63, doi:10.1016/j.revmic.2019.02.001, 2019.

Davis, B. A. S. and Stevenson, A. C.: The 8.2 ka event and Early-Mid Holocene forests, fires and flooding in the Central Ebro Desert, NE Spain, Quat. Sci. Rev., 26(13–14), doi:10.1016/j.quascirev.2007.04.007, 2007.

Davis, B. A. S., Brewer, S., Stevenson, A. C., Guiot, J., Allen, J., Almqvist-Jacobson, H., Ammann, B., Andreev, A. A., Argant, J., Atanassova, J., Balwierz, Z., Barnosky, C. D., Bartley, D. D., De Beaulieu, J. L., Beckett, S. C., Behre, K. E., Bennett, K. D., Berglund, B. E. B., Beug, H.-J., Bezusko, L., Binka, K., Birks, H. H., Birks, H. J. B., Björck, S., Bliakhartchouk, T., Bogdel, I., Bonatti, E., Bottema, S., Bozilova, E. D. B., Bradshaw, R., Brown, A. P., Brugiapaglia, E., Carrion, J., Chernavskaya, M., Clerc, J., Clet, M., Coûteaux, M., Craig, A. J., Cserny, T., Cwynar, L. C., Dambach, K., De Valk, E. J., Digerfeldt, G., Diot, M. F., Eastwood, W., Elina, G., Filimonova, L., Filipovitch, L., Gaillard-Lemdhal, M. J., Gauthier, A., Göransson, H., Guenet, P., Gunova, V., Hall, V. A. H., Harmata, K., Hicks, S., Huckerby, E., Huntley, B., Huttunen, A., Hyvärinen, H., Ilves, E., Jacobson, G. L., Jahns, S., Jankovská, V., Jóhansen, J., Kabailiene, M., Kelly, M. G., Khomutova, V. I., Königsson, L. K., Kremenetski, C., Kremenetskii, K. V., Krisai, I., Krisai, R., Kvavadze, E., Lamb, H., Lazarova, M. A., Litt, T., Lotter, A. F., Lowe, J. J., Magyari, E., Makohonienko, M., Mamakowa, K., Mangerud, J., Mariscal, B., Markgraf, V., McKeever, Mitchell, F. J. G., Munuera, M., Nicol-Pichard, S., Noryskiewicz, B., Odgaard, B. V., Panova, N. K., Pantaleon-Cano, J., Paus, A. A., Pavel, T., Peglar, S. M., Penalba, M. C., Pennington, W., Perez-Obiol, R., et al.: The temperature of Europe during the Holocene reconstructed from pollen data, Quat. Sci. Rev., 22(15–17), doi:10.1016/S0277-3791(03)00173-2, 2003.

Davis, B. A. S., Chevalier, M., Sommer, P., Carter, V. A., Finsinger, W., Mauri, A., Phelps, L. N., Zanon, M., Abegglen, R., Åkesson, C. M., Alba-Sánchez, F., Scott Anderson, R., Antipina, T. G., Atanassova, J. R., Beer, R., Belyanina, N. I., Blyakharchuk, T. A., Borisova, O. K., Bozilova, E., Bukreeva, G., Jane Bunting, M., Clò, E., Colombaroli, D., Combourieu-Nebout, N., Desprat, S., Di Rita, F., Djamali, M., Edwards, K. J., Fall, P. L., Feurdean, A., Fletcher, W., Florenzano, A., Furlanetto, G., Gaceur, E., Galimov, A. T., Gałka, M., García-Moreiras, I., Giesecke, T., Grindean, R., Guido, M. A., Gvozdeva, I. G., Herzschuh, U., Hjelle, K. L., Ivanov, S., Jahns, S., Jankovska, V., Jiménez-Moreno, G., Karpińska-Kołaczek, M., Kitaba, I., Kołaczek, P., Lapteva, E. G., Latałowa, M., Lebreton, V., Leroy, S., Leydet, M., Lopatina, D. A., López-Sáez, J. A., Lotter, A. F., Magri, D., Marinova, E., Matthias, I., Mavridou, A., Mercuri, A. M., Mesa-Fernández, J. M., Mikishin, Y. A., Milecka, K., Montanari, C., Morales-Molino, C., Mrotzek, A., Sobrino, C. M., Naidina, O. D., Nakagawa, T., Nielsen, A. B., Novenko, E. Y., Panajiotidis, S., Panova, N. K., Papadopoulou, M., Pardoe, H. S., Pędziszewska, A., Petrenko, T. I., Ramos-Román, M. J., Ravazzi, C., Rösch, M., Ryabogina, N., Ruiz, S. S., Sakari Salonen, J., Sapelko, T. V., Schofield, J. E., Seppä, H., Shumilovskikh, L., Stivrins, N., Stojakowits, P., Svitavska, H. S., Święta-Musznicka, J., Tantau, I., Tinner, W., Tobolski, K., Tonkov, S., Tsakiridou, M., et al.: The Eurasian Modern Pollen Database (EMPD), version 2, Earth Syst. Sci. Data, 12(4), 2423–2445, doi:10.5194/essd-12-2423-2020, 2020.

Davis M.B.: On the theory of pollen analysis. American Journal of Sciences, 26, 897–912, 1963.

Demay, L., Julien, M.A., Anghelinu, M., Shydlovskyi, P.S., Koulakovska, L.V., P´ean, S., Stupak, D.V., Vasyliev, P.M., Obˇada, T., Wojtal, P., Belyaeva, V.I.: Study of human behaviors during the Late Pleniglacial in the East European Plain through their relation to the animal world. Quat. Int. https://doi.org/10.1016/j. quaint.2020.10.047, 2021.

Douda, J., Doudová, J., Drašnarová, A., Kuneš, P., Hadincová, V., Krak, K., Zákravský, P. and Mandák, B.: Migration patterns of subgenus Alnus in Europe since the last glacial maximum: A systematic review, PLoS One, 9(2), doi:10.1371/journal.pone.0088709, 2014.

Duprat-Oualid, F., Rius, D., Bégeot, C., Magny, M., Millet, L., Wulf, S. and Appelt, O.: Vegetation response to abrupt climate changes in Western Europe from 45 to 14.7k cal a BP: the Bergsee lacustrine record (Black Forest, Germany), J. Quat. Sci., 32(7), 1008–1021, doi:10.1002/jqs.2972, 2017.

Dupre Ollivier, M.: Palinología y paleoambiente- nuevos datos españoles referencias, Universidad de Valencia., 1988.

Edwards, M. E., Anderson, P. M., Brubaker, L. B., Ager, T., Andreev, A. A., Bigelow, N. H., Cwynar, L. C., Eisner, W. R., Harrison, S. P., Hu, F.-S., Jolly, D., Lozhkin, A. V., MacDonald, G. M., Mock, C. J., Ritchie, J. C., Sher, A. V., Spear, R. W., Williams, J. & Yu, G.: Pollen-based biomes for Beringia 18,000, 6000 and 0 14C yr bp. *Journal of Biogeography*, **27**, 521– 554, doi: 10.1046/j.1365-2699.2000.00426.x, 2000.

Ehlers, J., Gibbard, P. L. and Hughes, P. D.: Quaternary Glaciations - Extent and Chronology A Closer Look, edited by J. Ehlers, P. L. Gibbard, and P. D. Hughes, Elsevier., 2011.

Elenga, H., Peyron, O., Bonnefille, R., Jolly, D., Cheddadi, R., Guiot, J., Andrieu, V., Bottema, S., Buchet, G., De Beaulieu, J. L., Hamilton, A. C., Maley, J., Marchant, R., Perez-Obiol, R., Reille, M., Riollet, G., Scott, L., Straka, H., Taylor, D., Van Campo, E., Vincens, A., Laarif, F. and Jonson, H.: Pollen-based biome reconstruction for southern Europe and Africa 18,000 yr BP, J. Biogeogr., 27(3), 621–634, doi:10.1046/j.1365-2699.2000.00430.x, 2000.

Ferguson, J. E., Henderson, G. M., Fa, D. A., Finlayson, J. C. and Charnley, N. R.: Increased seasonality in the Western Mediterranean during the last glacial from limpet shell geochemistry, Earth Planet. Sci. Lett., 308(3–4), 325–333, doi:10.1016/j.epsl.2011.05.054, 2011.

Feurdean A, Bhagwat SA, Willis KJ, Birks HJB, Lischke H, Hickler T.: Tree migration-rates: narrowing the gap between inferred post-glacial rates and projected rates. PLoS ONE 8: e71797, 2013.

Feurdean, A., Perşoiu, A., Tanţău, I., Stevens, T., Magyari, E. K., Onac, B. P., Marković, S., Andrič, M., Connor, S., Fărcaş, S., Gałka, M., Gaudeny, T., Hoek, W., Kolaczek, P., Kuneš, P., Lamentowicz, M., Marinova, E., Michczyńska, D. J., Perşoiu, I., Płóciennik, M., Słowiński, M., Stancikaite, M., Sumegi, P., Svensson, A., Tămaş, T., Timar, A., Tonkov, S., Toth, M., Veski, S., Willis, K. J. and Zernitskaya, V.: Climate variability and associated vegetation response throughout Central and Eastern Europe (CEE) between 60 and 8ka, Quat. Sci. Rev., 106, 206–224, doi:10.1016/j.quascirev.2014.06.003, 2014.

Fick, S. E. and Hijmans, R. J.: WorldClim 2: new 1-km spatial resolution climate surfaces for global land areas, Int. J. Climatol., 37(12), 4302–4315, doi:10.1002/joc.5086, 2017.

Fletcher, W. J., Goni, M. F. S., Peyron, O. and Dormoy, I.: Abrupt climate changes of the last deglaciation detected in a Western Mediterranean forest record, Clim. Past, 6(2), 245–264, doi:10.5194/cp-6-245-2010, 2010.

Gaillard, M. J., Sugita, S., Mazier, F., Trondman, A. K., Broström, A., Hickler, T., Kaplan, J. O., Kjellström, E., Kokfelt, U., Kuneš, P., Lemmen, C., Miller, P., Olofsson, J., Poska, A., Rundgren, M., Smith, B., Strandberg, G., Fyfe, R., Nielsen, A. B., Alenius, T., Balakauskas, L., Barnekow, L., Birks, H. J. B., Bjune, A., Björkman, L., Giesecke, T., Hjelle, K., Kalnina, L., Kangur, M., Van Der Knaap, W. O., Koff, T., Lageras, P., Latałowa, M., Leydet, M., Lechterbeck, J., Lindbladh, M., Odgaard, B., Peglar, S., Segerström, U., Von Stedingk, H.

and Seppä, H.: Holocene land-cover reconstructions for studies on land cover-climate feedbacks, Clim. Past, 6(4), 483–499, doi:10.5194/cp-6-483-2010, 2010.

García-Amorena, I., Gómez Manzaneque, F., Rubiales, J. M., Granja, H. M., Soares de Carvalho, G. and Morla, C.: The Late Quaternary coastal forests of western Iberia: A study of their macroremains, Palaeogeogr. Palaeoclimatol. Palaeoecol., 254(3–4), 448–461, doi:10.1016/j.palaeo.2007.07.003, 2007.

Genov, I.: The Black Sea level from the Last Glacial Maximum to the present time, Geol. Balc., 45(1–3), 3–19, 2016.

Giesecke, T.: Did thermophilous trees spread into central Europe during the Late Glacial?, New Phytol., 212(1), 15–18, doi:10.1111/nph.14149, 2016.

Giesecke, T., Davis, B., Brewer, S., Finsinger, W., Wolters, S., Blaauw, M., de Beaulieu, J.-L., Binney, H., Fyfe, R. M., Gaillard, M.-J., Gil-Romera, G., van der Knaap, W. O., Kuneš, P., Kühl, N., van Leeuwen, J. F. N., Leydet, M., Lotter, A. F., Ortu, E., Semmler, M. and Bradshaw, R. H. W.: Towards mapping the late Quaternary vegetation change of Europe, Veg. Hist. Archaeobot., 23(1), doi:10.1007/s00334-012-0390-y, 2014.

Geiger, R.: The climate near the ground. Cambridge: Blue Hill Met. Observ. Harvard University 1960

Giraudi, C.: Lake levels and climate for the last 30,000 years in the fucino area (Abruzzo-Central Italy) - A review, Palaeogeogr. Palaeoclimatol. Palaeoecol., 70(1–3), 249–260, doi:10.1016/0031-0182(89)90094-1, 1989.

Giraudi, C.: Climate evolution and forcing during the last 40 ka from the oscillations in Apennine glaciers and high mountain lakes, Italy, J. Quat. Sci., 32(8), 1085–1098, doi:10.1002/jqs.2985, 2017.

Guido, M. A., Molinari, C., Moneta, V., Branch, N., Black, S., Simmonds, M., Stastney, P. and Montanari, C.: Climate and vegetation dynamics of the Northern Apennines (Italy) during the Late Pleistocene and Holocene, Quat. Sci. Rev., 231, doi:10.1016/j.quascirev.2020.106206, 2020.

Hansen, M. C., Potapov, P. V., Moore, R., Hancher, M., Turubanova, S. A., Tyukavina, A., Thau, D., Stehman, S. V., Goetz, S. J., Loveland, T. R., Kommareddy, A., Egorov, A., Chini, L., Justice, C. O. and Townshend, J. R. G.: High-resolution global maps of 21st-century forest cover change, Science (80-.)., 342(6160), 850–853, doi:10.1126/science.1244693, 2013.

Grichuk, V. P.: Main types of vegetation (ecosystems) for the maximum cooling of the last glaciation. B. Frenzel, B. Pecsi, A.A. Velichko (Eds.), Atlas of Palaeoclimates and Palaeoenvironments of the Northern Hemisphere, NQUA/Hungarian Academy of Sciences, Budapest, pp. 123-124, doi: 10.2307/1551555, 1992.

Guiot, J., Torre, F., Jolly, D., Peyron, O., Boreux, J.J., Cheddadi, R.: Inverse vegetation modeling by Monte Carlo sampling to reconstruct palaeoclimates under changed precipitation seasonality and CO2 conditions: application to glacial climate in Mediterranean region. Ecol. Model. 127, 119–140. doi: 10.1016/ S0304-3800(99)00219-7, 2000.

Harrison, S. P., Yu, G. E. and Tarasov, P. E.: Late Quaternary Lake-Level Record from Northern Eurasia, Quat. Res., 45(2), 138–159, doi:10.1006/qres.1996.0016, 1996.

Harrison, S. P., Bartlein, P. J., Brewer, S., Prentice, I. C., Boyd, M., Hessler, I., Holmgren, K., Izumi, K. and Willis, K.: Climate model benchmarking with glacial and mid-Holocene climates, Clim. Dyn., 43(3–4), 671–688, doi:10.1007/s00382-013-1922-6, 2014.

Harrison, S. P., Bartlein, P. J., Izumi, K., Li, G., Annan, J., Hargreaves, J., Braconnot, P. and Kageyama, M.: Evaluation of CMIP5 palaeo-simulations to improve climate projections, Nat. Clim. Chang., 5(8), 735–743, doi:10.1038/nclimate2649, 2015.

Heiri, O., Koinig, K. A., Spötl, C., Barrett, S., Brauer, A., Drescher-Schneider, R., Gaar, D., Ivy-Ochs, S., Kerschner, H., Luetscher, M., Moran, A., Nicolussi, K., Preusser, F., Schmidt, R., Schoeneich, P., Schwörer, C., Sprafke, T., Terhorst, B. and Tinner, W.: Palaeoclimate records 60-8 ka in the Austrian and Swiss Alps and their forelands, Quat. Sci. Rev., 106, 186–205, doi:10.1016/j.quascirev.2014.05.021, 2014.

Heyman, B. M., Heyman, J., Fickert, T., Harbor, J. M. and Forest, B.: Paleo-climate of the central European uplands during the last glacial maximum based on glacier mass-balance modeling Bavarian Forest Republic, Quat. Res., 79(1), 49–54, doi:10.1016/j.yqres.2012.09.005, 2013.

Hughes, A. L. C., Gyllencreutz, R., Lohne, Ø. S., Mangerud, J. and Svendsen, J. I.: The last Eurasian ice sheets - a chronological database and time-slice reconstruction, DATED-1, Boreas, 45(1), 1–45, doi:10.1111/bor.12142, 2016.

Hughes, P. D. and Gibbard, P. L.: A stratigraphical basis for the Last Glacial Maximum (LGM), Quat. Int., 383(June 2014), 174–185, doi:10.1016/j.quaint.2014.06.006, 2015.

Hughes, P. D., Woodward, J. C. and Gibbard, P. L.: Late Pleistocene glaciers and climate in the Mediterranean, Glob. Planet. Change, 50(1–2), 83–98, doi:10.1016/j.gloplacha.2005.07.005, 2006.
Huntley, B.: Dissimilarity mapping between fossil and contemporary pollen spectra in Europe for the past 13,000 years, Quat. Res., 33(3), 360–376, doi:10.1016/0033-5894(90)90062-P, 1990.

Huntley B.: Dissimilarity mapping between fossil and contemporary pollen spectra in Europe for the past 13,000 years. Quaternary Research 33:360–376, 1990.

Huntley, B. and Allen, J. R. M.: Glacial environments III. Palaeovegetation patterns in late glacial Europe, in Neanderthals and modern humans in the European landscape during the last glaciation, edited by T. H. Van Andel and H. C. Davies, pp. 79–102, McDonald Institute for Archaeological Research, Cambridge., 2003.

Huntley, B. and Birks, H. J. B.: An Atlas of Past and Present Pollen Maps for Europe: 0–13,000 B.P. years ago, Cambridge University Press, Cambridge., 1983.

Jalut, G., Andrieu, V., Delibrias, G., Fontaugne, M. and Pages, P.: Palaeoenvironment of the valley of Ossau (Western French Pyrenees) during the last 27 000 year, Pollen et Spores, 30(3–4), 357–393, 1988.

Jalut, G., Marti, J. M., Fontugne, M., Delibrias, G., Vilaplana, J. M. and Julia, R.: Glacial to interglacial vegetation changes in the northern and southern Pyrénées: Deglaciation, vegetation cover and chronology, Quat. Sci. Rev., 11(4), 449–480, doi:10.1016/0277-3791(92)90027-6, 1992.

Jankovska, V.: Vegetation cover in West Carpathians during the Last Glacial period - analogy of present day siberian forest-tundra nad taiga, Palynol. Stratigr. geoecology, (SEPTEMBER 2008), 282–289, 2008.

Janská, V., Jiménez-Alfaro, B., Chytrý, M., Divíšek, J., Anenkhonov, O., Korolyuk, A., Lashchinskyi, N. and Culek, M.: Palaeodistribution modelling of European vegetation types at the Last Glacial Maximum using modern analogues from Siberia: Prospects and limitations, Quat. Sci. Rev., 159, 103–115, doi:10.1016/j.quascirev.2017.01.011, 2017.

Jost, A., Lunt, D., Abe-Ouchi, A., Abe-Ouchi, A., Peyron, O., Valdes, P. J. and Ramstein, G.: High-resolution simulations of the last glacial maximum climate over Europe: A solution to discrepancies with continental palaeoclimatic reconstructions?, Clim. Dyn., 24(6), 577–590, doi:10.1007/s00382-005-0009-4, 2005.

Juggins, S.: Quantitative reconstructions in palaeolimnology : new paradigm or sick science ?, Quat. Sci. Rev., 64, 20–32, doi:10.1016/j.quascirev.2012.12.014, 2013.

Juggins, S.: Rioja: Analysis of Quaternary Science Data, [online] Available from: https://cran.r-project.org/package=rioja, 2020.

Juggins, S. and Birks, H. J. B.: Quantitative Environmental Reconstructions from Biological Data, in Developments in Paleoenvironmental Research 5, edited by H. J. B. Birks, pp. 431–494, Springer ScienceCBusiness Media B.V., 2012.

Juřičková, L., Horáčková, J. and Ložek, V.: Direct evidence of central European forest refugia during the last glacial period based on mollusc fossils, Quat. Res. (United States), 82(1), 222–228, doi:10.1016/j.yqres.2014.01.015, 2014.

Kageyama, M., Laîné, A., Abe-Ouchi, A., Braconnot, P., Cortijo, E., Crucifix, M., de Vernal, A., Guiot, J., Hewitt, C. D., Kitoh, A., Kucera, M., Marti, O., Ohgaito, R., Otto-Bliesner, B., Peltier, W. R., Rosell-Melé, A., Vettoretti, G., Weber, S. L. and Yu, Y.: Last Glacial Maximum temperatures over the North Atlantic, Europe and western Siberia: a comparison between PMIP models, MARGO sea-surface temperatures and pollen-based reconstructions, Quat. Sci. Rev., 25(17–18), 2082–2102, doi:10.1016/j.quascirev.2006.02.010, 2006.

Kageyama, M., Harrison, S. P., Kapsch, M. L., Lofverstrom, M., Lora, J. M., Mikolajewicz, U., ... & Zhu, J. The PMIP4 Last Glacial Maximum experiments: preliminary results and comparison with the PMIP3 simulations. *Climate of the Past*, *17*(3), 1065-1089, 2021.

Kaltenrieder, P., Belis, C. A., Hofstetter, S., Ammann, B., Ravazzi, C. and Tinner, W.: Environmental and climatic conditions at a potential Glacial refugial site of tree species near the Southern Alpine glaciers. New insights from multiproxy sedimentary studies at Lago della Costa (Euganean Hills, Northeastern Italy), Quat. Sci. Rev., 28(25–26), 2647–2662, doi:10.1016/j.quascirev.2009.05.025, 2009.

Kaplan, J. O., Pfeiffer, M., Kolen, J. C. A. and Davis, B. A. S.: Large scale anthropogenic reduction of forest cover in last glacial maximum Europe, PLoS One, 11(11), doi:10.1371/journal.pone.0166726, 2016.

Kehrwald, N. M., McCoy, W. D., Thibeault, J., Burns, S. J. and Oches, E. A.: Paleoclimatic implications of the spatial patterns of modern and LGM European land-snail shell δ18O, Quat. Res., 74(1), 166–176, doi:10.1016/j.yqres.2010.03.001, 2010.

Kelly, A., Charman, D. J. and Newnham, R. M.: A last glacial maximum pollen record from bodmin moor showing a possible cryptic Northern refugium in Southwest England, J. Quat. Sci., 25(3), 296–308, doi:10.1002/jqs.1309, 2010.

Kolodny, Y., Stein, M. and Machlus, M.: Sea-rain-lake relation in the Last Glacial East Mediterranean revealed by δ18O-δ13C in Lake Lisan aragonites, Geochim. Cosmochim. Acta, 69(16), 4045–4060, doi:10.1016/j.gca.2004.11.022, 2005.

Kovács, J., Moravcová, M., Újvári, G. and Pintér, A. G.: Reconstructing the paleoenvironment of East Central Europe in the Late Pleistocene using the oxygen and carbon isotopic signal of tooth in large mammal remains, Quat. Int., 276–277, 145–154, doi:10.1016/j.quaint.2012.04.009, 2012.

Krebs, P., Pezzatti, G. B., Beffa, G., Tinner, W. and Conedera, M.: Revising the sweet chestnut (Castanea sativa Mill.) refugia history of the last glacial period with extended pollen and macrofossil evidence, Quat. Sci. Rev., 206, 111–128, doi:10.1016/j.quascirev.2019.01.002, 2019.

Kuneš, P., Pelánková, B., Chytrý, M., Jankovská, V., Pokorný, P. and Petr, L.: Interpretation of the last-glacial vegetation of eastern-central Europe using modern analogues from southern Siberia, J. Biogeogr., 35(12), 2223–2236, doi:10.1111/j.1365-2699.2008.01974.x, 2008.

Küster, H.: Postglaziale Vegetationsgeschichte Südbayerns. Geobotanische Studien zur Prähistorischen Landschaftskunde, Akademie Verlag, Berlin., 1995.

Lacey, J. H., Leng, M. J., Höbig, N., Reed, J. M., Valero-Garcés, B. and Reicherter, K.: Western Mediterranean climate and environment since Marine Isotope Stage 3: a 50,000-year record from Lake Banyoles, Spain, J. Paleolimnol., 55(2), 113–128, doi:10.1007/s10933-015-9868-9, 2016.

Latombe, G., Burke, A., Vrac, M., Levavasseur, G. and Dumas, C.: Comparison of spatial downscaling methods of general circulation model results to study climate variability during the Last Glacial Maximum, , 2563–2579, 2018.

Lefort J.P., Monnier J.L., Danukalova G.: Transport of Late Pleistocene loess particles by katabatic winds during the lowstands of the English Channel. Journal of the Geological Society 176: 1169–1181, doi: 10.1144/jgs2019-07, 2019.

Lehmkuhl, F., Nett, J.J., P€otter, S., Schulte, P., Sprafke, T., Jary, Z., Antoine, P.,Wacha, L., Wolf, D., Zerboni, A., Ho sek, J., Markovi c, S.B., Obreht, I., Sümegi, P., Veres, D., Zeeden, C., Boemke, B., Schaubert, V., Viehweger, J., Hambach, U.:Loess landscapes of Europe e mapping, geomorphology, and zonal differentiation. Earth Sci. Rev. 215, 103496. https://doi.org/10.1016/j.earscirev.2020.103496, 2021.

Leroy, S. A. G. and Arpe, K.: Glacial refugia for summer-green trees in Europe and south-west Asia as proposed by ECHAM3 time-slice atmospheric model simulations, J. Biogeogr., 34(12), 2115–2128, doi:10.1111/j.1365-2699.2007.01754.x, 2007.

Lev, L., Stein, M., Ito, E., Fruchter, N., Ben-Avraham, Z. and Almogi-Labin, A.: Sedimentary, geochemical and hydrological history of Lake Kinneret during the past 28,000 years, Quat. Sci. Rev., 209, 114–128, doi:10.1016/j.quascirev.2019.02.015, 2019.

Lister, A. M. and Stuart, A. J.: The impact of climate change on large mammal distribution and extinction: Evidence from the last glacial/interglacial transition, Comptes Rendus - Geosci., 340(9–10), 615–620, doi:10.1016/j.crte.2008.04.001, 2008.

López-García, J. M. and Blain, H. A.: Quaternary small vertebrates: State of the art and new insights, Quat. Sci. Rev., 233, doi:10.1016/j.quascirev.2020.106242, 2020.

Ludwig, P., Pinto, J. G., Raible, C. C. and Shao, Y.: Impacts of surface boundary conditions on regional climate model simulations of European climate during the Last Glacial Maximum, Geophys. Res. Lett., 44(10), 5086–5095, doi:10.1002/2017GL073622, 2017.

Luetscher, M., Boch, R., Sodemann, H., Spötl, C., Cheng, H., Edwards, R. L., Frisia, S., Hof, F. and Müller, W.: North Atlantic storm track changes during the Last Glacial Maximum recorded by Alpine speleothems, Nat. Commun., 6, 27–32, doi:10.1038/ncomms7344, 2015.

Magri, D.: Persistence of tree taxa in Europe and Quaternary climate changes, Quat. Int., 219(1–2), 145–151, doi:10.1016/j.quaint.2009.10.032, 2010.

Magri, D. and Parra, I.: Late Quaternary western Mediterranean pollen records and African winds, Earth Planet. Sci. Lett., 200(3–4), 401–408, doi:10.1016/S0012-821X(02)00619-2, 2002.

Magri, D. and Sadori, L.: Late Pleistocene and Holocene pollen stratigraphy at Lago di Vico, central Italy, Veg. Hist. Archaeobot., 8(4), 247–260, doi:10.1007/BF01291777, 1999.

Magyari, E., Jakab, G., Rudner, E. and Sümegi, P.: Palynological and plant macrofossil data on Late Pleistocene short-term climatic oscillations in NE-Hungary, Acta Palaeobot. Suppl., 2(January), 491–502, 1999.

Magyari, E. K., Kuneš, P., Jakab, G., Sümegi, P., Pelánková, B., Schäbitz, F., Braun, M. and Chytrý, M.: Late Pleniglacial vegetation in eastern-central Europe: Are there modern analogues in Siberia?, Quat. Sci. Rev., 95, 60–79, doi:10.1016/j.quascirev.2014.04.020, 2014a.

Magyari, E. K., Veres, D., Wennrich, V., Wagner, B., Braun, M., Jakab, G., Karátson, D., Pál, Z., Ferenczy, G., St-Onge, G., Rethemeyer, J., Francois, J. P., von Reumont, F. and Schäbitz, F.: Vegetation and environmental responses to climate forcing during the Last Glacial Maximum and deglaciation in the East Carpathians: Attenuated response to maximum cooling and increased biomass burning, Quat. Sci. Rev., 106, 278–298, doi:10.1016/j.quascirev.2014.09.015, 2014b.

Magyari, E. K., Pál, I., Vincze, I., Veres, D., Jakab, G., Braun, M., Szalai, Z., Szabó, Z. and Korponai, J.: Warm Younger Dryas summers and early late glacial spread of temperate deciduous trees in the Pannonian Basin during the last glacial termination (20-9 kyr cal BP), Quat. Sci. Rev., 225, doi:10.1016/j.quascirev.2019.105980, 2019.

Margari, V., Gibbard, P. L., Bryant, C. L. and Tzedakis, P. C.: Character of vegetational and environmental changes in southern Europe during the last glacial period; evidence from Lesvos Island, Greece, Quat. Sci. Rev., 28(13–14), 1317–1339, doi:10.1016/j.quascirev.2009.01.008, 2009.

Marsicek, J., Shuman, B. N., Bartlein, P. J., Shafer, S. L. and Brewer, S.: Reconciling divergent trends and millennial variations in Holocene temperatures, Nature, 554(7690), 92–96, doi:10.1038/nature25464, 2018.

Mauch Lenardić, J., Oros Sršen, A. and Radović, S.: Quaternary fauna of the Eastern Adriatic (Croatia) with the special review on the Late Pleistocene sites, Quat. Int., 494, 130–151, doi:10.1016/j.quaint.2017.11.028, 2018.

Mauri, A., Davis, B. A. S., Collins, P. M. and Kaplan, J. O.: The influence of atmospheric circulation on the mid-Holocene climate of Europe: A data-model comparison, Clim. Past, 10(5), 1925–1938, doi:10.5194/cp-10-1925-2014, 2014.

Mauri, A., Davis, B. A. S., Collins, P. M. and Kaplan, J. O.: The climate of Europe during the Holocene: A gridded pollen-based reconstruction and its multi-proxy evaluation, Quat. Sci. Rev., 112, doi:10.1016/j.quascirev.2015.01.013, 2015.

MARGE Project Members.: Constraints on the magnitude and patterns of ocean cooling at the Last Glacial Maximum, , (January), 1–6, doi:10.1038/ngeo411, 2009.

Mikolajewicz, U.: Modeling mediterranean ocean climate of the last glacial maximum, Clim. Past, 7(1), 161–180, doi:10.5194/cp-7-161-2011, 2011.

Miola, A., Bondesan, A., Corain, L., Favaretto, S., Mozzi, P., Piovan, S. and Sostizzo, I.: Wetlands in the Venetian Po Plain (northeastern Italy) during the Last Glacial Maximum:

Interplay between vegetation, hydrology and sedimentary environment, Rev. Palaeobot. Palynol., 141(1–2), 53–81, doi:10.1016/j.revpalbo.2006.03.016, 2006.

Mix, A. C., Bard, E. and Schneider, R.: Environmental processes of the ice age: Land, oceans, glaciers (EPILOG), Quat. Sci. Rev., 20(4), 627–657, doi:10.1016/S0277-3791(00)00145-1, 2001.

Moine, O., Rousseau, D. D., Jolly, D. and Vianey-Liaud, M.: Paleoclimatic reconstruction using mutual climatic range on terrestrial mollusks, Quat. Res., 57(1), 162–172, doi:10.1006/qres.2001.2286, 2002.

Monegato, G., Ravazzi, C., Donegana, M., Pini, R., Calderoni, G. and Wick, L.: Evidence of a two-fold glacial advance during the last glacial maximum in the Tagliamento end moraine system (eastern Alps), Quat. Res., 68(2), 284–302, doi:10.1016/j.yqres.2007.07.002, 2007.

Monegato, G., Ravazzi, C., Culiberg, M., Pini, R., Bavec, M., Calderoni, G., Jež, J. and Perego, R.: Sedimentary evolution and persistence of open forests between the south-eastern Alpine fringe and the Northern Dinarides during the Last Glacial Maximum, Palaeogeogr. Palaeoclimatol. Palaeoecol., 436, 23–40, doi:10.1016/j.palaeo.2015.06.025, 2015.

Moreno, A., González-Sampériz, P., Morellón, M., Valero-Garcés, B. L. and Fletcher, W. J.: Northern Iberian abrupt climate change dynamics during the last glacial cycle: A view from lacustrine sediments, Quat. Sci. Rev., 36, 139–153, doi:10.1016/j.quascirev.2010.06.031, 2012.

Nogues-Bravo D, Rodríguez-Sánchez F, Orsini L, de Boer E, Jansson R, Morlon, H., Fordham, D.A., Jackson, S.T.: Cracking the code of biodiversity responses to past climate change. *Trends Ecol. Evol.* 33:765–76, 2018.

~~Williams, J.W., Grimm, E.G., Blois, J., Charles, D.F., Davis, E., Goring, S.J., Graham, R., Smith, A.J., Anderson, M., Arroyo-Cabrales, J., Ashworth, A.C., Betancourt, J.L., Bills, B.W., Booth, R.K., Buckland, P., Curry, B., Giesecke, T., Hausmann, S., Jackson, S.T., Latorre, C., Nichols, J., Purdum, T., Roth, R.E., Stryker, M., Takahara, H. :The Neotoma Paleoecology Database: A multi-proxy, international community-curated data resource. Quat. Res. 89, 156-177, doi:10.1017/qua.2017.105, 2018.~~

Nolan, C., Overpeck, J. T., Allen, J. R. M., Anderson, P. M., Betancourt, J. L., Binney, H. A., Brewer, S., Bush, M. B., Chase, B. M., Cheddadi, R., Djamali, M., Dodson, J., Edwards, M. E., Gosling, W. D., Haberle, S., Hotchkiss, S. C., Huntley, B., Ivory, S. J., Kershaw, A. P., Kim, S. H., Latorre, C., Leydet, M., Lézine, A. M., Liu, K. B., Liu, Y., Lozhkin, A. V., McGlone, M. S., Marchant, R. A., Momohara, A., Moreno, P. I., Müller, S., Otto-Bliesner, B. L., Shen, C., Stevenson, J., Takahara, H., Tarasov, P. E., Tipton, J., Vincens, A., Weng, C., Xu, Q., Zheng, Z. and Jackson, S. T.: Past and future global transformation of terrestrial ecosystems under climate change, Science (80-.)., 361(6405), 920–923, doi:10.1126/science.aan5360, 2018.

Normand, S., Treier, U. A. and Odgaard, B. V.: Tree refugia and slow forest development in response to post - LGM warming in North - Eastern European Russia, , 2(4), 2–5, 2011.

Paganelli, A.: Evolution of vegetation and climate in the Veneto-Po Plain during the Late-Glacial and Early Holocene using pollen-strat-igraphical data, Alp. Mediterr. Quat., 9(2), 581–589, 1996.

Peyron, O., Guiot, J., Cheddadi, R., Tarasov, P., Reille, M., De Beaulieu, J. L., Bottema, S. and Andrieu, V.: Climatic Reconstruction in Europe for 18,000 YR B.P. from Pollen Data, Quat. Res., 49(2), 183–196, doi:10.1006/qres.1997.1961, 1998a.

Peyron, O., Cheddadi, R., Tarasov, P. and Reille, M.: Climatic Reconstruction in Europe for 18 , 000 YR B . P . from Pollen Data, , 196(49), 183–196, 1998b.

Pons, A. and Reille, M.: The Holocene- and upper Pleistocene pollen record from Padul (Granada, Spain): A new study, Palaeogeogr. Palaeoclimatol. Palaeoecol., 66(3–4), doi:10.1016/0031-0182(88)90202-7, 1988.

Potì, A., Kehl, M., Broich, M., Carrión Marco, Y., Hutterer, R., Jentke, T., Linstädter, J., López-Sáez, J. A., Mikdad, A., Morales, J., Pérez-Díaz, S., Portillo, M., Schmid, C., Vidal-Matutano, P. and Weniger, G. C.: Human occupation and environmental change in the western Maghreb during the Last Glacial Maximum (LGM) and the Late Glacial. New evidence from the Iberomaurusian site Ifri El Baroud (northeast Morocco), Quat. Sci. Rev., 220, 87–110, doi:10.1016/j.quascirev.2019.07.013, 2019.

Prentice, I. C., Cleator, S. F., Huang, Y. H., Harrison, S. P., and Roulstone, I.: Reconstructing ice-age palaeoclimates: Quantifying low-CO2 effects on plants, Global Planet. Change, 149, 166–176, https://doi.org/10.1016/j.gloplacha.2016.12.012, 2017.

Prentice, I. C. and Harrison, S. P.: Ecosystem effects of CO2 concentration: Evidence from past climates, Clim. Past, 5(3), 297–307, doi:10.5194/cp-5-297-2009, 2009.

Prentice, I. C., Guiot, J. and Harrison, S. P.: Mediterranean vegetation, lake levels and palaeoclimate at the Last Glacial Maximum, Nature, 360(6405), 658–660, doi:10.1038/360658a0, 1992.

Prentice, I. C., Guiot, J., Huntley, B., Jolly, D. and Cheddadi, R.: Reconstructing biomes from palaeoecological data: A general method and its application to European pollen data at 0 and 6 ka, Clim. Dyn., 12(3), 185–194, doi:10.1007/BF00211617, 1996.

Prentice, I. C., Harrison, S. P. and Bartlein, P. J.: Global vegetation and terrestrial carbon cycle changes after the last ice age, New Phytol., 189(4), 988–998, doi:10.1111/j.1469-8137.2010.03620.x, 2011.

Prud'homme, C., Lécuyer, C., Antoine, P., Moine, O., Hatté, C., Fourel, F., Martineau, F. and Rousseau, D. D.: Palaeotemperature reconstruction during the Last Glacial from δ18O of earthworm calcite granules from Nussloch loess sequence, Germany, Earth Planet. Sci. Lett., 442, 13–20, doi:10.1016/j.epsl.2016.02.045, 2016.

Prud'homme, C., Lécuyer, C., Antoine, P., Hatté, C., Moine, O., Fourel, F., Amiot, R., Martineau, F. and Rousseau, D. D.: δ13C signal of earthworm calcite granules: A new proxy for palaeoprecipitation reconstructions during the Last Glacial in western Europe, Quat. Sci. Rev., 179, 158–166, doi:10.1016/j.quascirev.2017.11.017, 2018.

Puzachenko, A. Y., Markova, A. K. and Pawłowska, K.: Evolution of Central European regional mammal assemblages between the late Middle Pleistocene and the Holocene (MIS7–MIS1), Quat. Int., (November), doi:10.1016/j.quaint.2021.11.009, 2021.

Ramstein, G., Kageyama, M., Guiot, J. and Wu, H.: How cold was Europe at the Last Glacial Maximum ? A synthesis of the progress achieved since the first PMIP model-data comparison, , 331–339, 2007.

Reille, M. and Andrieu, V.: The late Pleistocene and Holocene in the Lourdes Basin, Western Pyrénées, France: new pollen analytical and chronological data, Veg. Hist. Archaeobot., 4(1), 1–21, doi:10.1007/BF00198611, 1995.

Reille, M. and de Beaulieu, J. L.: History of the Würm and Holocene vegetation in western velay (Massif Central, France): A comparison of pollen analysis from three corings at Lac du Bouchet, Rev. Palaeobot. Palynol., 54(3–4), 233–248, doi:10.1016/0034-6667(88)90016-4, 1988.

Reimer, A., Landmann, G. and Kempe, S.: Lake Van, Eastern Anatolia, hydrochemistry and history, Aquat. Geochemistry, 15(1–2), 195–222, doi:10.1007/s10498-008-9049-9, 2009.

Rousseau, D. D.: Climatic transfer function from quaternary molluscs in European loess deposits, Quat. Res., 36(2), 195–209, doi:10.1016/0033-5894(91)90025-Z, 1991.

Royer, A., Montuire, S., Legendre, S., Discamps, E., Jeannet, M. and Lécuyer, C.: Investigating the influence of climate changes on rodent communities at a regional-scale (MIS 1-3, Southwestern France), PLoS One, 11(1), 1–25, doi:10.1371/journal.pone.0145600, 2016.

Ruiz-Zapata, M. B., Vegas, J., Garcia-Cortes, A., Gil Garcia, M. J., Torres, T., Ortiz, J. E. and Perez-Gonzalez, A.: Vegetation evolution during the Last Maximum Glacial Period in FU-1 sequence (Fuentillejo Lacustrin Maar, Campo de Calatrava, Ciudad Real), Polen, 18, 37–49, 2008.

Salonen, J.S., Ilvonen, L., Seppä, H., Holmström, L., Telford, R.J., Gaidamavicius, A., Stancikaite, M., Subetto, D., Comparing different calibration methods (WA/WA-PLS regression and Bayesian modelling) and different-sized calibration sets in pollen-based quantitative climate reconstruction. The Holocene 22, 413–424, 2012.

Samartin, S., Heiri, O., Kaltenrieder, P., Kühl, N. and Tinner, W.: Reconstruction of full glacial environments and summer temperatures from Lago della Costa, a refugial site in Northern Italy, Quat. Sci. Rev., 143, 107–119, doi:10.1016/j.quascirev.2016.04.005, 2016.

Sanchez Goñi, M.F., Harrison, S.P.: Millennial-scale climate variability and vegetation changes during the Last Glacial: concepts and terminology. Quaternary Science Reviews 29, 2823–2827, doi: 10.1016/j.quascirev.2009.11.014, 2010.

Sanchi, L., Ménot, G. and Bard, E.: Insights into continental temperatures in the northwestern Black Sea area during the Last Glacial period using branched tetraether lipids, Quat. Sci. Rev., 84, 98–108, doi:10.1016/j.quascirev.2013.11.013, 2014.

Satkūnas, J. and Grigienė, A.: Eemian-Weichselian palaeoenvironmental record from the Mickūnai glacial depression (Eastern Lithuania), Geologija, 54(2), 35–51, doi:10.6001/geologija.v54i2.2482, 2012.
Schäfer, I. K., Bliedtner, M., Wolf, D., Faust, D. and Zech, R.: Evidence for humid conditions during the last glacial from leaf wax patterns in the loess-paleosol sequence El Paraíso, Central Spain, Quat. Int., 407, 64–73, doi:10.1016/j.quaint.2016.01.061, 2016.

Scourse, J. D.: Late Pleistocene stratigraphy and palaeobotany of the Isles of Scilly, Philos. Trans. - R. Soc. London, B, 334(1271), 405–448, doi:10.1098/rstb.1991.0125, 1991.

Spötl, C., Koltai, G., Jarosch, A. H. and Cheng, H.: Increased autumn and winter precipitation during the Last Glacial Maximum in the European Alps, Nat. Commun., 12(1), doi:10.1038/s41467-021-22090-7, 2021.

Stewart, J. R. and Lister, A. M.: Cryptic northern refugia and the origins of the modern biota, Trends Ecol. Evol., 16(11), 608–613, doi:10.1016/S0169-5347(01)02338-2, 2001.

Stivrins, N., Soininen, J., Amon, L., Fontana, S. L., Gryguc, G., Heikkilä, M., Heiri, O., Kisielienė, D., Reitalu, T., Stančikaitė, M., Veski, S. and Seppä, H.: Biotic turnover rates during the Pleistocene-Holocene transition, Quat. Sci. Rev., 151, 100–110, doi:10.1016/j.quascirev.2016.09.008, 2016.

Strahl, J.: Zur Pollenstratigraphie des Weichselspätglazials von Berlin-Brandenburg [On the palynostratigraphy of the Late Weichselian in Berlin-Brandenburg], Brand. Geowissenschaftliche Beiträge, 12, 87–112, 2005.

Stute, M. and Deak, J.: Environmental isotope study (14C, 13C, 18O, D, noble gases) on deep groundwater circulation systems in Hungary with reference to paleoclimate, Radiocarbon, 31(3), 902–918, doi:10.1017/s0033822200012522, 1990.

Svenning, J., Normand, S. and Kageyama, M.: Glacial refugia of temperate trees in Europe : insights from species distribution modelling, , (Svenning 2003), 1117–1127, doi:10.1111/j.1365-2745.2008.01422.x, 2008.

Tarasov, P. E., Webb, T., Andreev, A. A., Afanas'eva, N. B., Berezina, N. A., Bezusko, L. G., Blyakharchuk, T. A., Bolikhovskaya, N. S., Cheddadi, R., Chernavskaya, M. M., Chernova, G. M., Dorofeyuk, N. I., Dirksen, V. G., Elina, G. A., Filimonova, L. V., Glebov, F. Z., Guiot, J., Gunova, V. S., Harrison, S. P., Jolly, D., Khomutova, V. I., Kvavadze, E. V., Osipova, I. M., Panova, N. K., Prentice, I. C., Saarse, L., Sevastyanov, D. V., Volkova, V. S. and Zernitskaya, V. P.: Present-day and mid-Holocene biomes reconstructed from pollen and plant macrofossil data from the former Soviet Union and Mongolia, J. Biogeogr., 25(6), 1029–1053, doi:10.1046/j.1365-2699.1998.00236.x, 1998.

Tarasov, P. E., Volkova, V. S., Webb, T., Guiot, J., Andreev, A. A., Bezusko, L. G., Bezusko, T. V., Bykova, G. V., Dorofeyuk, N. I., Kvavadze, E. V., Osipova, I. M., Panova, N. K. and Sevastyanov, D. V.: Last glacial maximum biomes reconstructed from pollen and plant macrofossil data from northern Eurasia, J. Biogeogr., 27(3), 609–620, doi:10.1046/j.1365-2699.2000.00429.x, 2000.

Tarasov, P.E., Andreev, A.A., Anderson, P.M., Lozhkin, A.V., Haltia-Hovi, E., Nowaczyk, N.R., Wennrich, V., Brigham-Grette, J., Melles, M.: A pollen-based biome reconstruction over the last 3.562 million years in the Far East Russian Arctic e new insights on climate-vegetation relationships at the regional scale. Clim. Past 9, 2759-2775, doi: 10.5194/cp-9-2759-2013, 2013.

Telford, R. J. and Birks, H. J. B.: Evaluation of transfer functions in spatially structured environments, Quat. Sci. Rev., 28(13–14), 1309–1316, doi:10.1016/j.quascirev.2008.12.020, 2009.

Turner, M. G., Wei, D., Prentice, I. C., & Harrison, S. P. The impact of methodological decisions on climate reconstructions using WA-PLS. *Quaternary Research*, *99*, 341-356, 2021.

Valero-Garcés, B. L., González-Sampériz, P., Navas, A., Machin, J., Delgado-Huertas, A., Pena-Monné, J. L., Sancho-Marcén, C., Stevenson, T. and Davis, B.: Paleohydrological fluctuations and steppe vegetation during the last glacial maximum in the central Ebro valley (NE Spain), Quat. Int., 122(1 SPEC. ISS.), doi:10.1016/j.quaint.2004.01.030, 2004.

Valsecchi, V., Sanchez Goñi, M. F. and Londeix, L.: Vegetation dynamics in the Northeastern Mediterranean region during the past 23 000 yr: Insights from a new pollen record from the Sea of Marmara, Clim. Past, 8(5), 1941–1956, doi:10.5194/cp-8-1941-2012, 2012.

Vandenberghe, J., French, H. M., Gorbunov, A., Marchenko, S., Velichko, A. A., Jin, H., Cui, Z., Zhang, T. and Wan, X.: The Last Permafrost Maximum (LPM) map of the Northern Hemisphere: Permafrost extent and mean annual air temperatures, 25-17ka BP, Boreas, 43(3), 652–666, doi:10.1111/bor.12070, 2014.

Varsányi, I., Palcsu, L. and Kovács, L. Ó.: Groundwater flow system as an archive of palaeotemperature: Noble gas, radiocarbon, stable isotope and geochemical study in the Pannonian Basin, Hungary, Appl. Geochemistry, 26(1), 91–104, doi:10.1016/j.apgeochem.2010.11.006, 2011.

Vegas-Vilarrúbia, T., González-Sampériz, P., Morellón, M., Gil-Romera, G., Pérez-Sanz, A. and Valero-Garcés, B.: Diatom and vegetation responses to late glacial and early holocene climate changes at lake estanya (southern pyrenees, NE spain), Palaeogeogr. Palaeoclimatol. Palaeoecol., 392, 335–349, doi:10.1016/j.palaeo.2013.09.011, 2013.

Vegas, J., Ruiz-Zapata, B., Ortiz, J. E., Galán, L., Torres, T., García-Cortés, Á., Gil-García, M. J., Pérez-González, A. and Gallardo-Millán, J. L.: Identification of arid phases during the last 50 cal. ka BP from the Fuentillejo maar-lacustrine record (Campo de Calatrava Volcanic Field, Spain), J. Quat. Sci., 25(7), 1051–1062, doi:10.1002/jqs.1262, 2010.

Velasquez, P., Kaplan, J. O., Messmer, M., Ludwig, P. and Raible, C. C.: The role of land cover in the climate of glacial Europe, Clim. Past, 17(3), 1161–1180, doi:10.5194/cp-17-1161-2021, 2021.

Vicente-Serrano, S. M., Trigo, R. M., López-Moreno, J. I., Liberato, M. L. R., Lorenzo-Lacruz, J., Beguería, S., Morán-Tejeda, E. and El Kenawy, A.: Extreme winter precipitation in the Iberian Peninsula in 2010: Anomalies, driving mechanisms and future projections, Clim. Res., 46(1), 51–65, doi:10.3354/cr00977, 2011.

Williams, J.W., Grimm, E.G., Blois, J., Charles, D.F., Davis, E., Goring, S.J., Graham, R., Smith, A.J., Anderson, M., Arroyo-Cabrales, J., Ashworth, A.C., Betancourt, J.L., Bills, B.W., Booth, R.K., Buckland, P., Curry, B., Giesecke, T., Hausmann, S., Jackson, S.T., Latorre, C., Nichols, J., Purdum, T., Roth, R.E., Stryker, M., Takahara, H. :The Neotoma Paleoecology Database: A multi-proxy, international community-curated data resource. Quat. Res. 89, 156-177, doi:10.1017/qua.2017.105, 2018.

Williams, J. W. and Jackson, S. T.: Palynological and AVHRR observations of modern vegetational gradients in eastern North America, , 4, 485–497, 2003.

Williams, J. W., Webb, T., Shurman, B. N. and Bartlein, P. J.: Do Low CO 2 Concentrations Affect Pollen-Based Reconstructions of LGM Climates? A Response to "Physiological Significance of Low Atmospheric CO 2 for Plant–Climate Interactions" by Cowling and Sykes, Quat. Res., 53(3), 402–404, doi:10.1006/qres.2000.2131, 2000.

Willis, K. J. and Van Andel, T. H.: Trees or no trees? The environments of central and eastern Europe during the Last Glaciation, Quat. Sci. Rev., 23(23–24), 2369–2387, doi:10.1016/j.quascirev.2004.06.002, 2004.

Wu, H., Guiot, J., Brewer, S. and Guo, Z.: Climatic changes in Eurasia and Africa at the last glacial maximum and mid-Holocene: Reconstruction from pollen data using inverse vegetation modelling, Clim. Dyn., 29(2–3), 211–229, doi:10.1007/s00382-007-0231-3, 2007.

Yu, G. and Harrison, S. P.: Lake status records from Europe: data base documentation, NOAA Paleoclimatology Publications Series, Boulder, Colorado., 1995.

Zaarur, S., Affek, H. P. and Stein, M.: Last glacial-Holocene temperatures and hydrology of the Sea of Galilee and Hula Valley from clumped isotopes in Melanopsis shells, Geochim. Cosmochim. Acta, 179, 142–155, doi:10.1016/j.gca.2015.12.034, 2016.

Zanon, M., Davis, B. A. S., Marquer, L., Brewer, S. and Kaplan, J. O.: European forest cover during the past 12,000 years: A palynological reconstruction based on modern analogs and remote sensing, Front. Plant Sci., 9, doi:10.3389/fpls.2018.00253, 2018.

Zech, M., Buggle, B., Leiber, K., Marković, S., Glaser, B., Hambach, U., Huwe, B., Stevens, T., Sümegi, P., Wiesenberg, G. and Zöller, L.: Reconstructing Quaternary vegetation history in the Carpathian Basin, SE-Europe, using n-alkane biomarkers as molecular fossils: Problems and possible solutions, potential and limitations, Quat. Sci. J., 58(2), 148–155, doi:10.3285/eg.58.2.03, 2010.

Tables

Site	Site Name	Country/Ocean	Latitude	Longitude	Elevation	Site Type	Data Type	Samples	Source	Reference
1	MD95-2039 (M)	Atlantic	40.578333	-10.348333	-3381	Marine	Raw Count	21	EPD (E#1472)	Roucoux et al. 2005
2	SU81-18 (M)	Atlantic	37.77	-9.82	-3135	Marine	Raw Count	10	ACER	Turon et al. 2003
3	MD99-2331 (M)	Atlantic	41.15	-9.68	-2110	Marine	Raw Count	41	ACER	Naughton et al. 2006
4	Carn Morval	United Kingdom	49.926111	-6.313889	5	Lake	Digitised	1	Publication	Scourse 1991
5	Gorham Cave	Spain	36.132826	-5.347358	0	Cave	Digitised	1	Publication	Carrion et al. 2008
6	Dozmary Pool	United Kingdom	50.5347222	-4.5358333	265	Lake	Raw Count	32	Author	Kelly et al. 2010
7	Bajondillo	Spain	36.619722	-4.496389	20	Cave	Raw Count	1	EPD (E#1570)	Cortes-Sanchez et al 2011
8	Laguna del maar de Fuentillejo	Spain	38.937996	-4.0539	637	Lake	Digitised	1	Publication	Ruiz-Zapata et al. 2009
9	Padul-1	Spain	37.016338	-3.608503	785	Peat Bog	Digitised	13	Publication	Pons & Reille 1988
10	Padul-2	Spain	37.010833	-3.603889	726	Peat Bog	Digitised	1	Publication	Camuera et al. 2019
11	Cova di Carihuela	Spain	37.4489	-3.4297	1020	Cave	Digitised	1	Publication	Carrion 1992
12	Ifri El Baroud	Morocco	34.75	-3.3	539	Cave	Digitised	1	Publication	Poti et al. 2019
13	MD95-2043 (M)	Mediterranean	36.14	-2.621	-1841	Marine	Raw Count	7	ACER	Fletcher et al. 2008
14	San Rafael	Spain	36.773611	-2.601389	0	Peat Bog	Raw Count	2	EPD (E#574)	Pantaléon-Cano 1997
15	Siles	Spain	38.24	-2.3	1320	Lake	Digitised	1	Publication	Carrion 2002
16	Torrecilla de Valmadrid	Spain	41.4469444	-0.895	570	Colluvium	Digitised	1	Publication	Valero-Garces et al. 2004
17	Navarrés-1	Spain	39.1	-0.683333	225	Peat Bog	Raw Count	1	EPD (E#469)	Carrión & Dupré-Olivier 1996
18	Navarrés-2	Spain	39.1	-0.683333	225	Peat Bog	Raw Count	1	EPD (E#470)	Carrión & Dupré-Olivier 1996
19	Tourbiere de l'Estarres	France	43.0933	-0.3792	356	Lake	Digitised	1	Publication	Jalut et al. 1988
20	Cova de les Malladetes	Spain	39.058	-0.321	20	Cave	Digitised	1	Publication	Dupré Ollivier 1988
21	Lourdes	France	43.033333	-0.075	430	Lake	Digitised	15	Publication	Reille & Andrieu 1995
22	Lake Estanya	Spain	42.0333333	0.53333333	670	Lake	Digitised	1	Publication	Vegas-Villarubia et al. 2013
23	Freychinede	France	42.7833	1.4333	1350	Lake	Digitised	1	Publication	Jalut et al. 1992
24	Banyoles	Spain	42.133333	2.75	173	Lake	Raw Count	13	EPD (E#931)	Pérez-Obiol & Julia 1994
25	Lac du Bouchet B5	France	44.916667	3.783333	1200	Lake	Digitised	14	Publication	Reille & de Beaulieu 1988
26	MD99-2348 (103) (M)	Mediterranean	42.692778	3.841667	-296	Marine	Raw Count	41	EPD (E#1474)	Beaudouin et al. 2007
27	Les Echets G	France	45.9	4.93	267	Peat Bog	Digitised	136	ACER	de Beaulieu & Reille 1984
28	La Grotte Walou	Belgium	50.585278	5.536389	252	Cave	Digitised	1	Publication	Damblon 2011
29	Bergsee	Germany	47.5722222	7.93638889	382	Lake	Digitised	1	Publication	Duprat-Oualid et al. 2017
30	Garaat El-Ouez	Algeria	36.818333	8.33333	45	Peat Bog	Raw Count	6	EPD (E#1501)	Benslama et al 2010
31	Pian del Lago	Italy	44.321561	9.485682	833	Lake	Digitised	1	Publication	Guido et al. 2020
32	Pilsensee	Germany	48.0267	11.1883	534	Lake	Digitised	1	Publication	Küster 1995
33	Orgiano	Italy	45.29	11.43	19	Peat Bog	Digitised	1	Publication	Paganelli 1996
34	Lago della Costa	Italy	45.2702778	11.7430556	7	Lake	Digitised	8	Publication	Kaltenrieder et al. 2009
35	Lagaccione	Italy	42.566667	11.85	355	Lake	Raw Count	7	ACER	Magri 1999
36	Lago Vico	Italy	42.3166667	12.1666667	510	Lake	Digitised	15	Publication	Magri & Sadori 1999
37	Stracciacappa	Italy	42.13	12.32	220	Lake	Raw Count	2	ACER	Giardini 2007
38	Lago di Monterosi	Italy	42.2166667	12.4333333	237	Lake	Raw Count	1	Publication	Bonatti 1970
39	Venice	Italy	45.629523	12.654086	0	Peat Bog	Digitised	1	Publication	Miola et al. 2006
40	Azzano Decimo	Italy	45.8833	12.7165	10	Alluvial Fan	Raw Count	6	ACER	Pini et al. 2009
41	Valle di Castiglione	Italy	41.89	12.75	44	Lake	Raw Count	2	ACER	Follieri et al. 1989
42	Travesio	Italy	46.2	12.87	220	Lake	Digitised	1	Publication	Monegato et al. 2007
43	Orvenco	Italy	46.252088	13.169771	380	Alluvial Fan	Digitised	1	Publication	Monegato et al. 2007
44	Rio Doidis	Italy	46.12	13.19	152	Lake	Digitised	1	Publication	Monegato et al. 2007
45	Billerio	Italy	46.22	13.21	300	Lake	Digitised	1	Publication	Monegato et al. 2007
46	Kersdorf-Briesen	Germany	52.333704	14.269142	44	Lake	Digitised	1	Publication	Strahl 2005
47	Lago Grande di Monticchio	Italy	40.944444	15.6	1326	Lake	Raw Count	6	EPD (E#932)	Watts et al. 1996
48	Nagymohos	Hungary	48.326944	20.436389	297	Peat Bog	Raw Count	14	Publication	Magyari et al 1999
49	Safarka	Slovakia	48.8819444	20.575	600	Peat Bog	Digitised	1	Publication	Jankovska 2008
50	Feher Lake	Hungary	46.45	20.65	86	Lake	Raw Count	10	Publication	Magyari et al. 2014
51	Ioannina	Greece	39.75	20.85	470	Peat Bog	Raw Count	20	ACER	Tzedakis et al. 2004
52	Kokad	Hungary	47.4027778	21.9286111	112	Peat Bog	Raw Count	2	Publication	Magyari et al. 2019
53	Lake Xinias	Greece	39.05	22.27	500	Lake	Raw Count	5	EPD (E#976)	Bottema 1979
54	Mickunai	Lithuania	54.722114	25.532218	143	Lake	Digitised	1	Publication	Satkunas & Grigiene 2012
55	Lake Sfanta Anna	Romania	46.1263889	25.8880556	946	Lake	Digitised	1	Publication	Magyari et al. 2014
56	Megali Limni	Greece	39.1	26.3	323	Lake	Digitised	1	Publication	Margari et al. 2009
57	Straldzha	Bulgaria	42.630278	26.77	138	Peat Bog	Raw Count	3	Publication	Connor et l. 2013
58	MD01-2430 (M)	Turkey	40.796833	27.725166	-580	Marine	Digitised	1	Publication	Valsecchi et al. 2012
59	Lake Iznik	Turkey	40.433889	29.533056	88	Lake	Raw Count	7	EPD (E#714)	Miebach et al 2016
60	M72/5 628-1 (M)	Black Sea	42.1035	36.62383	-418	Marine	Raw Count	6	Pangaea (833387)	Shumilovskikh et al. 2014
61	Dziguta	Georgia	42.99	41.07	35	Peat Bog	Digitised	1	Publication	Arslanov et al. 2007
62	Lake Van LG	Turkey	38.667	42.669	1649	Lake	Raw Count	10	Pangaea (853779)	Pickarski et al. 2015
63	Lake Zeribar	Iran	35.533333	46.116667	1286	Lake	Raw Count	17	EPD (E#714)	van Zeist & Bottema 1977

Table 1. List of selected sites

Site	Site Name	COHMAP Quality	Upper 14C	Upper Cal. BP	Lower 14C	Lower Cal. BP
1	MD95-2039 (M)	3C	14830±80	18166±269	19950±210	23883±374
2	SU81-18 (M)	2C	17510±270	20952±404	21250±280	25420±441
3	MD99-2331 (M)	2C	16170±130	19325±303	19770±170	23682±336
4	Carn Morval	4C		18600±3700	21500±890/800	25867±1127
5	Gorham Cave	4D			18440±160	22055±341
6	Dozmary Pool	2C	14568±129	17569±523	18325±216	21769±602
7	Bajondillo	1C		18701±2154		
8	Laguna del maar de Fuentillejo	5D	16540±90	19847±308		
9	Padul-1	3D	18300±300	21821±412	19100±160	22922±308
10	Padul-2	1D			17450±539	21082±539
11	Cova di Carihuela	2C	15700±220	18958±280	21430±130	25659±226
12	Ifri El Baroud	2D	17296±87	20761±293		
13	MD95-2043 (M)	2C	15440±90	18533±294	18260±120	21951±335
14	San Rafael	3D	9980±60	11464±133	16860±120	20083±292
15	Siles	2D	17030±80	20345±351		
16	Torrecilla de Valmadrid	2D	17100±85	20456±366		
17	Navarrés-1	4D	18360±195	22001±353	20700±295	24664±411
18	Navarrés-2	5D	5150±50	5881±85	16000±	19144±
19	Tourbiere de l'Estarres	1C	17150±250	20522±470	18970±160	22847±317
20	Cova de les Malladetes	5D	16300±1500	19686±1723		
21	Lourdes	4D	18510±130	22112±130	20025±175	23952±355
22	Lake Estanya	5D		9498±50		19184±251
23	Freychinede	3C	14800±800	17912±856	21300±760	25615±1030
24	Banyoles	4C		19878±100		27862±3000
25	Lac du Bouchet B5	2C	15350±350	18513±435	19200±300	23006±384
26	MD99-2348 (103) (M)	1D	17660±60	21065±310	19350±90	23111±271
27	Les Echets G	1C	17530±270	20970±407	18030±250	21704±473
28	La Grotte Walou	1D				21200±700
29	Bergsee	2D			17780±90	21244±306
30	Garaat El-Ouez	2C	16010±320	19200±801		
31	Pian del Lago	2D				21260±320
32	Pilsensee	6D	15860±250	19073±290		
33	Orgiano	2D	17760±160	21221±373	19290±520	23141±621
34	Lago della Costa	2C	15400±150	18484±330	19285±160	23052±302
35	Lagaccione	2C	16080±450	19369±527	20615±940	24746±1201
36	Lago Vico	3C	14385±140	17541±272	20500±230	24430±376
37	Stracciacappa	4C	12060±130	14093±281	19745±820	22675±955
38	Lago di Monterosi	2D	17040±350	20398±544		
39	Venice	5D			18640±100	22277±336
40	Azzano Decimo	2D	18000±300	21637±529	21025±245	25179±449
41	Valle di Castiglione	3C	14220±145	17443±270	20300±700	24266±842
42	Travesio	5D			18780±200	22483±406
43	Orvenco	2D	17760±160	21221±373	19290±520	23141±621
44	Rio Doidis	5D			18860±190	22390±373
45	Billerio	3D			18165±200	21872±382
46	Kersdorf-Briesen	1D			17622±94	21183±356
47	Lago Grande di Monticchio	2C		20204±		24014±
48	Nagymohos	2C	14246±144	17361±425	18159±247	21735±622
49	Safarka	3D			18287±1512	21912±1781
50	Feher Lake	1D	17715±250	21190±463	19911±81	23841±313
51	Ioannina	3C	15330±140	18420±312	20760±230	24748±330
52	Kokad	5D	14326±63	17433±443	16280±90	19685±538
53	Lake Xinias	6C	11150±130	13049±160	21390±430	25671±648
54	Mickunai	1D		21000±2200		
55	Lake Sfanta Anna	1D	17626±96	20955±432		
56	Megali Limni	6D	19072±237	22906±340		
57	Straldzha	6C	14696±65	18022±364	23653±114	28580±390
58	MD01-2430 (M)	4C	12050±75	14904±324	18310±380	21746±968
59	Lake Iznik	7D	16910±100	19515±115		
60	M72/5 628-1 (M)	2C	16835±85	18490±	19495±90	21280±
61	Dziguta	4C	12990±160	15839±483	20560±880	24666±1126
62	Lake Van LG	2C		18590±62		23290±596
63	Lake Zeribar	4C	13650±160	16610±399	22000±500	26462±880

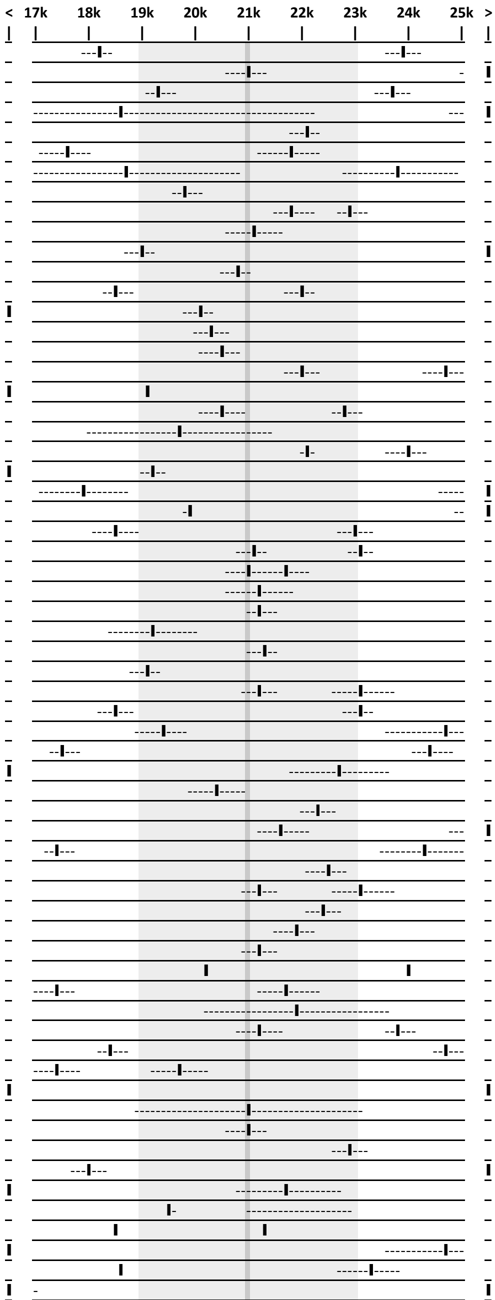

~~COHMAP chronological quality classification:~~
~~1C: Bracketing dates within 2000 14C (2360 Cal.) yr interval about the time being assessed~~
~~2C: Bracketing dates, one within 2000 14C (2360 Cal.) yr and the second within 4000 14C (4682 Cal.) yr of the time being assessed~~
~~3C: Bracketing dates within 4000 14C (4682 Cal.) yr interval about the time being assessed~~
~~4C: Bracketing dates, one being within 4000 14C (4682 Cal.) yr and the second being within 6000 14C (7490 Cal.) yr of the time being assessed~~
~~5C: Bracketing dates within 6000 14C (7490 Cal.) yr interval about the time being assessed~~
~~6C: Bracketing dates, one within 6000 14C (7490 Cal.) yr and the second within 8000 14C (9681 Cal.) yr of the time being assessed~~
~~7C: Poorly dated~~
~~1D: Date within 250 14C (206 Cal.) yr of the time being assessed~~
~~2D: Date within 500 14C (684 Cal.) yr of the time being assessed~~
~~3D: Date within 750 14C (975 Cal.) yr of the time being assessed~~
~~4D: Date within 1000 14C (1123 Cal.) yr of the time being assessed~~
~~5D: Date within 1500 14C (1881 Cal.) yr of the time being assessed~~
~~6D: Date within 2000 14C (2360 Cal.) yr of the time being assessed~~
~~7D: Poorly dated~~

~~Table 2. Chronological control~~

	RMSE	R2
TANN	2.28	0.9
TDJF	3.35	0.91
TJJA	2.21	0.81
PANN	224.94	0.69
PDJF	78.51	0.69
PJJA	52.49	0.75
Tree Cover	21.03	0.52

Table 2~~3~~. MAT performance statistics based on the modern pollen sample training set. This includes Mean Annual Temperature and Precipitation (TANN and PANN), Mean Winter Temperature and Precipitation (TDJF and PDJF) and Mean Summer Temperature and Precipitation (TJJA and PJJA).

Figures

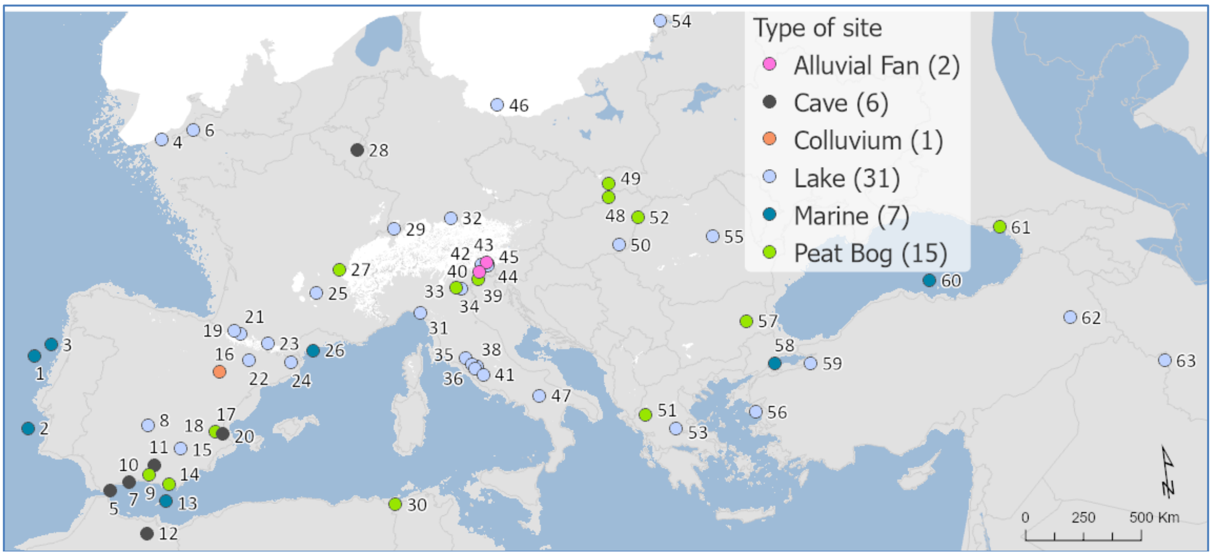

Figure 1. Site locations and archives (Site numbers are as shown in Table 1)

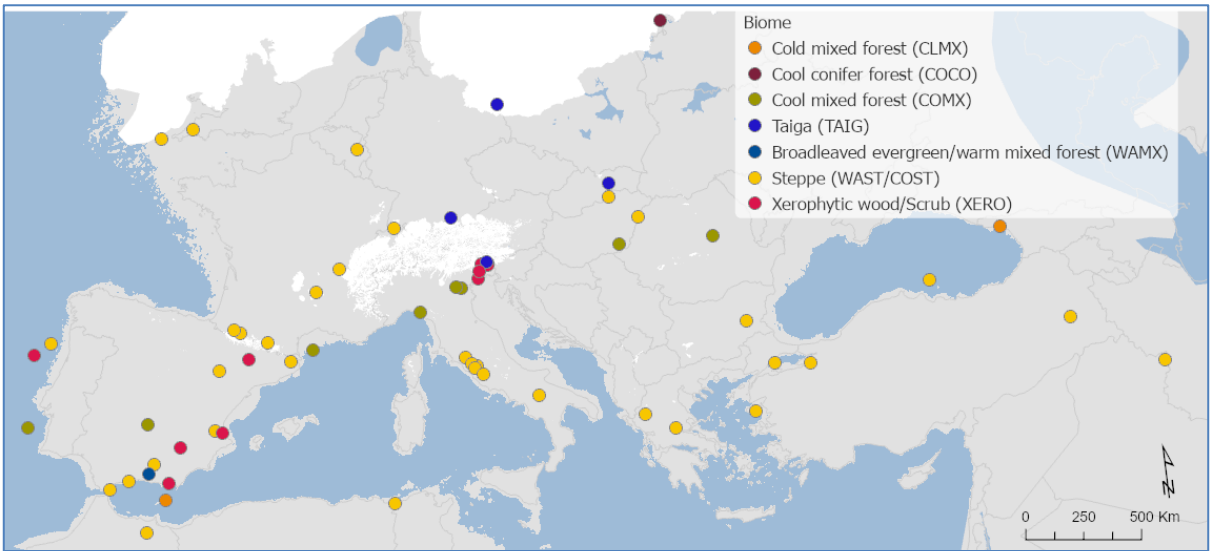

Figure 2. Pollen biomes

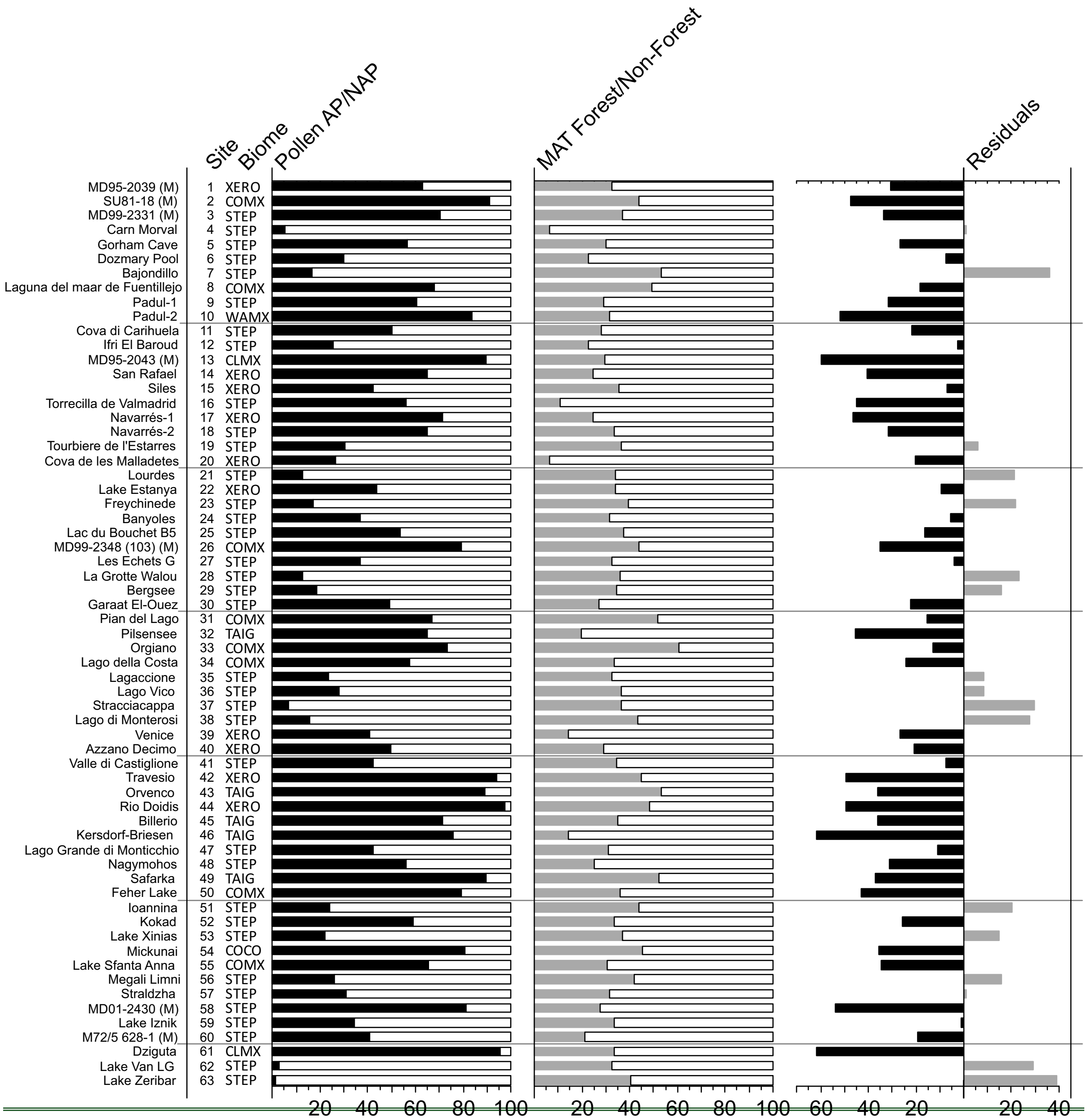

~~Figure 3. Pollen biomes (see figure 2 for key), Arboreal Pollen (AP) % forest cover, MAT % forest cover and residuals (AP % compared to MAT Forest %)~~

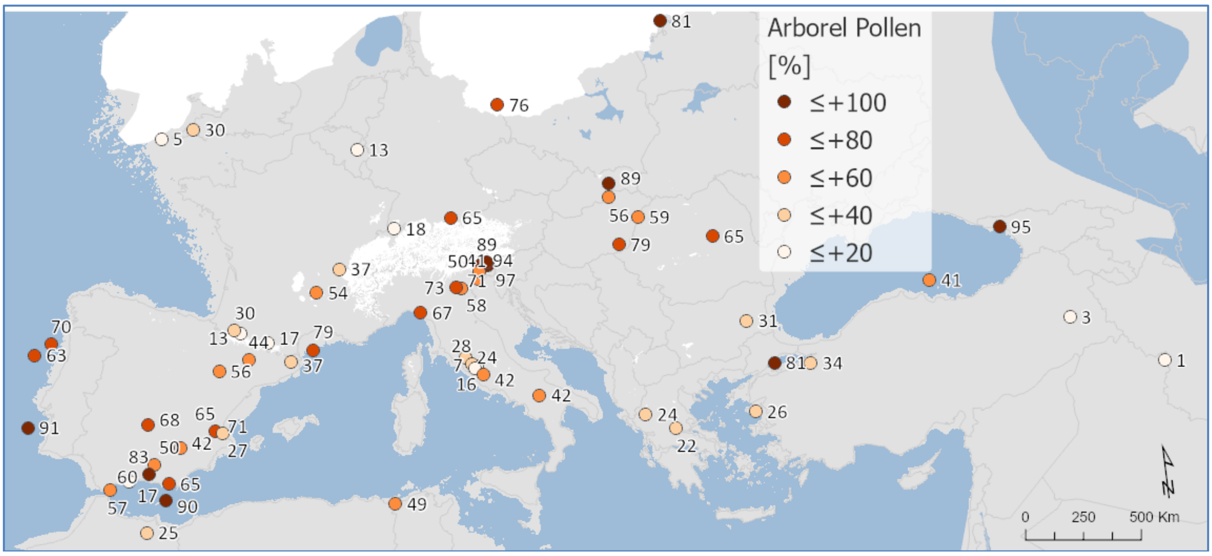

Figure 34. Arboreal Pollen (AP) % forest cover

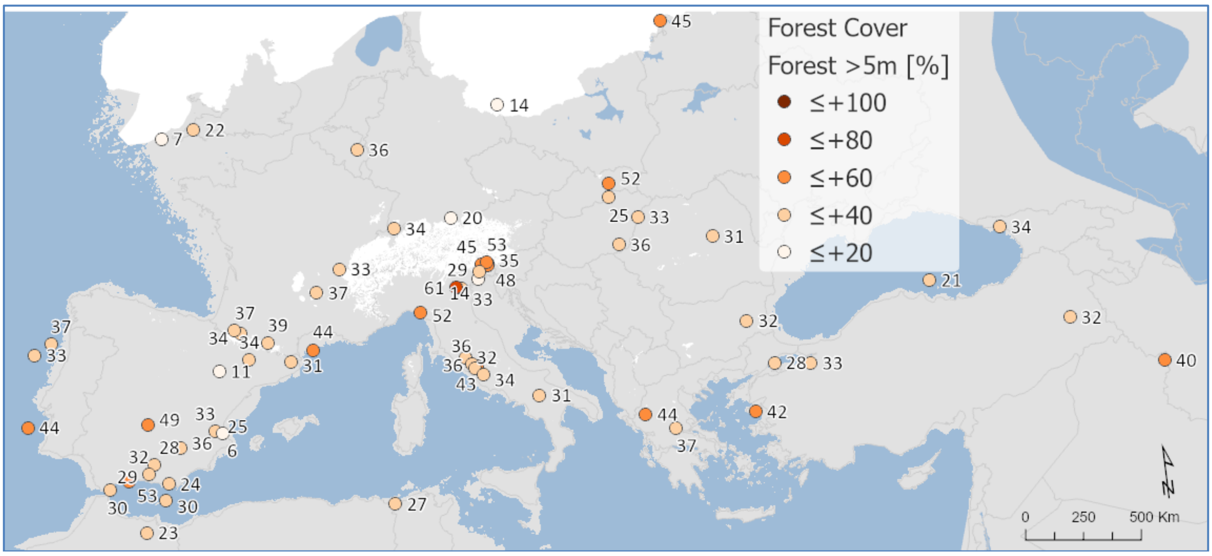

Figure ~~5~~4. Modern Analogue Technique (MAT) % forest cover

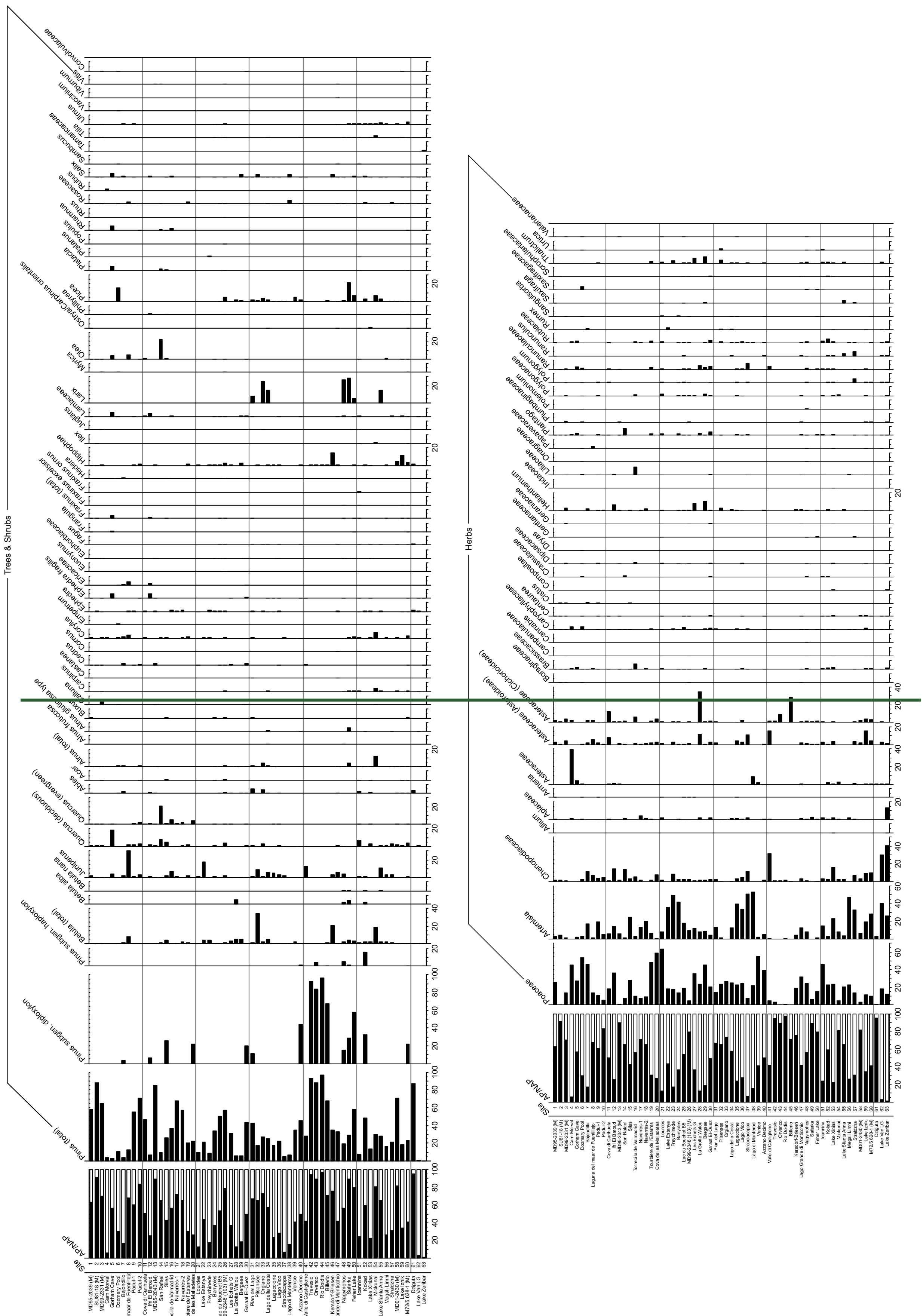

Figure 6. Pollen taxa percentages for all LGM sites/records

2291

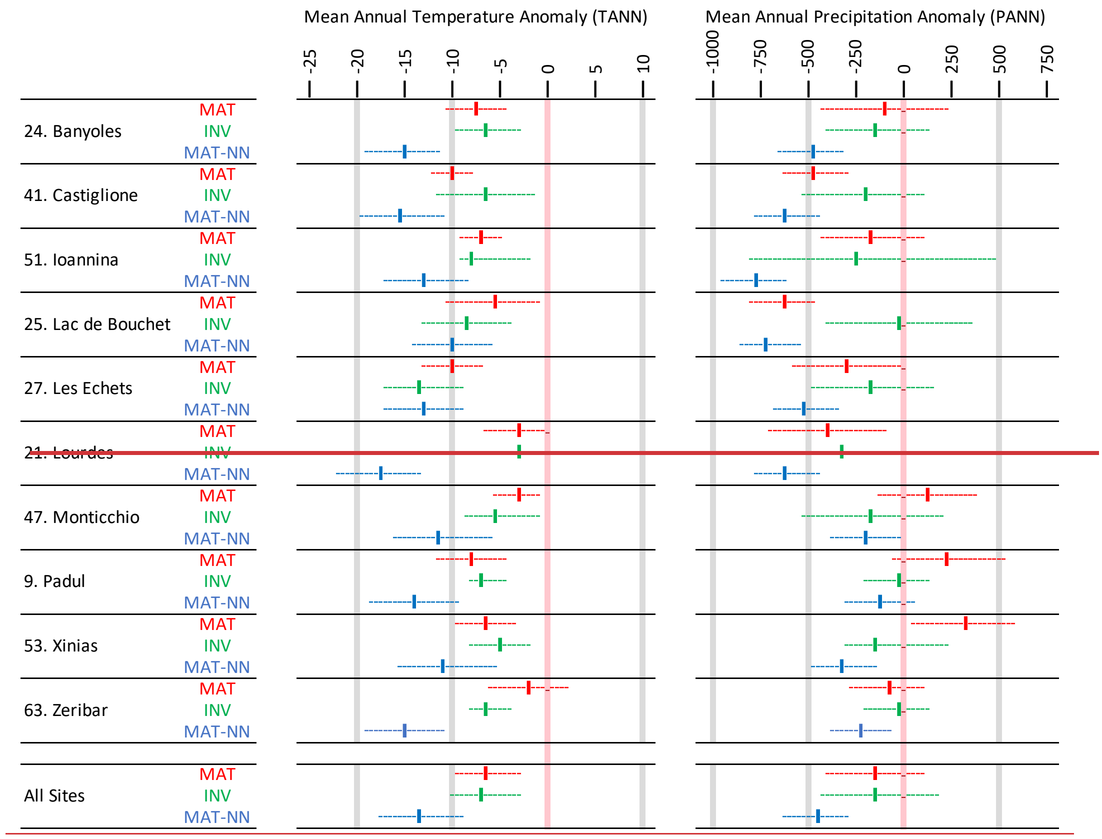

Figure 7. A site-by-site comparison between LGM pollen-climate reconstructions based on Modern Analogue Technique MAT (this study), neural-networks MAT-NN (Peyron et al., 1998), and Inverse Modelling INV (Wu et al., 2007). The results show that MAT and INV give similar climate reconstructions, but MAT-NN is significantly cooler/drier.

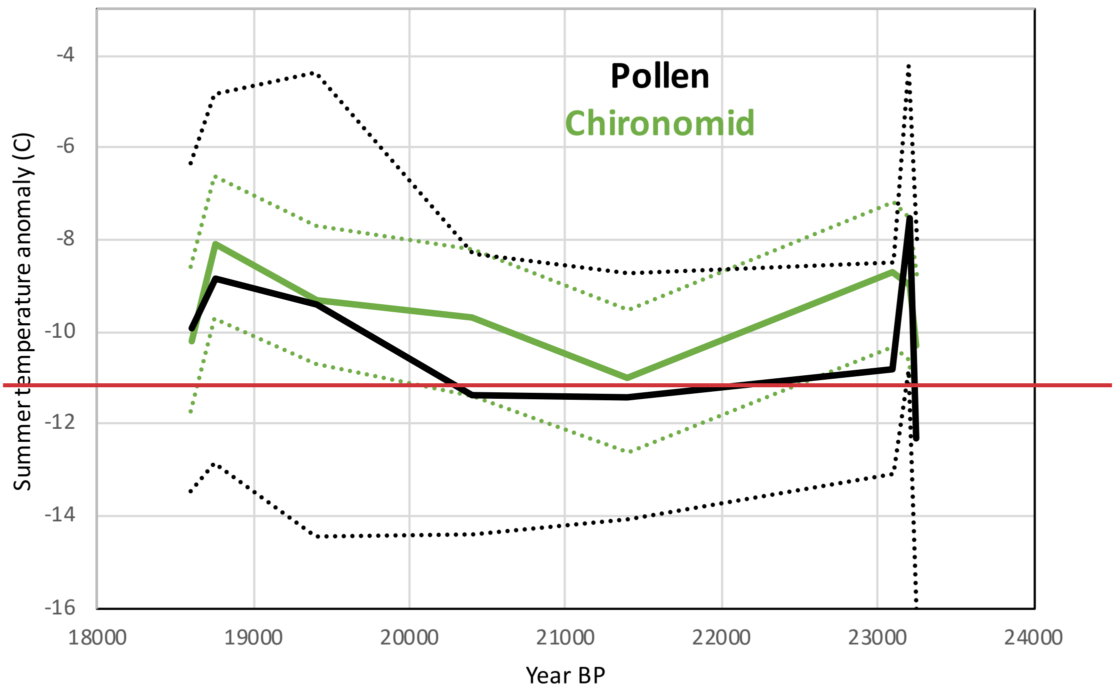

Figure 8. Comparison between LGM pollen-climate MAT and chironomid summer temperature reconstructions at Lago della Costa, Italy (chironomid reconstruction and pollen data from Samartin et al., 2016). Dash lines show uncertainties.

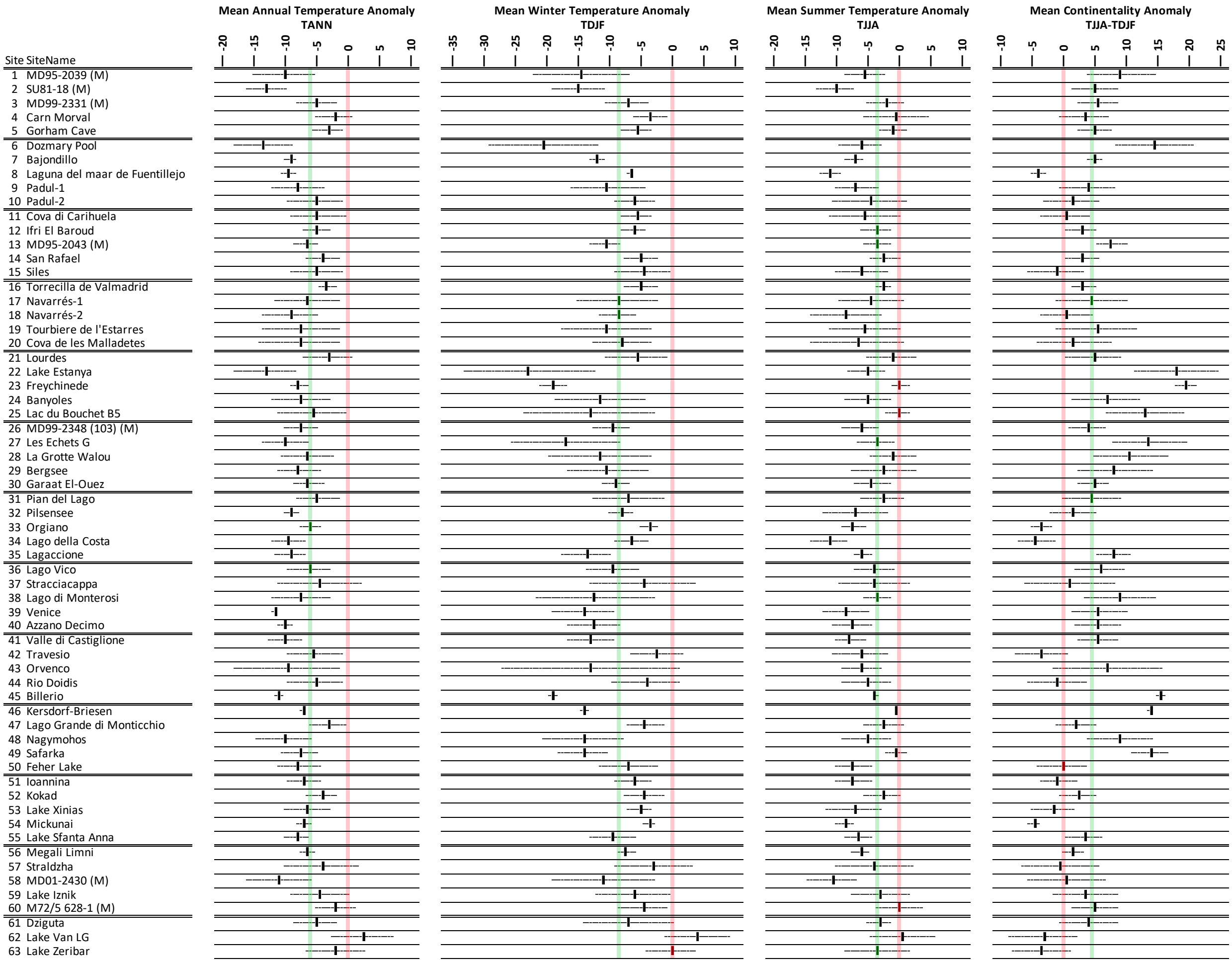

Figure 59. Pollen-based MAT reconstructions for LGM annual, winter and summer temperature anomalies (uncertainties represent one standard deviation). Continentality represents the difference in temperature between summer and winter, with positive anomalies indicating an increase in the temperature difference between summer and winter. All values are expressed as anomalies compared with the present day. The green line indicates the mean for all the sites.

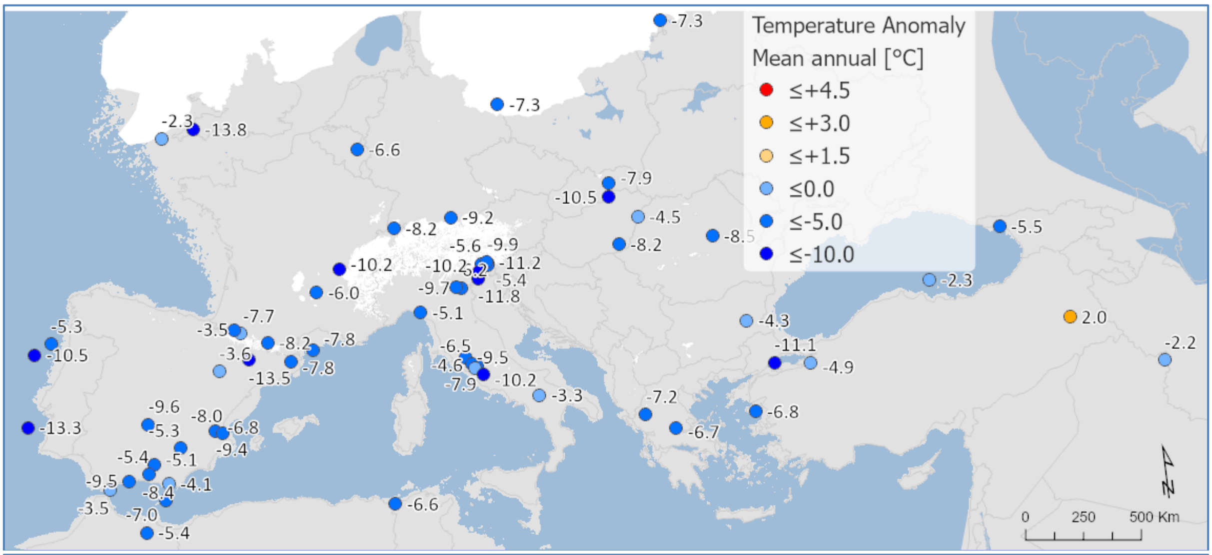
Temperature Anomaly
Mean annual [°C]
≤+4.5
≤+3.0
≤+1.5
≤0.0
≤-5.0
≤-10.0
0 250 500 Km

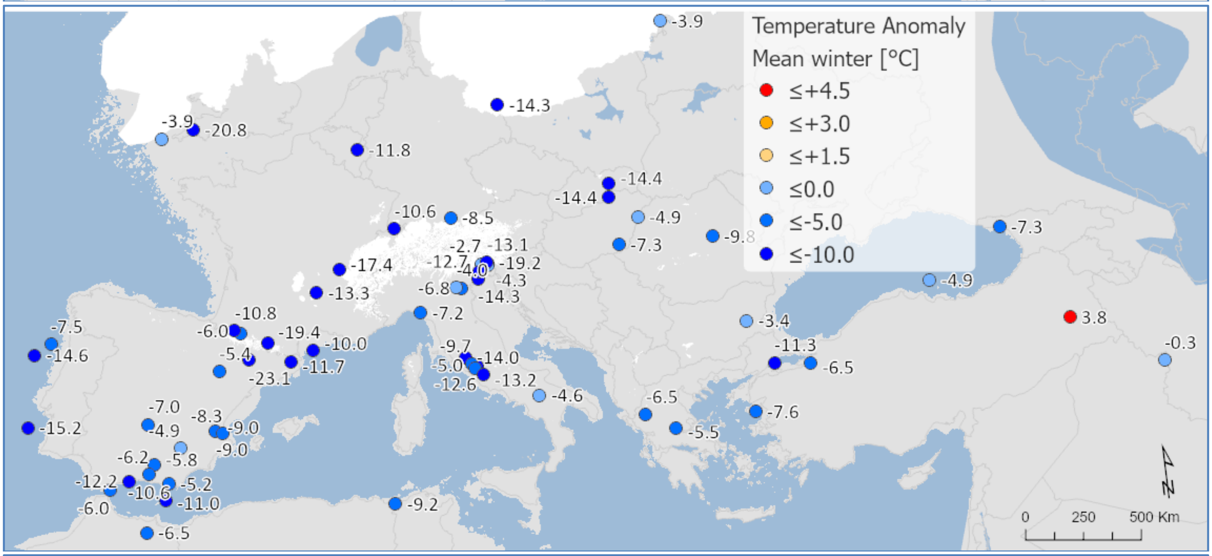
Temperature Anomaly
Mean winter [°C]
≤+4.5
≤+3.0
≤+1.5
≤0.0
≤-5.0
≤-10.0
0 250 500 Km

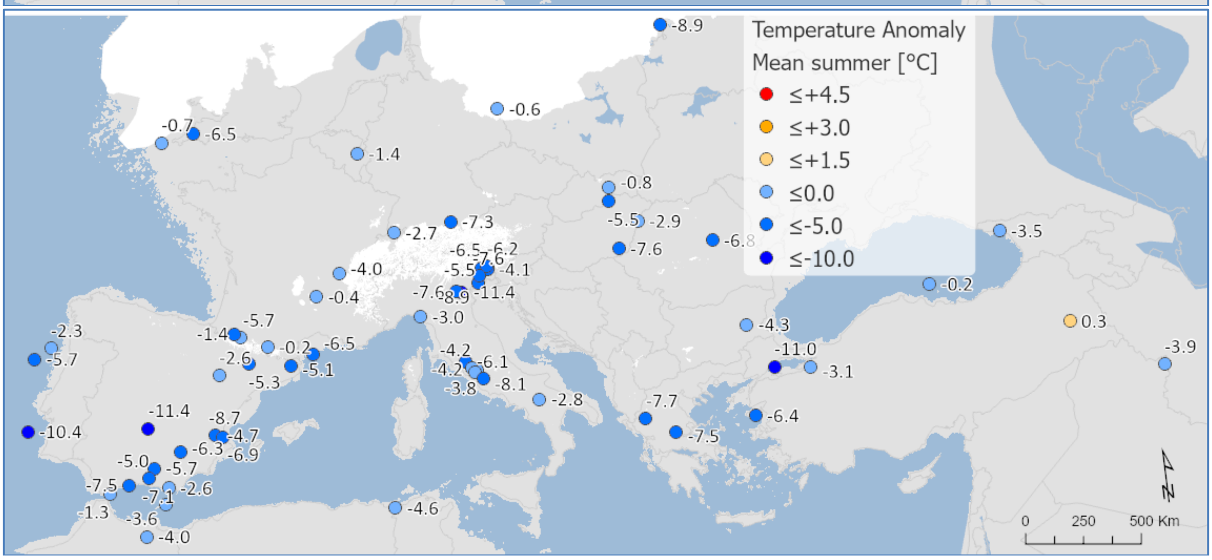
Temperature Anomaly
Mean summer [°C]
≤+4.5
≤+3.0
≤+1.5
≤0.0
≤-5.0
≤-10.0
0 250 500 Km

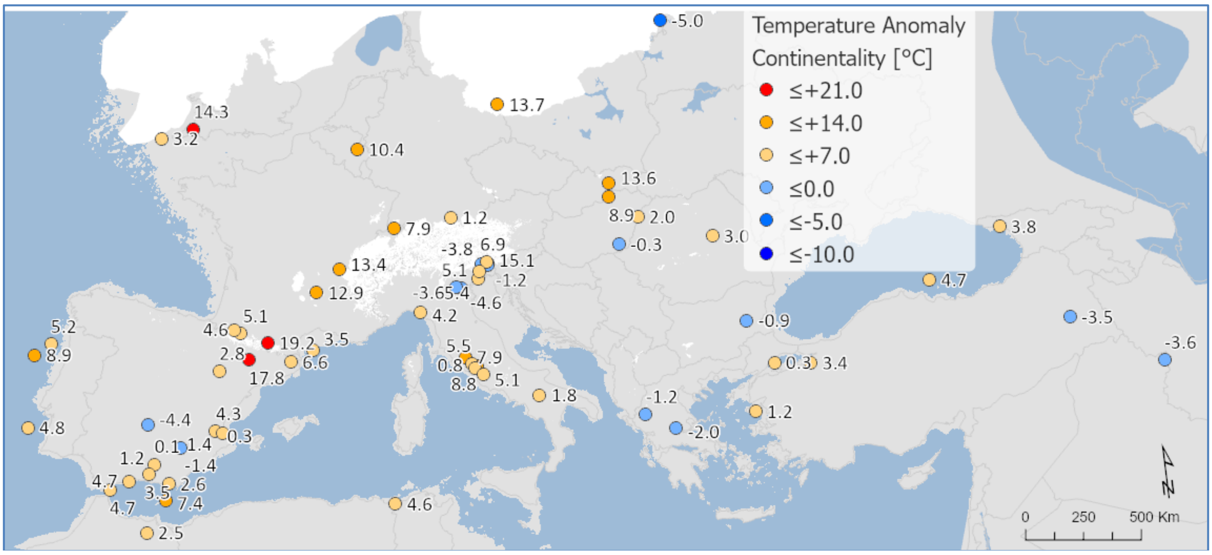

Figure 6~~10~~. Maps of pollen-based MAT reconstructions for LGM annual, winter and summer temperature anomalies (as shown in figure 9). Continentality represents the difference in temperature between summer and winter, with positive anomalies indicating an increase in the temperature difference between summer and winter. All values are expressed as anomalies compared with the present day.

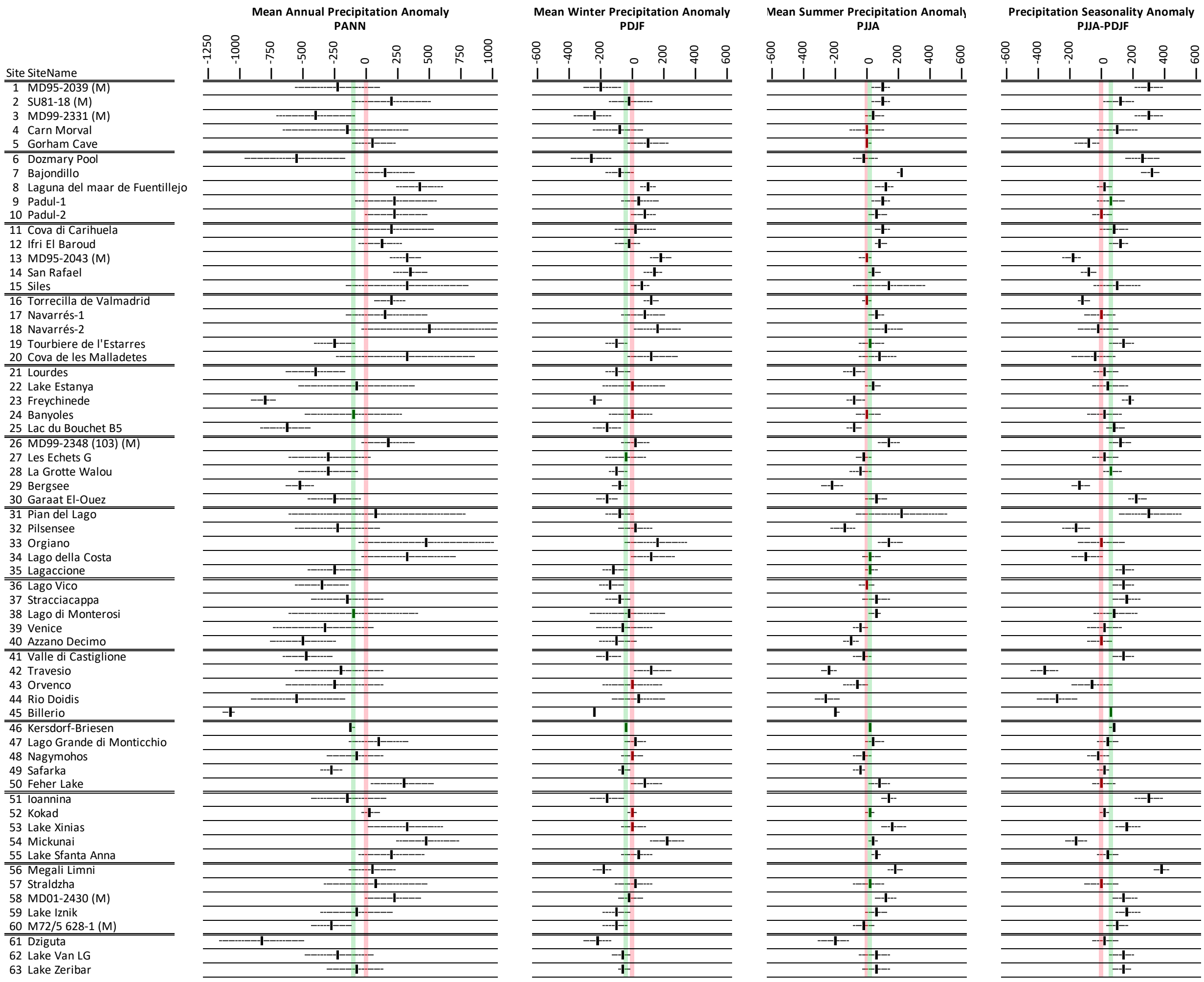

Figure ~~11~~7. Pollen-based MAT reconstructions for LGM annual, winter and summer precipitation anomalies (uncertainties represent one standard deviation). Seasonality represents the difference in precipitation between summer and winter, with positive anomalies indicating an increase in summer precipitation compared to winter. All values are expressed as anomalies compared with the present day. The green line indicates the mean for all the sites.

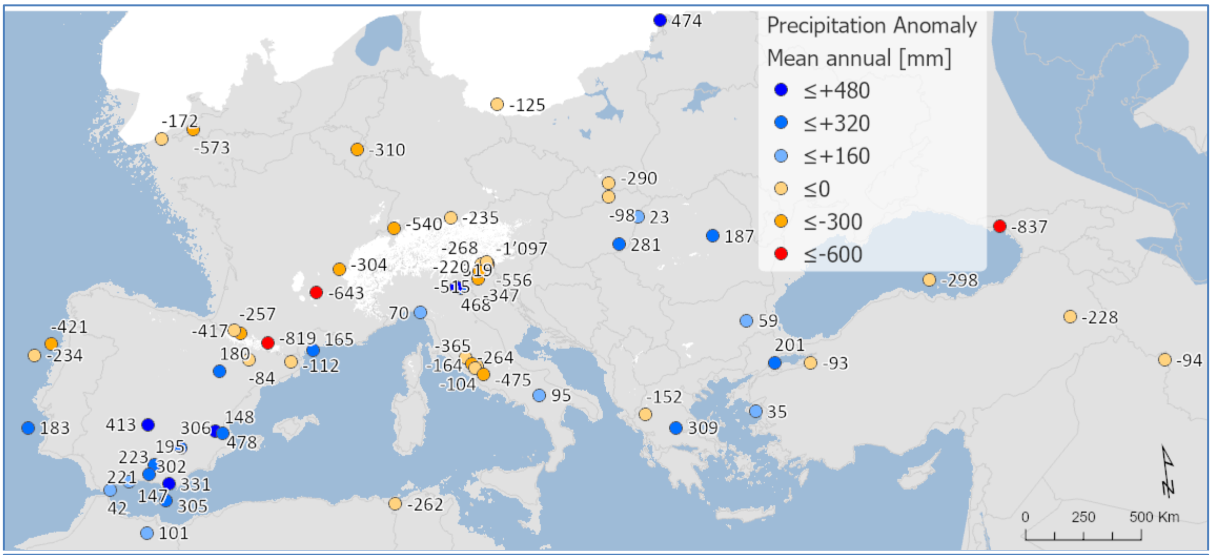
Precipitation Anomaly
Mean annual [mm]
≤+480
≤+320
≤+160
≤0
≤-300
≤-600
0 250 500 Km

2342

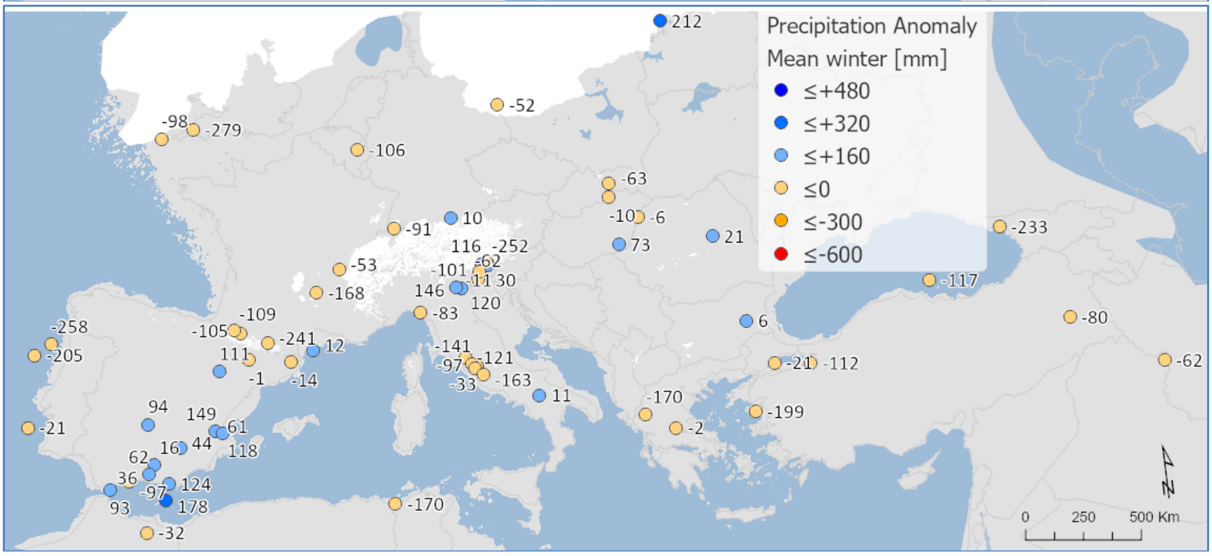
Precipitation Anomaly
Mean winter [mm]
≤+480
≤+320
≤+160
≤0
≤-300
≤-600
0 250 500 Km

2343

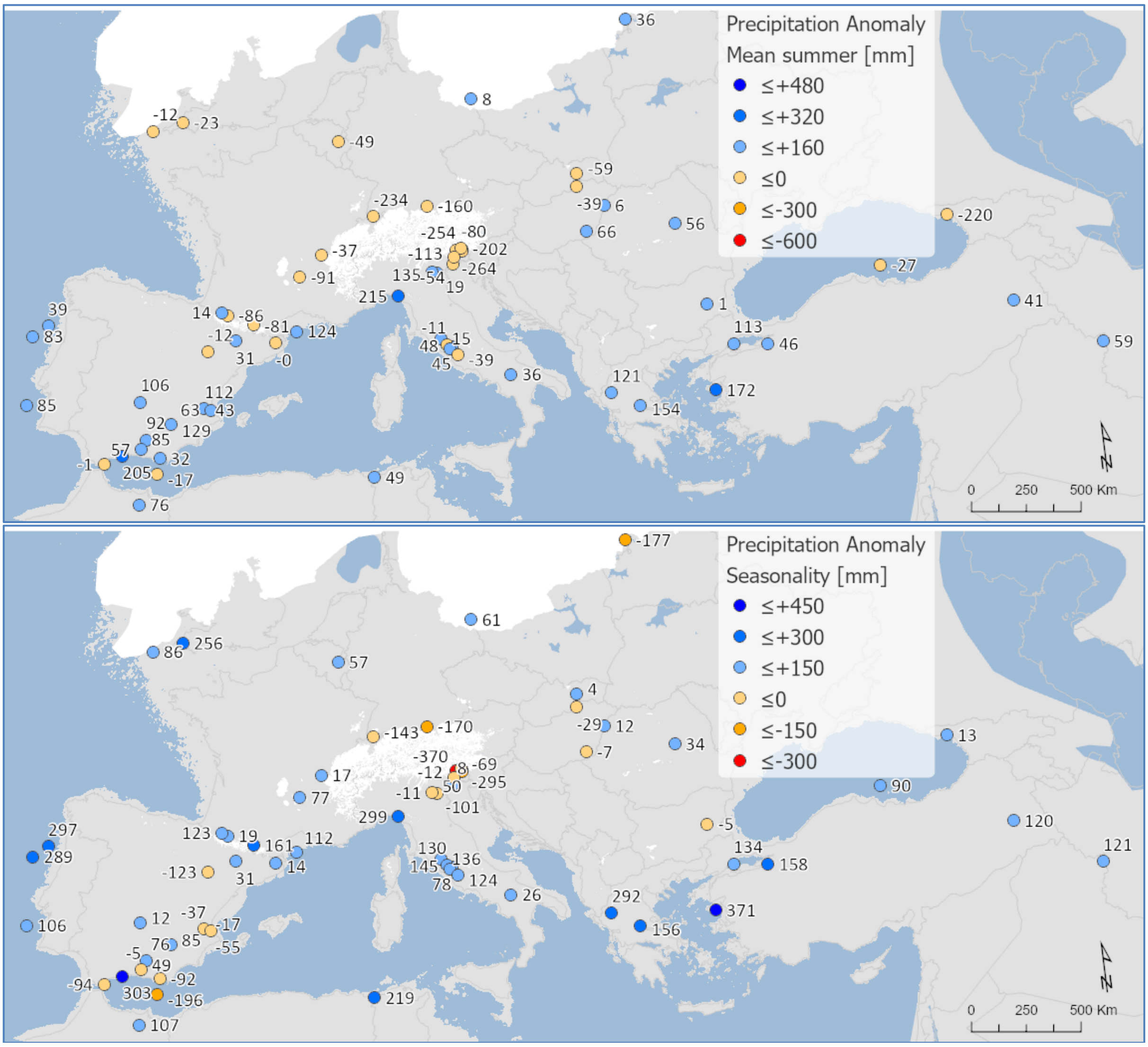

Figure ~~12~~8. Maps of pollen-based MAT reconstructions for LGM annual, winter and summer precipitation anomalies (as shown in figure 11). Seasonality represents the difference in precipitation between summer and winter, with positive anomalies indicating an increase in summer precipitation compared to winter. All values are expressed as anomalies compared with the present day.

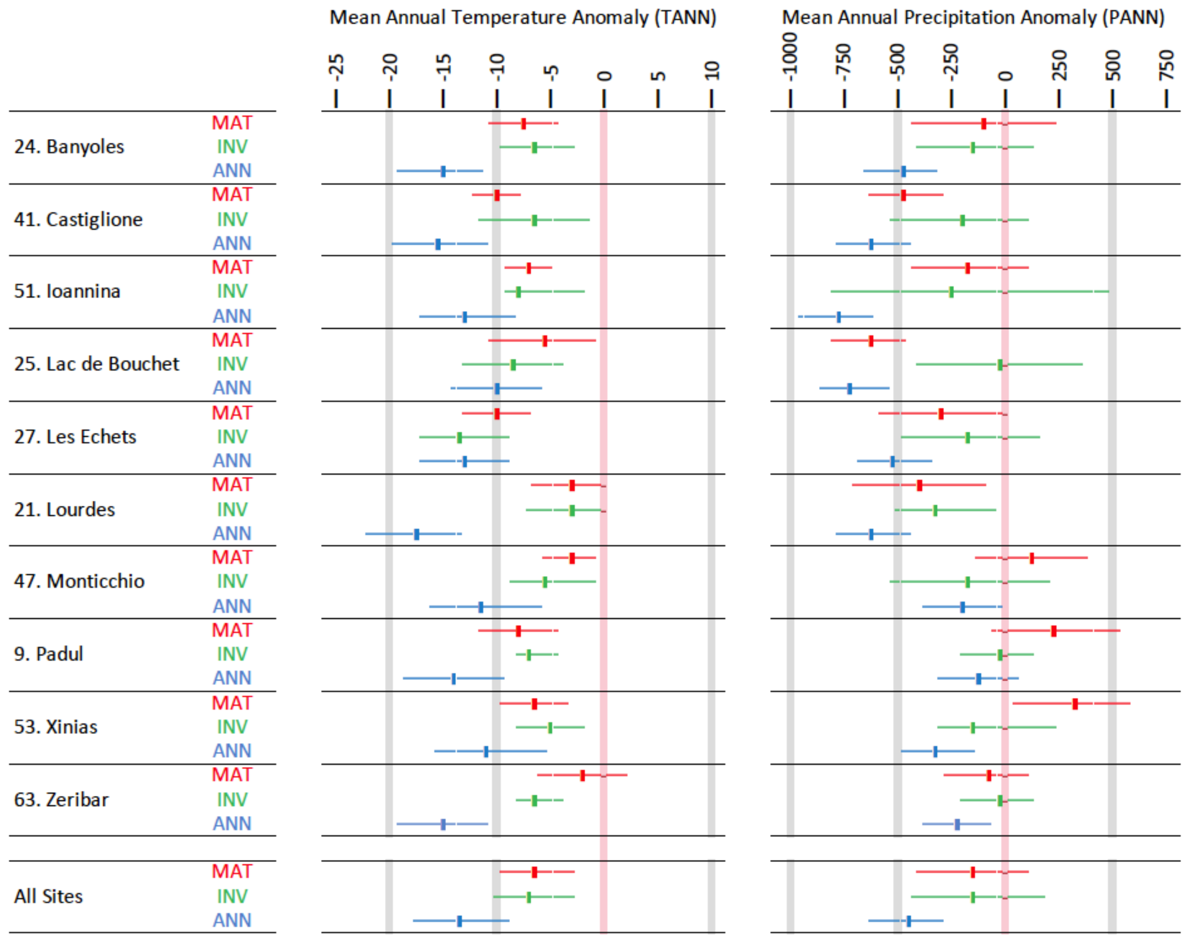

Figure 9. A site-by-site comparison between LGM pollen-climate reconstructions based on Modern Analogue Technique MAT (this study), neural-networks ANN (Peyron et al., 1998), and Inverse Modelling INV (Wu et al., 2007). The results show that MAT and INV give similar climate reconstructions, but ANN is significantly cooler/drier.

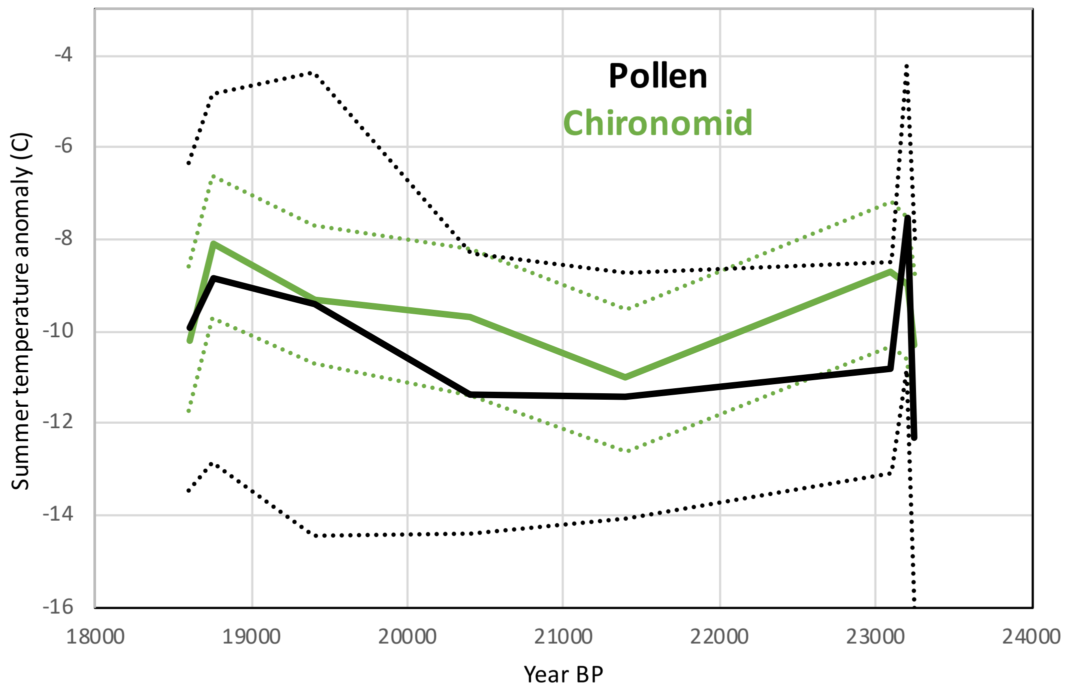

Figure 10. Comparison between LGM pollen-climate MAT and chironomid summer temperature reconstructions at Lago della Costa, Italy (chironomid reconstruction and pollen data from Samartin et al., 2016). Dash lines show uncertainties.

Appendix

Site	Site Name	COHMAP Quality	Upper 14C	Upper Cal. BP	Lower 14C	Lower Cal. BP
1	MD95-2039 (M)	3C	14830±80	18166±269	19950±210	23883±374
2	SU81-18 (M)	2C	17510±270	20952±404	21250±280	25420±441
3	MD99-2331 (M)	2C	16170±130	19325±303	19770±170	23682±336
4	Carn Morval	4C		18600±3700	21500±890/800	25867±1127
5	Gorham Cave	4D			18440±160	22055±341
6	Dozmary Pool	2C	14568±129	17569±523	18325±216	21769±602
7	Bajondillo	1C		18701±2154		
8	Laguna del maar de Fuentillejo	5D	16540±90	19847±308		
9	Padul-1	3D	18300±300	21821±412	19100±160	22922±308
10	Padul-2	1D			17450±539	21082±539
11	Cova di Carihuela	2C	15700±220	18958±280	21430±130	25659±226
12	Ifri El Baroud	2D	17296±87	20761±293		
13	MD95-2043 (M)	2C	15440±90	18533±294	18260±120	21951±335
14	San Rafael	3D	9980±60	11464±133	16860±120	20083±292
15	Siles	2D	17030±80	20345±351		
16	Torrecilla de Valmadrid	2D	17100±85	20456±366		
17	Navarrés-1	4D	18360±195	22001±353	20700±295	24664±411
18	Navarrés-2	5D	5150±50	5881±85	16000±	19144±
19	Tourbiere de l'Estarres	1C	17150±250	20522±470	18970±160	22847±317
20	Cova de les Malladetes	5D	16300±1500	19686±1723		
21	Lourdes	4D	18510±130	22112±130	20025±175	23952±355
22	Lake Estanya	5D		9498±50		19184±251
23	Freychinede	3C	14800±800	17912±856	21300±760	25615±1030
24	Banyoles	4C		19878±100		27862±3000
25	Lac du Bouchet B5	2C	15350±350	18513±435	19200±300	23006±384
26	MD99-2348 (103) (M)	1D	17660±60	21065±310	19350±90	23111±271
27	Les Echets G	1C	17530±270	20970±407	18030±250	21704±473
28	La Grotte Walou	1D				21200±700
29	Bergsee	2D			17780±90	21244±306
30	Garaat El-Ouez	2C	16010±320	19200±801		
31	Pian del Lago	2D				21260±320
32	Pilsensee	6D	15860±250	19073±290		
33	Orgiano	2D	17760±160	21221±373	19290±520	23141±621
34	Lago della Costa	2C	15400±150	18484±330	19285±160	23052±302
35	Lagaccione	2C	16080±450	19369±527	20615±940	24746±1201
36	Lago Vico	3C	14385±140	17541±272	20500±230	24430±376
37	Stracciacappa	4C	12060±130	14093±281	19745±820	22675±955
38	Lago di Monterosi	2D	17040±350	20398±544		
39	Venice	5D			18640±100	22277±336
40	Azzano Decimo	2D	18000±300	21637±529	21025±245	25179±449
41	Valle di Castiglione	3C	14220±145	17443±270	20300±700	24266±842
42	Travesio	5D			18780±200	22483±406
43	Orvenco	2D	17760±160	21221±373	19290±520	23141±621
44	Rio Doidis	5D			18860±190	22390±373
45	Billerio	3D			18165±200	21872±382
46	Kersdorf-Briesen	1D			17622±94	21183±356
47	Lago Grande di Monticchio	2C		20204±		24014±
48	Nagymohos	2C	14246±144	17361±425	18159±247	21735±622
49	Safarka	3D			18287±1512	21912±1781
50	Feher Lake	1D	17715±250	21190±463	19911±81	23841±313
51	Ioannina	3C	15330±140	18420±312	20760±230	24748±330
52	Kokad	5D	14326±63	17433±443	16280±90	19685±538
53	Lake Xinias	6C	11150±130	13049±160	21390±430	25671±648
54	Mickunai	1D		21000±2200		
55	Lake Sfanta Anna	1D	17626±96	20955±432		
56	Megali Limni	6D	19072±237	22906±340		
57	Straldzha	6C	14696±65	18022±364	23653±114	28580±390
58	MD01-2430 (M)	4C	12050±75	14904±324	18310±380	21746±968
59	Lake Iznik	7D	16910±100	19515±115		
60	M72/5 628-1 (M)	2C	16835±85	18490±	19495±90	21280±
61	Dziguta	4C	12990±160	15839±483	20560±880	24666±1126
62	Lake Van LG	2C		18590±62		23290±596
63	Lake Zeribar	4C	13650±160	16610±399	22000±500	26462±880

COHMAP chronological quality classification:
1C: Bracketing dates within 2000 14C (2360 Cal.) yr interval about the time being assessed
2C: Bracketing dates, one within 2000 14C (2360 Cal.) yr and the second within 4000 14C (4682 Cal.) yr of the time being assessed
3C: Bracketing dates within 4000 14C (4682 Cal.) yr interval about the time being assessed
4C: Bracketing dates, one being within 4000 14C (4682 Cal.) yr and the second being within 6000 14C (7490 Cal.) yr of the time being assessed
5C: Bracketing dates within 6000 14C (7490 Cal.) yr interval about the time being assessed
6C: Bracketing dates, one within 6000 14C (7490 Cal.) yr and the second within 8000 14C (9681 Cal.) yr of the time being assessed
7C: Poorly dated
1D: Date within 250 14C (206 Cal.) yr of the time being assessed
2D: Date within 500 14C (684 Cal.) yr of the time being assessed
3D: Date within 750 14C (975 Cal.) yr of the time being assessed
4D: Date within 1000 14C (1123 Cal.) yr of the time being assessed
5D: Date within 1500 14C (1881 Cal.) yr of the time being assessed
6D: Date within 2000 14C (2360 Cal.) yr of the time being assessed
7D: Poorly dated

Table A12. Chronological control

Site Number	Site Name	Site Type	TANN	TDJF	TJJA	PANN	PDJF	PJJA
1	MD95-2039 (M)	Marine	15.7	10.7	20.8	1047	427	70
2	SU81-18 (M)	Marine	20.8	15.3	26.5	629	282	25
3	MD99-2331 (M)	Marine	14.6	9.8	19.4	1239	507	88
4	Carn Morval	Lake	12.5	8.7	16.9	1183	392	206
5	Gorham Cave	Cave	18.3	13.4	23.7	740	336	25
6	Dozmary Pool	Lake	10.3	6.0	15.2	1271	422	236
7	Bajondillo	Cave	16.6	10.5	23.4	542	223	27
8	Laguna del maar de Fuentillejo	Lake	16.1	8.1	25.4	474	156	47
9	Padul-1	Peat Bog	16.6	9.6	24.9	417	157	23
10	Padul-2	Peat Bog	16.6	9.6	24.9	417	157	23
11	Cova di Carihuela	Cave	15.7	8.1	25.1	551	187	57
12	Ifri El Baroud	Cave	16.9	10.7	24.0	457	184	22
13	MD95-2043 (M)	Marine	17.9	12.4	24.0	214.2	37	72
14	San Rafael	Peat Bog	18.1	11.9	24.9	243	87	14
15	Siles	Lake	14.4	6.8	23.4	658	195	92
16	Torrecilla de Valmadrid	Colluvium	14.2	6.6	22.5	390	75	82
17	Navarrés-1	Peat Bog	17.0	10.9	23.8	421	96	51
18	Navarrés-2	Peat Bog	17.0	10.9	23.8	421	96	51
19	Tourbiere de l'Estarres	Lake	13.0	6.1	20.4	1045	272	217
20	Cova de les Malladetes	Cave	18.1	12.1	24.8	478	117	60
21	Lourdes	Lake	12.6	5.5	20.1	1002	256	212
22	Lake Estanya	Lake	12.8	5.1	21.0	641	125	152
23	Freychinede	Lake	10.8	3.9	19.0	1128	257	277
24	Banyoles	Lake	14.3	7.7	21.9	698	157	139
25	Lac du Bouchet B5	Lake	8.2	1.3	15.9	1070	251	221
26	MD99-2348 (103) (M)	Marine	14.6	8.0	21.9	618	158	95
27	Les Echets G	Peat Bog	11.4	3.6	19.6	876	175	215
28	La Grotte Walou	Cave	10.3	3.2	17.0	903	215	249
29	Bergsee	Lake	9.6	1.4	17.6	1048	189	387
30	Garaat El-Ouez	Peat Bog	17.3	11.0	24.3	830	360	33
31	Pian del Lago	Lake	12.4	5.1	20.0	995	266	149
32	Pilsensee	Lake	9.3	0.6	17.7	947	151	374
33	Orgiano	Peat Bog	13.0	3.3	22.3	907	200	228
34	Lago della Costa	Lake	12.9	3.3	22.1	888	196	224
35	Lagaccione	Lake	14.2	7.2	21.7	705	203	109
36	Lago Vico	Lake	13.7	6.4	21.5	870	258	132
37	Stracciacappa	Lake	14.6	7.3	22.4	867	266	115
38	Lago di Monterosi	Lake	15.0	7.7	22.9	837	248	115
39	Venice	Peat Bog	13.4	4.5	22.1	1050	221	277
40	Azzano Decimo	Alluvial Fan	13.3	4.4	22.1	1170	241	311
41	Valle di Castiglione	Lake	16.3	9.1	24.0	988	294	144
42	Travesio	Lake	12.6	3.7	21.3	1415	281	375
43	Orvenco	Alluvial Fan	13.0	3.3	22.3	907	200	228
44	Rio Doidis	Lake	12.8	4.1	21.2	1529	315	392
45	Billerio	Lake	12.8	4.1	21.2	1529	315	392
46	Kersdorf-Briesen	Lake	8.8	-1.0	17.9	538	110	175
47	Lago Grande di Monticchio	Lake	11.5	4.1	19.8	518	154	76
48	Nagymohos	Peat Bog	9.5	-1.5	19.1	616	103	230
49	Safarka	Peat Bog	7.0	-3.2	16.0	755	119	280
50	Feher Lake	Lake	11.0	-0.1	20.7	546	112	185
51	Ioannina	Peat Bog	14.7	6.5	23.3	1000	364	98
52	Kokad	Peat Bog	10.2	-0.9	19.8	601	130	204
53	Lake Xinias	Lake	15.6	7.5	24.1	563	211	47
54	Mickunai	Lake	6.0	-5.0	16.3	682	131	230
55	Lake Sfanta Anna	Lake	11.6	5.2	18.4	867	253	172
56	Megali Limni	Lake	15.5	8.2	23.4	684	357	28
57	Straldzha	Peat Bog	12.5	2.6	21.8	591	158	135
58	MD01-2430 (M)	Marine	18.0	8.7	27.5	595	219	75
59	Lake Iznik	Lake	13.9	6.1	21.8	677	250	85
60	M72/5 628-1 (M)	Marine	14.5	8.0	21.6	857	251	156
61	Dziguta	Peat Bog	14.1	6.6	21.7	1549	409	373
62	Lake Van LG	Lake	12.0	0.9	23.1	635	201	34
63	Lake Zeribar	Lake	17.1	5.0	29.0	427	167	6

Table A2. Modern climate values for each site used in the calculation of anomalies (taken from WorldClim 2, Fick & Hijmans 2017)

	All surface samples		Steppe only	
	RMSE	**R2**	**RMSE**	**R2**
TANN	2.28	0.9	2.51	0.87
TDJF	3.35	0.91	3.26	0.88
TJJA	2.21	0.81	2.49	0.82
PANN	224.94	0.69	185.7	0.71
PDJF	78.51	0.69	66.5	0.66
PJJA	52.49	0.75	43.8	0.79

Table A3. A comparison of MAT performance statistics based on the modern pollen sample training set using all surface samples from the EMPD2 used in the LGM reconstruction (as shown in Table 3), and a subset of 1588 samples from the EMPD2 that were classified as steppe. The results show little difference between the two different types of samples. The table includes Mean Annual Temperature and Precipitation (TANN and PANN), Mean Winter Temperature and Precipitation (TDJF and PDJF) and Mean Summer Temperature and Precipitation (TJJA and PJJA).

Site Name	Site#	Pollen Biome	Modern Analogue Biome	Modern Analogue Ecoregion
MD95-2039	1	XERO	Mediterranean Forests, woodlands and scrubs	Iberian conifer forests
SU81-18	2	COMX	Mediterranean Forests, woodlands and scrubs	Iberian conifer forests
MD99-2331	3	STEP	Mediterranean Forests, woodlands and scrubs	Alps conifer and mixed forests
Carn Morval	4	STEP	Temperate broadleaf and mixed forests	North Atlantic moist mixed forests
Gorham Cave	5	STEP	Mediterranean Forests, woodlands and scrubs	Cyprus Mediterranean forests
Dozmary Pool	6	STEP	Temperate Coniferous Forest	Alps conifer and mixed forests
Bajondillo	7	STEP	Temperate broadleaf and mixed forests	Central European mixed forests
Laguna del maar de Fuentillejo	8	COMX	Mediterranean Forests, woodlands and scrubs	Northwest Iberian montane forests
Padul	9	STEP	Mediterranean Forests, woodlands and scrubs	Central Anatolian steppe
Padul-15-05	10	WAMX	Mediterranean Forests, woodlands and scrubs	Iberian sclerophyllous and semi-deciduous forests
Cova di Carihuela	11	STEP	Deserts and xeric shrublands	Azerbaijan shrub desert and steppe
Ifri El Baroud	12	STEP	Mediterranean Forests, woodlands and scrubs	Iberian sclerophyllous and semi-deciduous forests
MD95-2043	13	CLMX	Mediterranean Forests, woodlands and scrubs	Southern Anatolian montane conifer and deciduous forests
San Rafael	14	XERO	Mediterranean Forests, woodlands and scrubs	Tyrrhenian-Adriatic Sclerophyllous and mixed forests
Siles	15	XERO	Mediterranean Forests, woodlands and scrubs	Northwest Iberian montane forests
Torrecilla de Valmadrid	16	STEP	Mediterranean Forests, woodlands and scrubs	Southern Anatolian montane conifer and deciduous forests
Navarres	17	XERO	Mediterranean Forests, woodlands and scrubs	Iberian sclerophyllous and semi-deciduous forests
Navarres	18	STEP	Temperate broadleaf and mixed forests	Pyrenees conifer and mixed forests
Tourbiere de lEstarres	19	STEP	Temperate grasslands, savannas and shrublands	Eastern Anatolian montane steppe
Cova de les Malladetes	20	XERO	Mediterranean Forests, woodlands and scrubs	Pyrenees conifer and mixed forests
Lourdes	21	STEP	Temperate broadleaf and mixed forests	Gissaro-Alai open woodlands
Estanya	22	XERO	Temperate broadleaf and mixed forests	Western Siberian hemiboreal forests
Freychinede	23	STEP	Temperate grasslands, savannas and shrublands	Mongolian-Manchurian grassland
Lake Banyoles	24	STEP	Temperate grasslands, savannas and shrublands	Gissaro-Alai open woodlands
Lac du Bouchet B5	25	STEP	Temperate grasslands, savannas and shrublands	Gissaro-Alai open woodlands
MD99-2348-103	26	COMX	Temperate broadleaf and mixed forests	Rodope montane mixed forests
Les Echets G - DIGI	27	STEP	Temperate broadleaf and mixed forests	Western Siberian hemiboreal forests
La Grotte Walou	28	STEP	Temperate broadleaf and mixed forests	Kazakh forest steppe
Bergsee	29	STEP	Temperate broadleaf and mixed forests	Kazakh forest steppe
Garaat El-Ouez	30	STEP	Mediterranean Forests, woodlands and scrubs	Anatolian conifer and deciduous mixed forests
Pian del Lago	31	COMX	Temperate broadleaf and mixed forests	Western European broadleaf forests
Pilsensee	32	TAIG	Tundra	Kola Peninsula tundra
Orgiano	33	COMX	Temperate broadleaf and mixed forests	Western European broadleaf forests
Lago della Costa	34	COMX	Temperate Coniferous Forest	Alps conifer and mixed forests
Lagaccione	35	STEP	Temperate grasslands, savannas and shrublands	Gissaro-Alai open woodlands
Lago Vico	36	STEP	Temperate grasslands, savannas and shrublands	Gissaro-Alai open woodlands
Stracciacappa	37	STEP	Mediterranean Forests, woodlands and scrubs	Western European broadleaf forests
Lago di Monterosi	38	STEP	Temperate grasslands, savannas and shrublands	Northwest Iberian montane forests
Venice	39	XERO	Tundra	Scandinavian Montane Birch forest and grasslands
Azzano Decimo	40	XERO	Temperate broadleaf and mixed forests	Scandinavian Montane Birch forest and grasslands
Valle di Castiglione	41	STEP	Temperate broadleaf and mixed forests	Tian Shan montane steppe and meadows
Travesio	42	XERO	Mediterranean Forests, woodlands and scrubs	Iberian conifer forests
Orvenco	43	TAIG	Temperate broadleaf and mixed forests	Western Siberian hemiboreal forests
Rio Doidis	44	XERO	Mediterranean Forests, woodlands and scrubs	Cyprus Mediterranean forests
Billerio	45	TAIG	Temperate broadleaf and mixed forests	Western Siberian hemiboreal forests
Kersdorf-Briesen	46	TAIG	Temperate broadleaf and mixed forests	Western Siberian hemiboreal forests
Lago Grande di Monticchio	47	STEP	Temperate broadleaf and mixed forests	Tian Shan montane steppe and meadows
Nagymohos Pleistocene	48	STEP	Tundra	Sarmatic mixed forests
Safarka	49	TAIG	Boreal forests / Taiga	Ural montane forests and tundra
Feher-to	50	COMX	Temperate Coniferous Forest	Alps conifer and mixed forests
Ioannina	51	STEP	Temperate broadleaf and mixed forests	Central European mixed forests
Kokad	52	STEP	Temperate broadleaf and mixed forests	East European forest steppe
Lake Xinias	53	STEP	Temperate broadleaf and mixed forests	Western European broadleaf forests
Mickunai	54	COCO	Tundra	Scandinavian Montane Birch forest and grasslands
Lake Sfanta Anna	55	COMX	Temperate Coniferous Forest	Alps conifer and mixed forests
Lesvos ML01 Megali Limni	56	STEP	Temperate broadleaf and mixed forests	Rodope montane mixed forests
Straldzha	57	STEP	Temperate broadleaf and mixed forests	Aegean and Western Turkey sclerophyllous and mixed forests
MD01-2430	58	STEP	Temperate broadleaf and mixed forests	Euxine-Colchic broadleaf forests
Lake Iznik	59	STEP	Temperate broadleaf and mixed forests	Tian Shan montane steppe and meadows
M72/5 628-1	60	STEP	Deserts and xeric shrublands	Azerbaijan shrub desert and steppe
Dziguta Core 1	61	CLMX	Temperate broadleaf and mixed forests	Northeastern Spain and Southern France Mediterranean forests
Lake Van LG	62	STEP	Mediterranean Forests, woodlands and scrubs	Aegean and Western Turkey sclerophyllous and mixed forests
Lake Zeribar	63	STEP	Temperate grasslands, savannas and shrublands	Pontic steppe

Notes: Modern analogue Biomes and Ecoregions were calculated as the most commonly occuring amongst all 6 best modern analogue pollen samples in all LGM samples for each pollen site/record. These are taken from the EMPD2 (Davis et al 2020), using the classification of Olsen et al 2001.

Table A4. The biome and ecoregion of the modern surface samples used as analogues in the pollen-climate reconstructions.

Figures

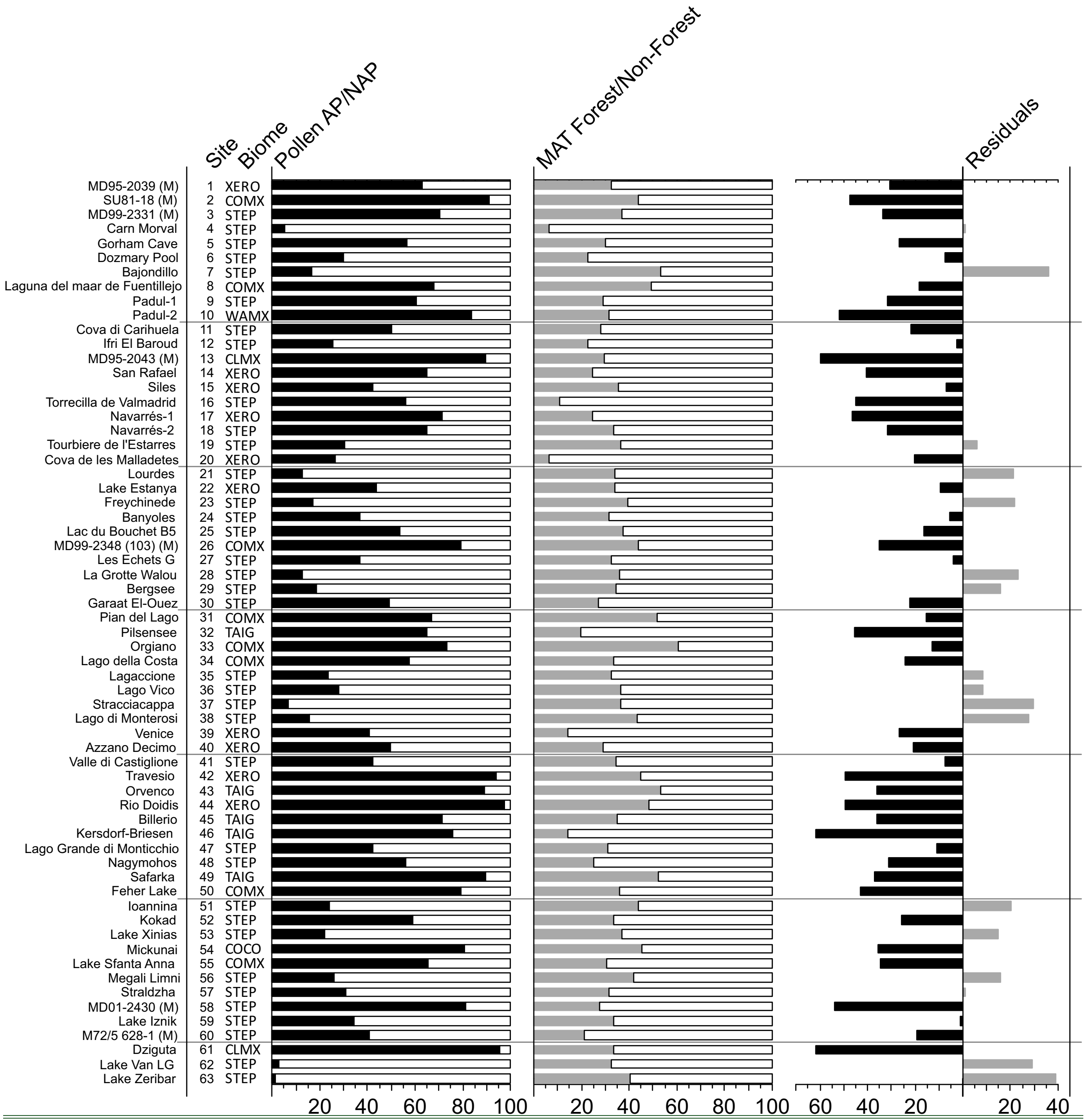

Figure A1~~3~~. Pollen biomes (see figure 2 for key), Arboreal Pollen (AP) % forest cover, MAT % forest cover and residuals (AP % compared to MAT Forest %)

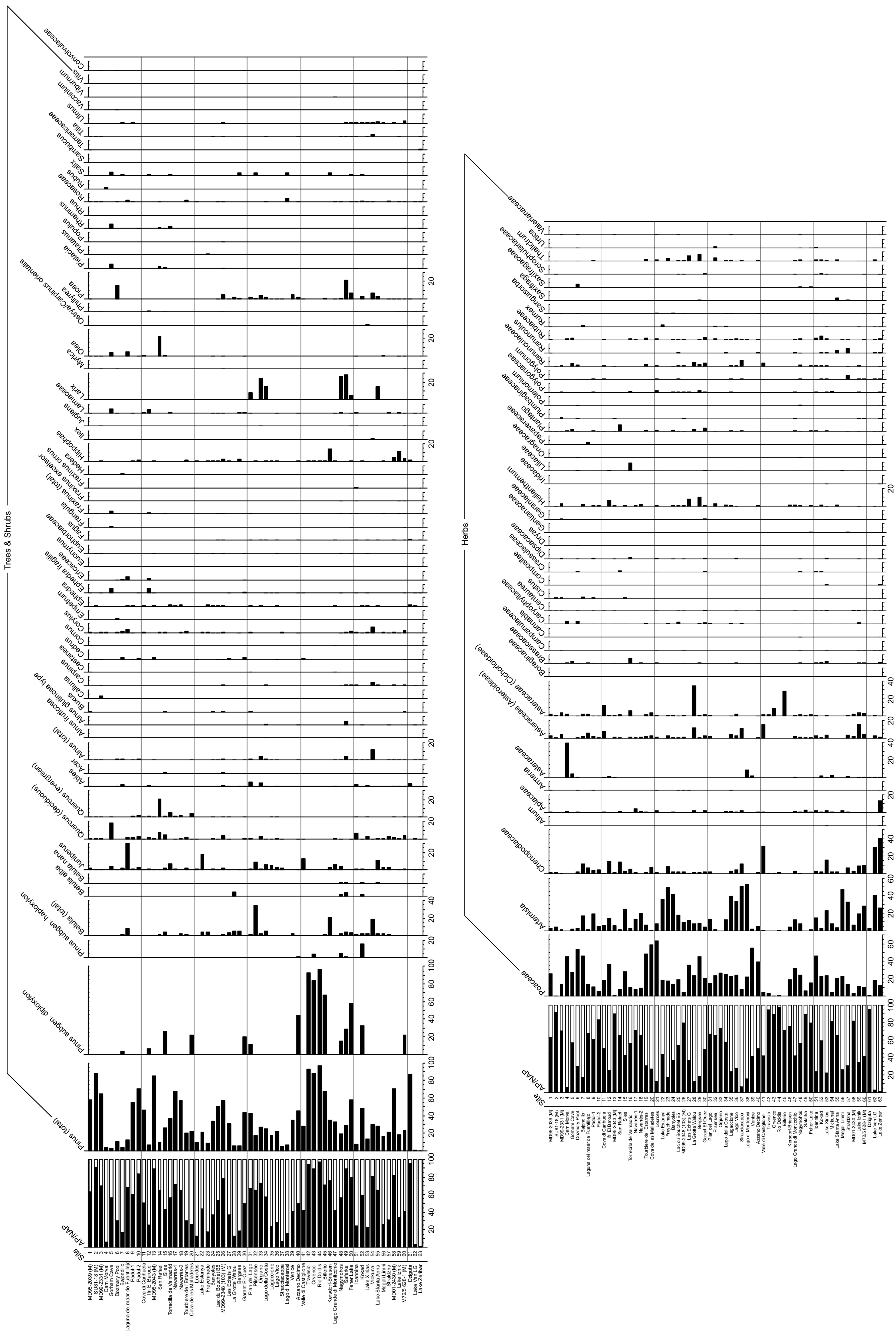

Figure A2~~6~~. Pollen taxa percentages for all LGM sites/records

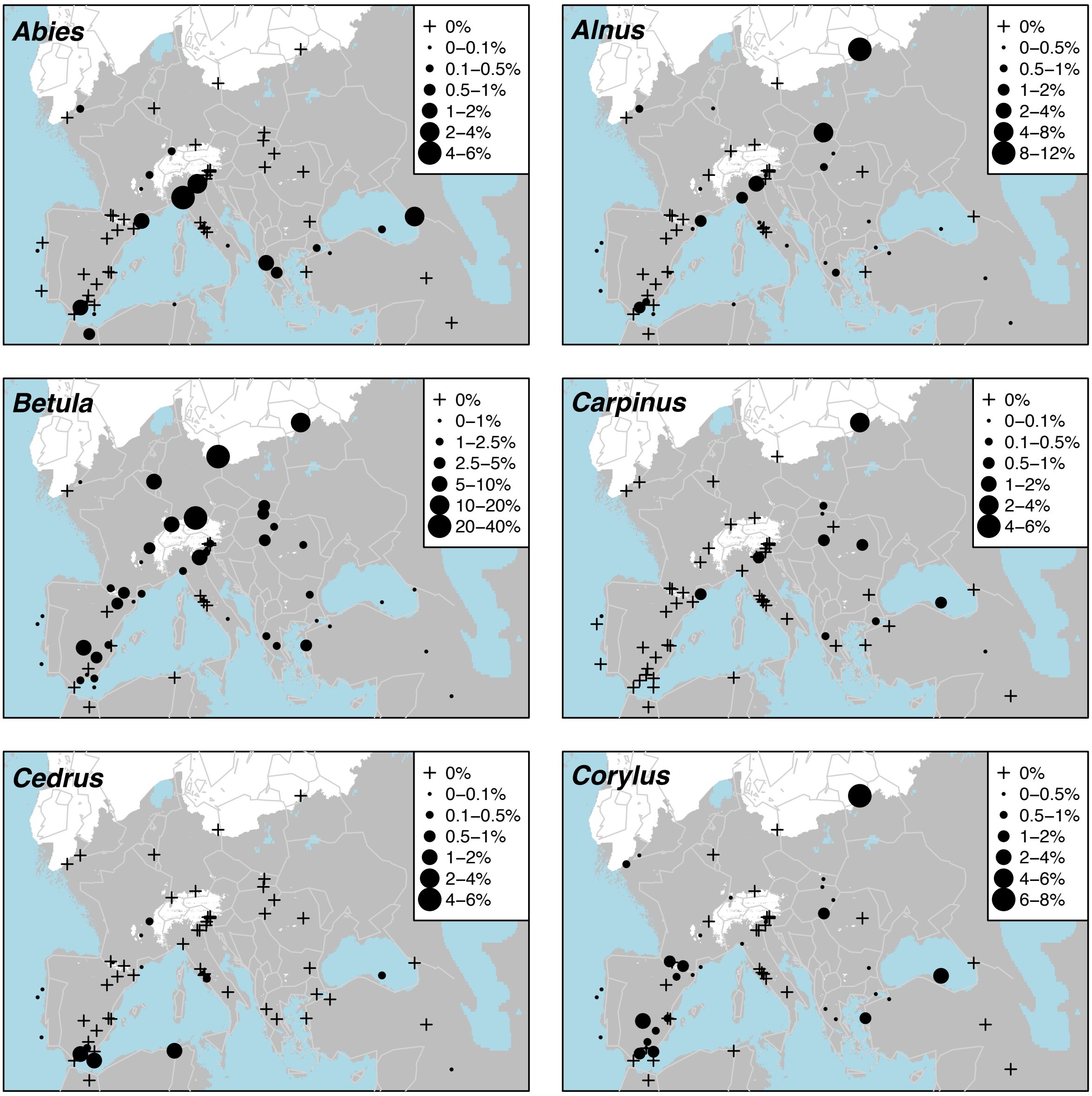

Figure ~~A1a~~A3a. Percentage maps of *Abies*, *Alnus*, *Betula*, *Car~~pinus~~Pinus*, *Cedrus* and *Corylus*

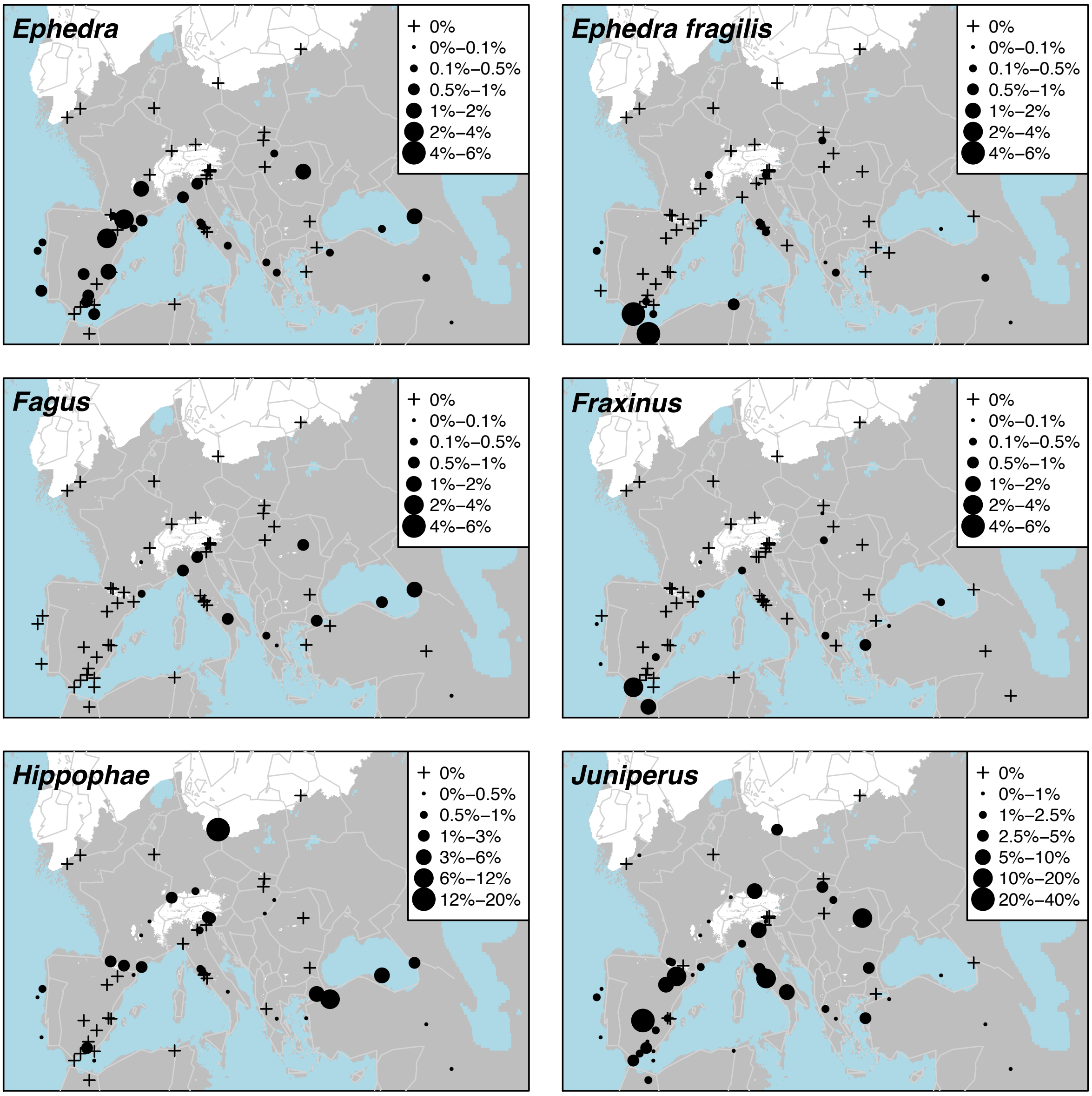

Figure A31b. Percentage maps of *Ephedra*, *Ephedra fragilis*, *Fagus*, *Fraxinus*, *Hippophae* and *Juniperus*

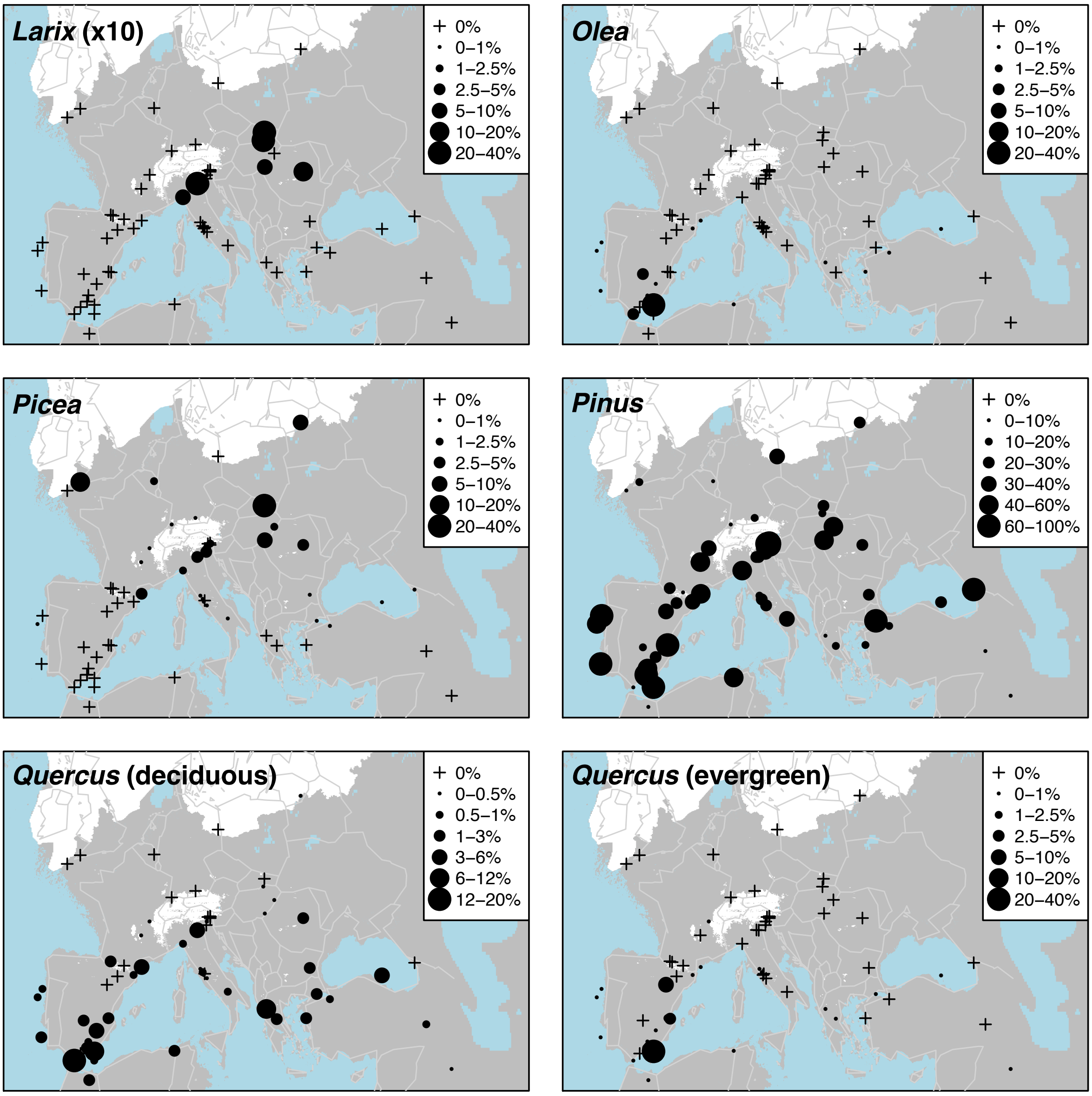

Figure ~~A1c~~A3c. Percentage maps of *Larix* (x10 exaggeration), *Olea*, *Picea*, ~~*Pinus*~~*Pinus*, *Quercus* (deciduous) and *Quercus* (evergreen)

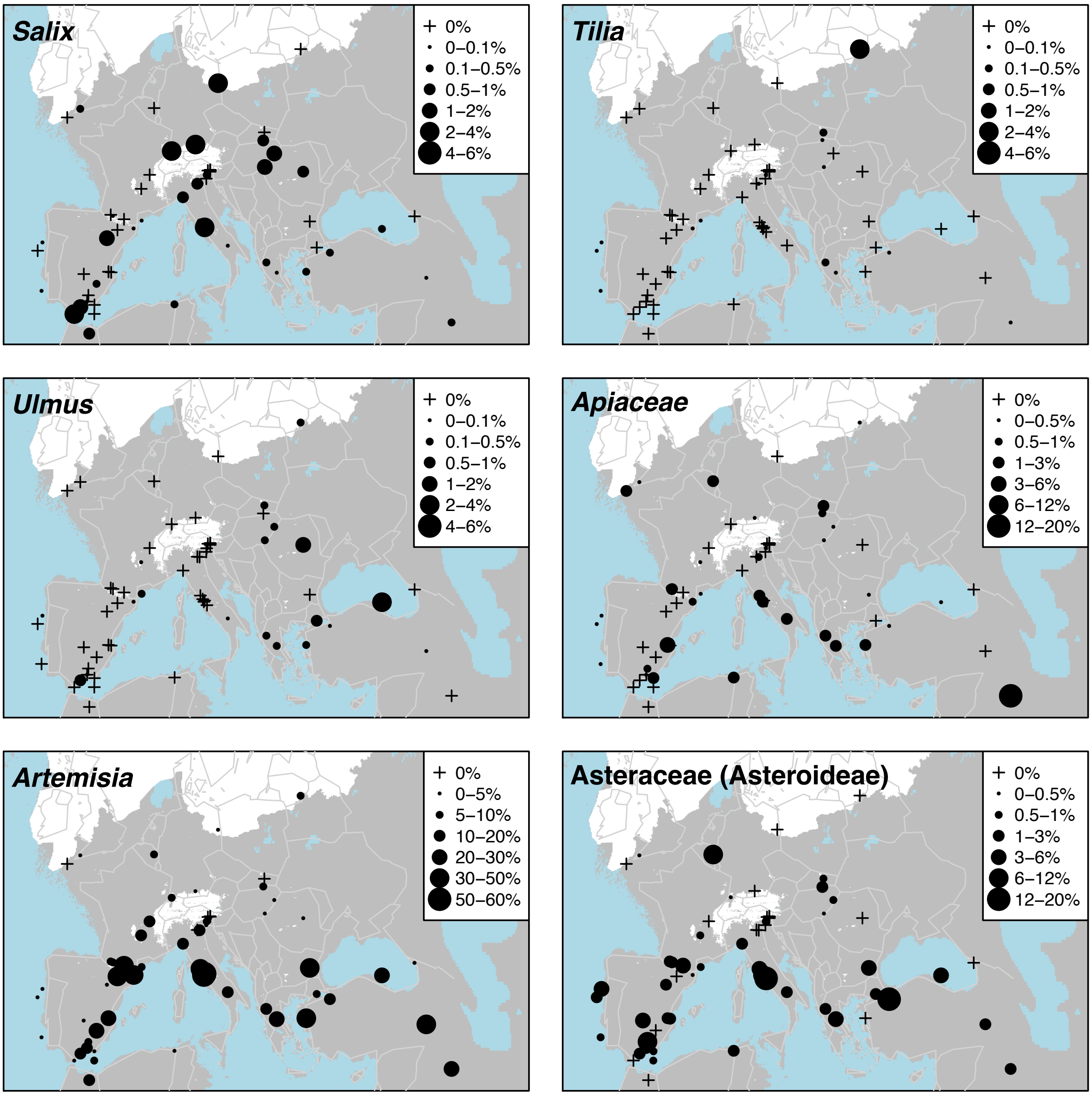

Figure ~~A1d~~A3d. Percentage maps of *Salix*, *Tilia*, *Ulmus*, Apiaceae, *Artemisia* and Asteraceae (Asteroideae)

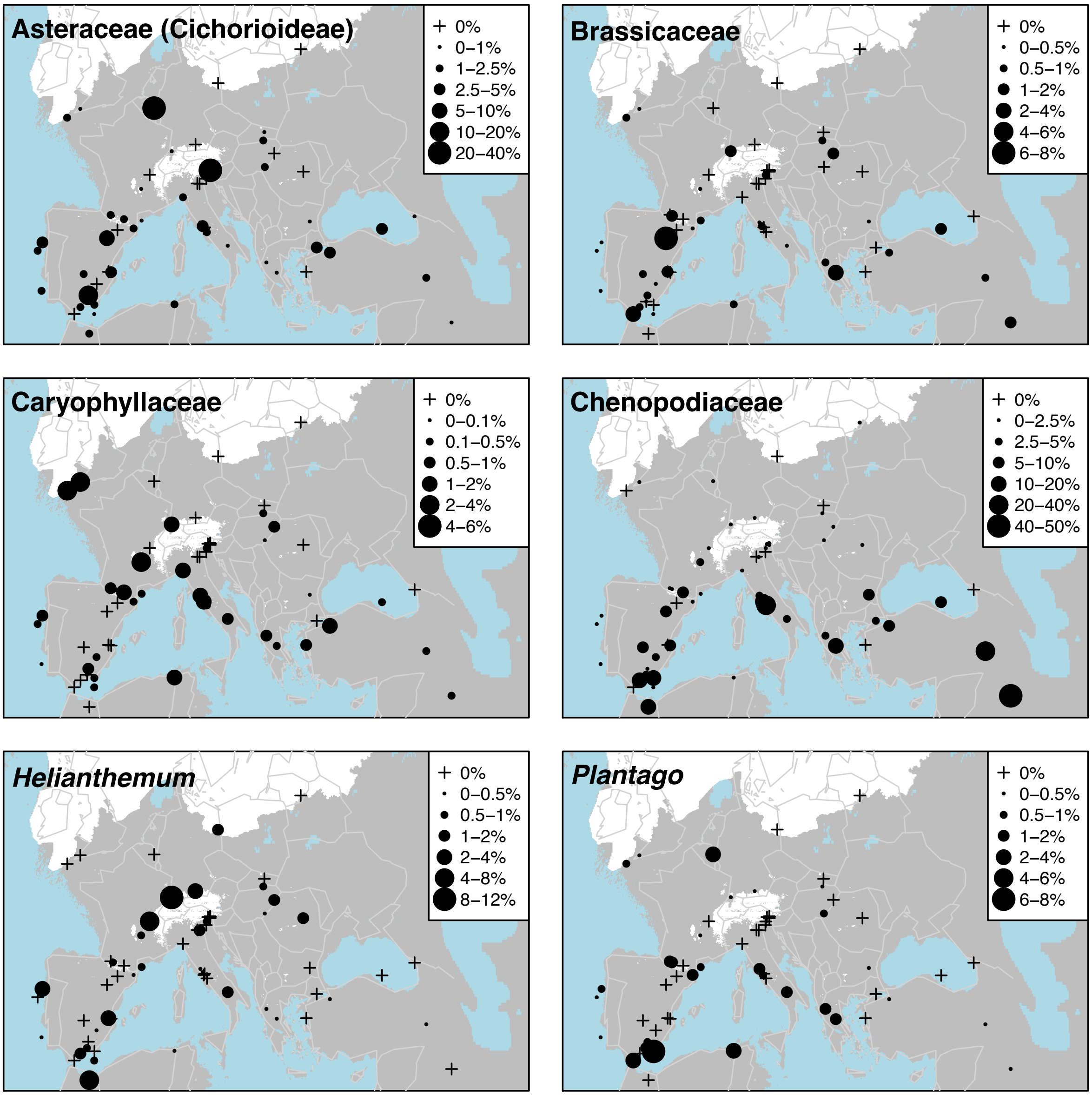

Figure ~~A1e~~A3e. Percentage maps of Asteraceae (Cichorioideae), Brassicaceae, Caryophyllaceae, Chenopodiaceae, Helianthemum and *Plantago*

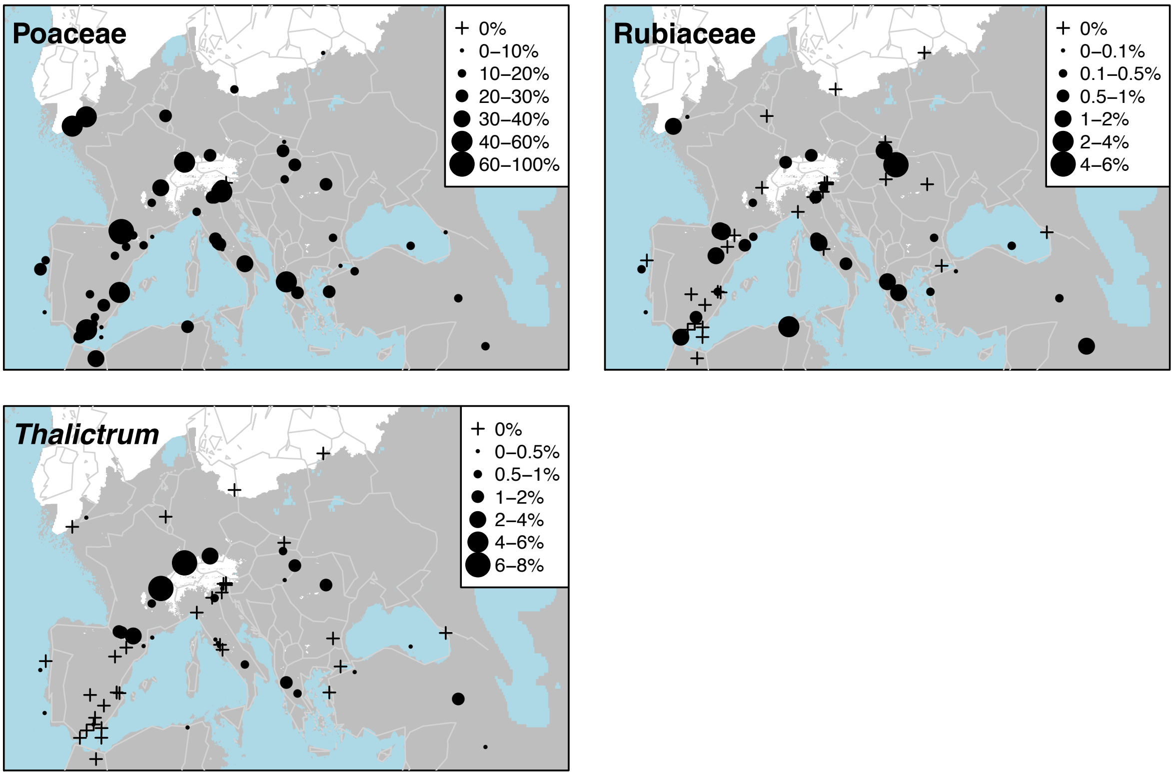

Figure ~~A1f~~A3f. Percentage maps of Poaceae, Rubiaceae and *Thalictrum*

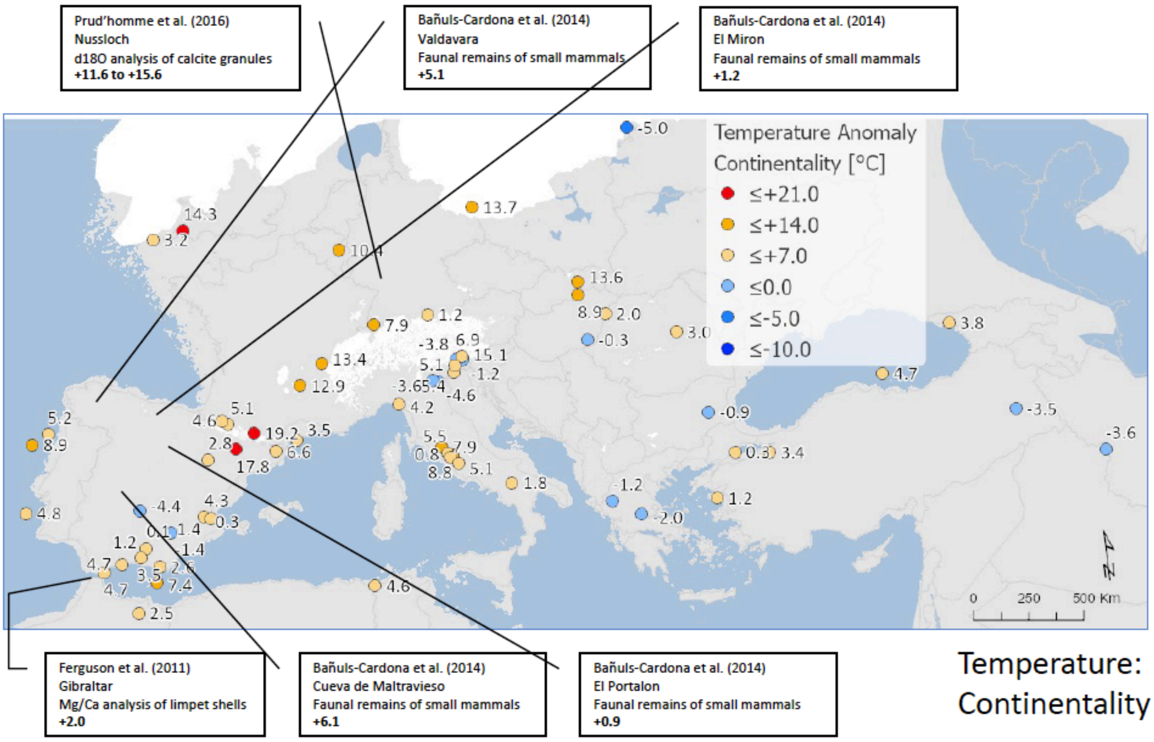
Prud'homme et al. (2016)
Nussloch
d18O analysis of calcite granules
+11.6 to +15.6
Bañuls-Cardona et al. (2014)
Valdavara
Faunal remains of small mammals
+5.1
Bañuls-Cardona et al. (2014)
El Miron
Faunal remains of small mammals
+1.2
Temperature Anomaly
Continentality [°C]
≤+21.0
≤+14.0
≤+7.0
≤0.0
≤-5.0
≤-10.0
0 250 500 Km
Ferguson et al. (2011)
Gibraltar
Mg/Ca analysis of limpet shells
+2.0
Bañuls-Cardona et al. (2014)
Cueva de Maltravieso
Faunal remains of small mammals
+6.1
Bañuls-Cardona et al. (2014)
El Portalon
Faunal remains of small mammals
+0.9
Temperature:
Continentality

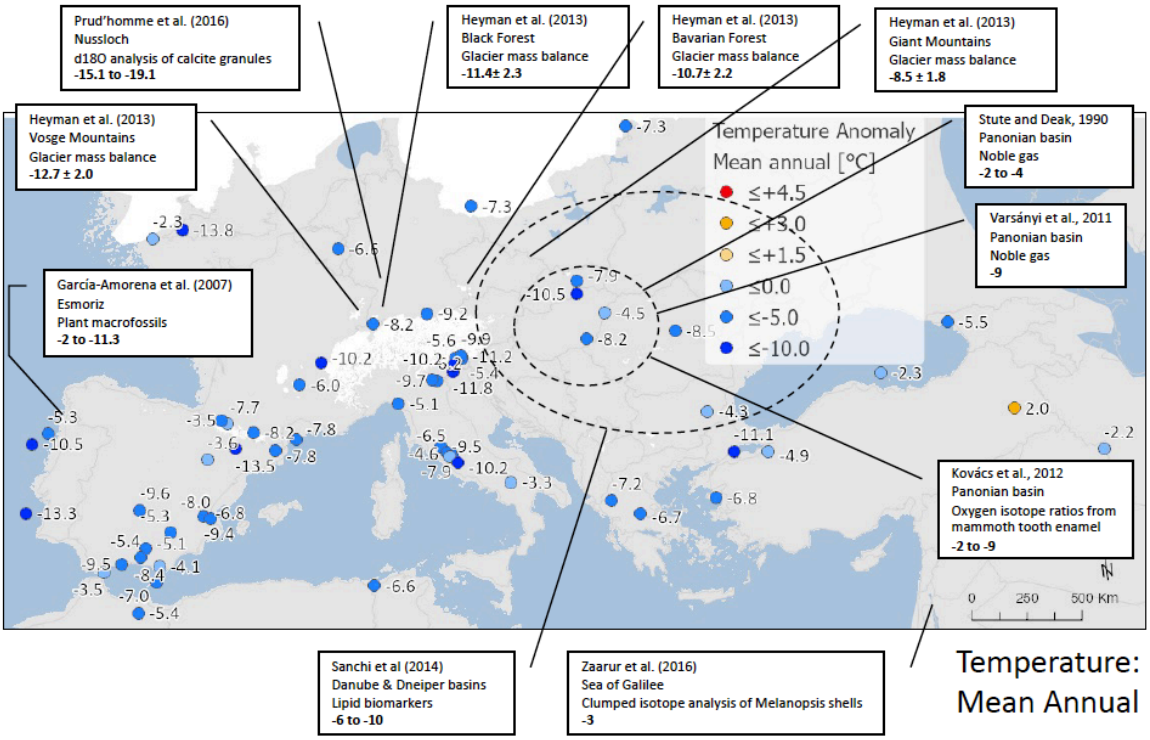
Prud'homme et al. (2016)
Nussloch
d18O analysis of calcite granules
-15.1 to -19.1
Heyman et al. (2013)
Black Forest
Glacier mass balance
-11.4± 2.3
Heyman et al. (2013)
Bavarian Forest
Glacier mass balance
-10.7± 2.2
Heyman et al. (2013)
Giant Mountains
Glacier mass balance
-8.5 ± 1.8
Heyman et al. (2013)
Vosge Mountains
Glacier mass balance
-12.7 ± 2.0
Temperature Anomaly
Mean annual [°C]
≤+4.5
≤+3.0
≤+1.5
≤0.0
≤-5.0
≤-10.0
Stute and Deak, 1990
Panonian basin
Noble gas
-2 to -4
Varsányi et al., 2011
Panonian basin
Noble gas
-9
García-Amorena et al. (2007)
Esmoriz
Plant macrofossils
-2 to -11.3
Kovács et al., 2012
Panonian basin
Oxygen isotope ratios from mammoth tooth enamel
-2 to -9
0 250 500 Km
Sanchi et al (2014)
Danube & Dneiper basins
Lipid biomarkers
-6 to -10
Zaarur et al. (2016)
Sea of Galilee
Clumped isotope analysis of Melanopsis shells
-3
Temperature:
Mean Annual

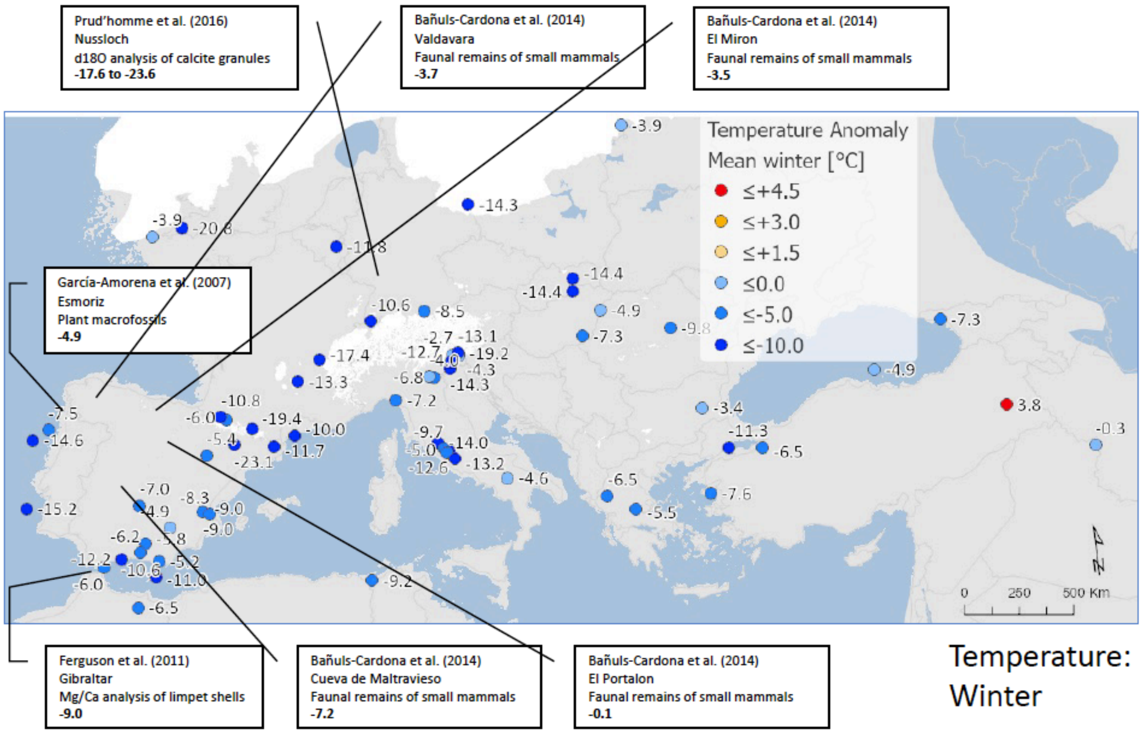

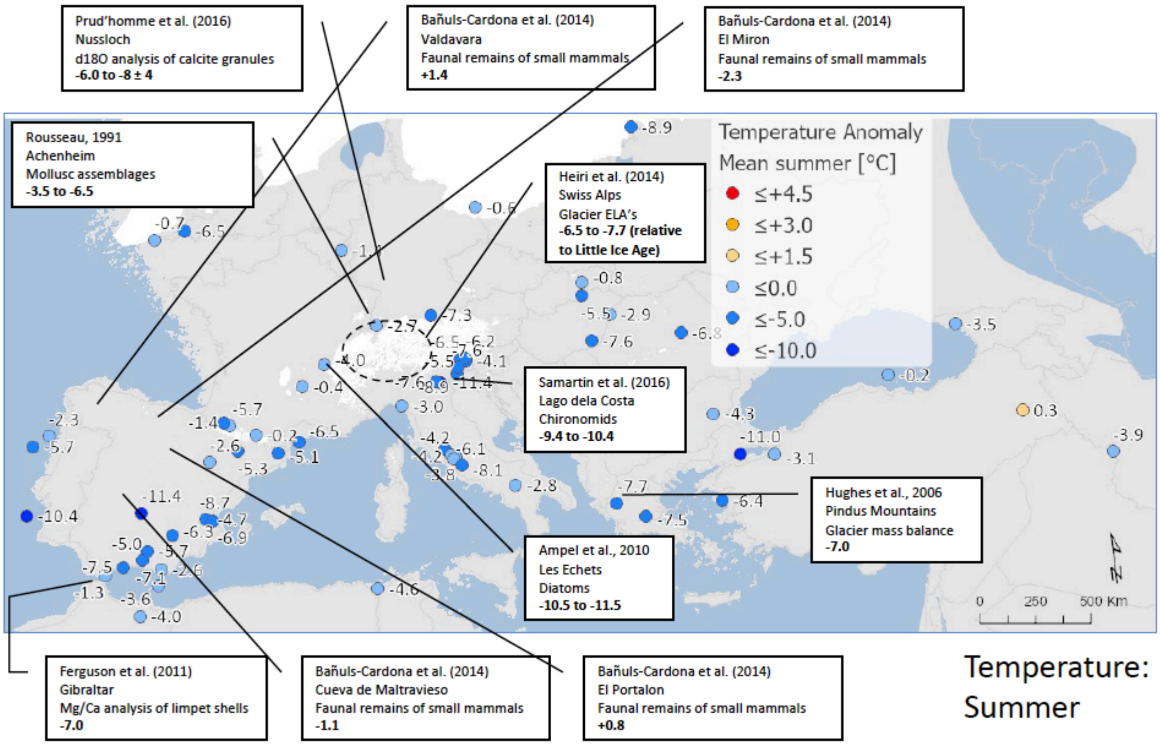

Figure A4. Maps of pollen-based MAT reconstructions for LGM annual, winter and summer temperature anomalies (as shown in figure 10), shown together with the results of other published studies. Continentality represents the difference in temperature between summer and winter, with positive anomalies indicating an increase in the temperature difference between summer and winter. All values are expressed as anomalies compared with the present day unless otherwise indicated.

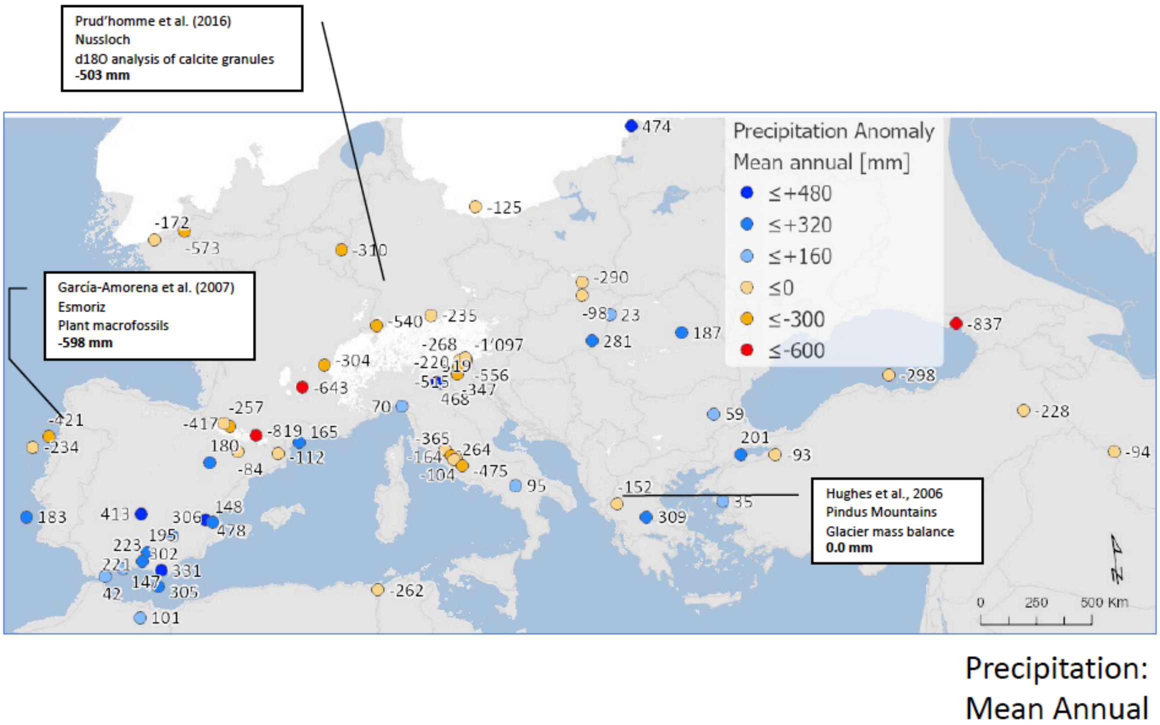

Figure A5. Maps of pollen-based MAT reconstructions for LGM annual precipitation anomalies (as shown in figure 12), shown together with the results of other published studies. All values are expressed as anomalies compared with the present day.